2017-01-01

Development of an Alternative Laboratory Testing Procedure for Tensile Characterization of Cement Stabilized Base Layers

Jose Antonio Tarin
University of Texas at El Paso, jatarin2@miners.utep.edu

DEVELOPMENT OF AN ALTERNATIVE LABORATORY TESTING PROCEDURE FOR TENSILE CHARACTERIZATION OF CEMENT STABILIZED BASE LAYERS

JOSE ANTONIO TARIN

Master's Program in Civil Engineering

APPROVED:

Reza S. Ashtiani, Ph.D.

Diane Doser, Ph.D.

Soheil Nazarian, Ph.D.

Charles Ambler, Ph.D.
Dean of the Graduate School

Dedication

This thesis is dedicated to my parents and sister for their love and continuous support.

DEVELOPMENT OF AN ALTERNATIVE LABORATORY TESTING PROCEDURE FOR TENSILE CHARACTERIZATION OF CEMENT STABILIZED BASE LAYERS

by

JOSE ANTONIO TARIN, BSCE

THESIS

Presented to the Faculty of the Graduate School of

The University of Texas at El Paso

in Partial Fulfillment

of the Requirements

for the Degree of

Master of Science

Department of Civil Engineering

THE UNIVERSITY OF TEXAS AT EL PASO

May, 2017

Acknowledgements

I would like to express sincerely my thankfulness to my academic advisor, Dr. Reza Ashtiani for providing me the opportunity to labor at the Center for Transportation Infrastructure Systems (CTIS) in the Tx-06812 Research Project and for his continuous academic guidance, indispensable advice, information, cooperation and support on different aspects of this study. My honest appreciation and gratitude to Dr. Soheil Nazarian for serving in my thesis committee, his academic guidance and support in this study. I would also like to thank to Dr. Diane Doser for serving in my committee, taking time to talk with me on several occasions and providing me appreciated general comments in this writing.

I would also want to extend my gratitude to the Texas Department of Transportation (TxDOT) for providing the funding of this study and also to Mr. Jose Garibay and Dr. Imad Abdala for their laboratory assistance, cooperation and experience in every aspect of the experimental work of this study.

I would like to thank the undergraduate students that participated in this study: Paloma Zamarripa, Diana Cabrera, Uriel Rocha, Miguel Perez, and to my graduate friends and colleagues: Uriel Arteaga, Mauricio Valenzuela, Jorge Navarrete and Victor Garcia.

Lastly but definitively not least, I would like to express my cordial gratitude to my father Antonio, my mother Carolina and my sister Estefania for their love, patience, encouragement, and fundamental support throughout my study. My gratitude is also dedicated to my uncle Cesar and my grandmother Cleotilde for their unconditionally support in this country.

Abstract

Proper characterization of the fatigue performance of stabilized materials in the laboratory is an integral component of the structural design of stabilized layers in multi-layer pavements. The new mechanistic pavement design protocols require modulus of rupture of the stabilized base layers as an input to the fatigue performance models. This study discusses the practical and theoretical discrepancies associated with the traditional tensile strength tests, and provides an alternative testing procedure for the determination of the tensile strength of the stabilized materials in the laboratory. To achieve this objective, a full factorial laboratory experiment design consisted of four aggregate sources with distinct lithology, four stabilizer contents, and two curing conditioning procedures were incorporated in the experiment matrix. The stabilized systems were subjected to unconfined compressive strength test, submaximal modulus test at different strength ratios, static and dynamic indirect diametrical tension tests, free-free resonant column test and dielectric test, to identify the mechanical behavior of stabilized materials in the laboratory. A moisture susceptibility test was also incorporated in the study to monitor the degradation of the mechanical properties with moisture intrusion in stabilized materials. A multi-dimensional aggregate feature database was developed based on 570 fabricated laboratory specimens in this study. The trend analysis of the laboratory data revealed the capability of the new laboratory procedure to provide an efficient and repeatable measure of the tensile strength of stabilized materials subjected to high number of load cycles in the laboratory.

Table of Contents

List of Tables

List of Figures

Chapter 1: Introduction

SIGNIFICANCE

Structural pavements are multi-layer systems commonly composed of a surface layer, base layer and subgrade level. The principal role of the supporting layers is to minimize the stresses induced by the traffic wheels to a tolerable level that the natural soil can sustain. Furthermore, the surface layer has the obligation to provide environmental protection to safeguard the granular layers against moisture intrusion with the purpose of sustaining the entire integrity of the pavement system. However, pavements in general tend to develop two common modes of failure categorized as permanent deformation and fatigue cracking. In order to minimize these failure potentials, several departments of transportation (DOT) in the US and other countries have implemented the practice of soil stabilization in base layers. An important motive of stabilizing the granular base layer is to supply a more rigid structural platform to the surface layer and protect the subgrade level.

For that reason, soil stabilization is used frequently on granular base layers especially for heavy-duty traffic conditions. Providing stabilized base layers in the system improves the fatigue resistance and reduces the permanent deformation potential of the pavement structure. The favorable effect of the fatigue resistance improvement is usually credited to a notable reduction in the critical tensile strain at the bottom fibers of the surface layer. Flintsch et al. (2008) demonstrated that providing a cement treated base in the pavement system would significantly decrease the tensile strain at the bottom fibers of the asphalt layer. Therefore, the fatigue life of the pavement structure is improved by applying a stabilized base layer in the system. However, the author found a crucial shifting in the location of the critical tensile strain in the multi-layer system. The critical tensile strain moves from the bottom fibers of the asphalt layer to the bottom

fibers of the cement treated base layer as Figure 1.1 illustrates. Therefore, the tensile characteristics of stabilized base layers are of predominant importance to reduce the fatigue cracking potential of such layers.

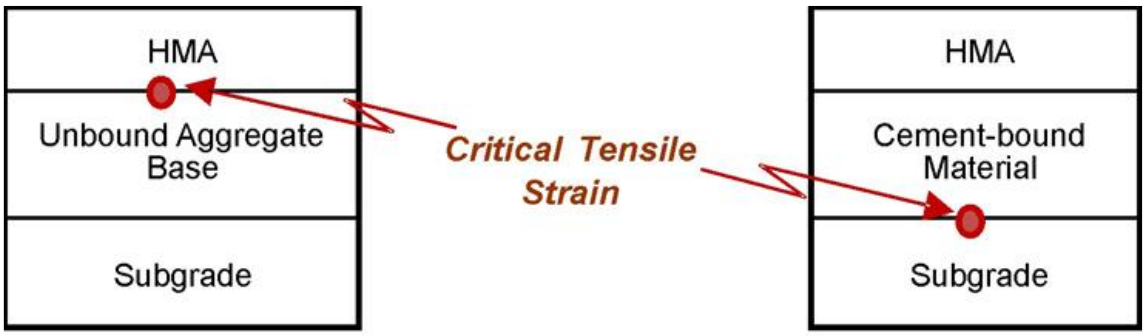

Figure 1.1: Shift in Critical Strain Location from Traditional Flexible Pavement to Pavement with Cement-Treated Base (Flintsch et al. 2008)

In stabilized base layers, a fatigue crack emerges when the tensile stresses imposed by the traffic wheel load exceed the tensile strength of the material. Additionally, these cracks have the tendency to extend from the bottom to the top of the layer. Consequently, the crack propagates through the surface layer region reaching the uppermost segment of the pavement system; this mode of failure is considered as reflective cracks. According to Adaska et al. (2004), such as reflective cracks are very common in pavement structures and usually they do not reduce the pavement performance or serviceability. However, wide cracks (greater than 6 mm) can be responsible for poor load transfer and a notable increment of the stress affecting in the pavement, consequently developing serious pavement performance problems. Additionally, wide cracks cause water infiltration within the pavement structure, which causes erosion of the subgrade level in a process termed pumping. Figure 1.2 illustrates wide reflective cracks in a pavement section due the brakeage of the stabilized base layer. This is an indication of the importance of the stabilized layer's role when subjected to cyclic loading and emphasizes the necessity of a proper tensile characterization.

Figure 1.2: Wide Reflective Cracks on Asphalt Layer (Adaska et al. 2004)

Thus, the horizontal tensile strain at the bottom fibers of cement treated layers has been considered as the decisive component that controls the fatigue performance in the most innovative pavement design approaches. Recent pavement design analysis includes mechanistic-empirical models to develop a precise characterization of the fatigue performance of stabilized layers under repeated loading conditions. Equation 1.1 supplies the general form on the subject of fatigue performance in the new mechanistic pavement design guide. This equation contains a strain-strength ratio where the modulus of rupture provides a measure of the tensile strength of stabilized materials. It is imperative to mention that the tensile characteristics are of significant importance to properly characterize the fatigue performance of stabilized materials.

$$N_f = 10^{\{[0.972\beta_{C1} - (\sigma_t / M_{Rup})]/0.0825\beta_{C2}\}} \quad (1.1)$$

Where:

N_f = Number of load repetitions to reach fatigue failure

σ_t = Tensile stress by Traffic Load

M_{rup}= Modulus of Rupture

β_i: Fitting Parameters

STATE OF THE PROBLEM

Usually the fatigue characterization of stabilized bases consists in the determination of strength measurements generally in terms of Unconfined Compressive Strength (UCS) test and Flexural Strength (M_{rup}) as Equation 1.1 demonstrates. Additionally, many districts in Texas tend to utilize compressive strength requirements to select the amount of stabilizer needed in a specific base layer. However, the compressive and tensile properties of stabilized materials can behave very dissimilarly to each other. Other districts design a stabilized base layer based on the experience of other projects previously developed. Nonetheless, the material characteristics may be significantly different from one location to another.

Traditionally the four-point bending beam test measures a tensile strength parameter expressed as the flexural strength or modulus of rupture. The modulus of rupture is a decisive characteristic that governs the fatigue life equation of stabilized materials. This destructive test originally was designed for concrete characterization where large concrete beams are subjected to strain-controlled loading protocol to induce fracture failure at the bottom fibers of the beams as Figure 1.3 illustrates.

Figure 1.3: Large Beam Fatigue Test after Failure at The University of Texas at El Paso (UTEP)

Many engineers have favored this test because the laboratory conditions simulate the field conditions. However, due to the extrapolation of this test from concrete to stabilized materials, several practical and theoretical discrepancies emerged immediately. For these reasons, the purpose of this section is to provide a detailed discussion on the subject of systematic errors and practical concerns associated with the implementation of the ordinary four-point bending beam test to stabilized granular materials.

Technical Discrepancies

Many researchers have reported technical difficulties with respect to sample preparation and handling activities in the laboratory. A major technical concern related to sample preparation is the non-uniform level of compaction effort along the stabilized beam. Similarly, the uniformity of density cannot be guaranteed due to the long and relatively shallow shape of the molds in ordinary four-point bending beam specimens of 6 x 6 x 20 in (152 x 152 x 508 mm) dimensions. Occasionally, void pockets of trapped air are observed between the rigid mold and the specimen perimeter. This clearly is an indication of the irregularity of the compaction effort along the beam. Figure 1.4 demonstrates a beam specimen containing 3 percent cement where the surface clearly shows air void in most of the outside perimeter. These concerns tend to potentially reduce the reliability and repeatability of the test results.

Additionally, stabilized beams at low stabilizer content such as 1 or 2 percent tend to disintegrate by their own weight during the handling, transportation and curing process in the laboratory. Paul and Gnanendran (2012) experienced technical problems preparing beam specimens containing 1 percent of cement content. The stabilized specimens developed damage during curing procedures and the specimens were not tested.

Figure 1.4: Large Beam Fatigue Test Setup at UTEP

Figure 1.5 demonstrates fragmented stabilized specimens during removing from the mold and during the curing process at UTEP. This result requires more than one operator to carefully prepare and handle the specimens and hence increases the test cost.

Figure 1.5: Sample Breakage during Demolding and Curing at the CTIS Laboratory

Theoretical Discrepancies

Moreover, there are several theoretical concerns related to the four-point bending beam test. The modulus of rupture is calculated by the standard flexural formula using the dimensions

of the beam and the maximum load at failure. This formula, assumes that the stress is proportional to the distance from the neutral axis based on a linear stress-strain relationship. However, according to Hudson and Kennedy (1968) such a relationship does not exist for most materials. More important is the fact that even in the most elastic materials, this assumption is seriously incorrect mainly at failure conditions. Consequently, the modulus of rupture does not correctly represent the tensile properties of materials. The modulus of rupture is calculated using equation 1.2.

$$M_{rup} = \frac{PL}{bd^2} \tag{1.2}$$

Where:

M_{rup}= Modulus of Rupture

P = Load at Failure

L = Specimen Length

b = Specimen Width

d = Specimen Depth

However, equation 1.2 is not valid if the crack occurs outside of the middle third of the span length. In this case, the modulus rupture is calculated using Equation 1.3 where the fracture is outside by not more than 5 percent of the span length.

$$M_{rup} = \frac{3Pa}{bd^2} \tag{1.3}$$

Where

a = the average distance between the crack and the nearest support measured from the bottom surface of the beam namely tension region.

Furthermore, another error associated with the bending beam test is the overestimation of the tensile properties of cementation materials. The modulus of rupture tends to overestimate the tensile strength significantly. Grieb (1952) and Thaulow (1947) estimate that for concrete the modulus of rupture is equal to or greater than two times the tensile strength. Similarly, Price (1952) found that in some cases the modulus of rupture value overestimates the tensile strength by 50 to 100 percent. Table 1.1 illustrates the modulus of rupture, compressive and tensile strength values of cementation materials.

Table 1.1: Relationship between Tensile Strength and the Modulus of Rupture (After Price, 1952)

Strength of Concrete (MPa)			**Ratio (%)**		
Compressive	**Modulus of Rupture**	**Tensile**	**Modulus of Rupture to Compressive Strength**	**Tensile Strength to Compressive Strength**	**Tensile Strength to Modulus of Rupture**
7	2	1	23.0	11.0	48
14	3	1	18.8	10.0	53
21	3	2	16.2	9.2	57
28	4	2	14.5	8.5	59
34	5	3	13.5	8.0	59
41	5	3	12.8	7.7	60
48	6	4	12.2	7.4	61
55	6	4	11.6	7.2	62
62	7	4	11.2	7.0	63

Price mentioned that this incongruence has to do generally with the modulus of rupture equation where a linear stress-strain relationship is assumed along the cross section. According to Mehta (2006) the actual stress distributions compared to the assumed stress distributions in the four-point beam test are significant different especially at the top and bottom portions of the beam cross section. Figure 1.6 shows the distinction between the assumed and actual stress

distributions where the critical tensile stress situated at the bottom of the beam is less than the assumed.

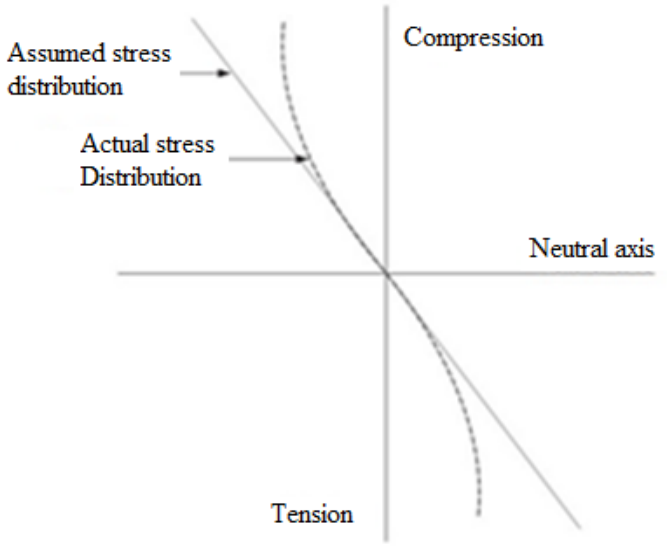

Figure 1.6: Diagrammatic Arrangements of the Traditional Flexural Four-Point Stress Distributions (Mehta, 2006)

In order to verify these observations made by previous researchers, a series of finite element analyses were performed to evaluate the stress distributions on beams of 6 x 6 x 20 inch dimensions during the bending beam test. Figure 1.7 provides the stress distributions in the beam where the red color indicates tensile stresses and blue colors are an indication of compression in the structure. The colors indicate that the top portion is performing in compression while the bottom portion is acting in tension due the bending mechanism of the bending beam test. According to Hudson (1968), the location of the neutral axis is a function of material properties, loading rate and the load magnitude during test.

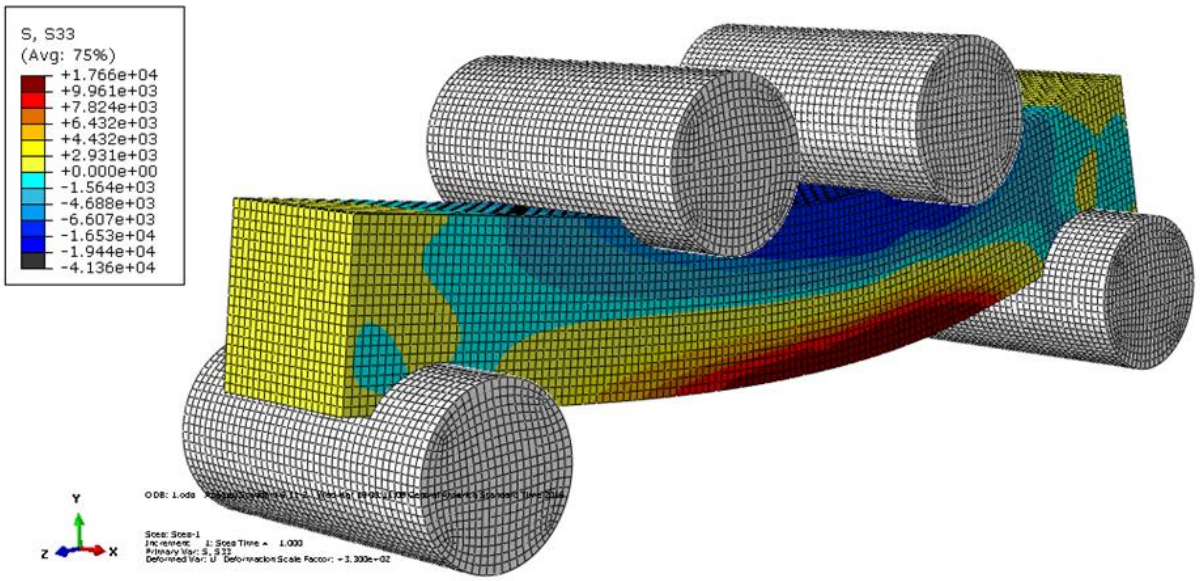

Figure 1.7: Distribution of the Stresses in the Four-Point Beam Test

A better visualization of the non-linear behavior of the stress distributions is more evident in the beam cross section of previous figure shown in Figure 1.8. This figure demonstrates that approximately 60 percent of the beam is acting in compression due the pure bending mechanism according to the parameters selected in the finite element analysis. This analysis is a confirmation of the argument presented by Price (2012) and Mehta (2006) on the systematic error of using simplified linear stress distribution to calculate the modulus of rupture in cementation materials.

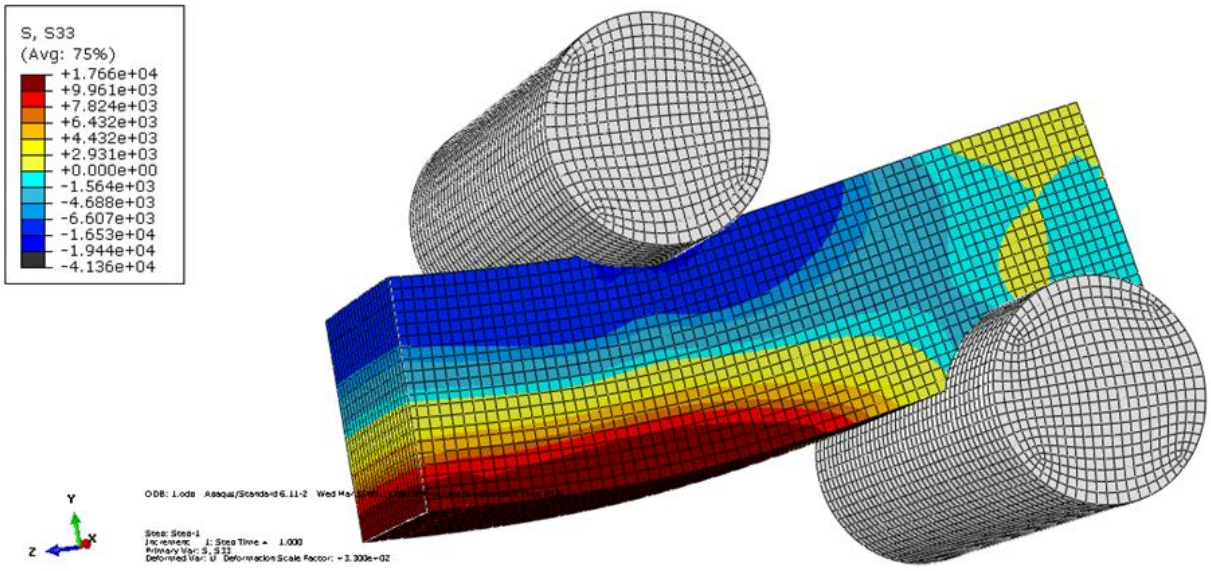

Figure 1.8: Distribution of the Stresses in the Transverse Cross-Section in the Mid-Span of the Prismatic Beam

Moreover, the degree of non-linearity of lightly stabilized materials is significantly elevated compared to traditional concrete. This component combined with the theoretical issues and practical aspects of the four-point bending beam test emphasize the necessity of developing an alternative tensile testing protocol to effectively and efficiently estimate the tensile characteristics of stabilized materials in the laboratory.

SCOPE AND LIMITATIONS

This study focuses on providing an innovative tensile testing protocol for the practice of tensile characterization of stabilized granular materials. An important component of this study was to create an extensive literature search of the current state of tensile characterization for stabilized materials in the laboratory. Such a developed test should be derived from current tensile testing procedures to avoid the necessity of new equipment in the laboratory. Additionally, such a test should follow theoretical principals with the least amount on uncertainly in the assumption of its related equations. Developing an experiment matrix is also a vital

constituent of this study in order to verify the implementation of such a tensile test to stabilized materials. This tensile testing procedure should recognize the properties that tend to develop fatigue cracking during pavement service life.

Additionally, this new approach should be inclusive with specimens subjected to different environmental conditions such as moisture susceptibility related to the aggregate mineralogy and stabilizer content. Moreover, this new testing protocol should be effortless to complete in the laboratory to facilitate reliable and repeatable results. However, this study does not pretend to characterize the fatigue performance of stabilized materials based on the developed tensile test.

Tensile Protocol Requirements

1. Technically speaking, the testing procedure process must be easy to perform in the laboratory with the least amount of difficulty including sample preparation, transportation and handling activities.

2. It must be capable of being implemented for several materials with different mineralogies and amounts of stabilizer content, especially low cement contents.

3. It must be derived from a current laboratory tensile test to prevent the need to acquire new laboratory equipment.

4. It must follow theoretical principals with the least amount of uncertainly in the assumptions.

Chapter 2: Literature Review

INTRODUCTION

The objective of this chapter is to present an extended and general description of the current methodology used to characterize the strength, modulus and fatigue performance of stabilized materials in the laboratory. As mentioned in the previous chapter, there are two principal modes of failure in pavement structures namely permanent deformation and fatigue cracking. Fatigue cracking is one mode of failure observed in the pavement structure under cyclic load conditions such as traffic loading and environmental conditions. Consequently, current pavement design analyses consider mechanistic-empirical models to determine the pavement properties in terms of fatigue cracking. Therefore, the most important objective of the literature search consists in the identification of the current situation of the testing protocols and the analysis techniques used to characterize the fatigue properties of cement-stabilized layers.

BACKGROUND

Molennar and Pu (2002) developed a relationship based on the field fatigue performance of sandy cement treated bases. The authors used the SHRP-NL database to analyze the relationship based on pavements that contain sandy cement treated bases. The data obtained contained visual condition, falling weight deflectometer results, and traffic readings for a 10-year period. The first observation that the authors noted was that the crack initially occured at the bottom of the stabilized layer and then it propagated to the surface. The tensile strain at the bottom of the stabilized base layer and the traffic analysis of data collected were the precursor parameters to develop the relationship presented in Equation 2.1 to predict the fatigue life of cement treated bases.

$$logN = 8.5 - 0.034\ \varepsilon \qquad (2.1)$$

Where;

N =allowable number of 100kN equivalent single axles

Ɛ =Tensile strain at the bottom of the cement treated base due to 50 kN loading condition (μm/m)

Flintsch et al. (2008) demonstrated that providing a cement treated base in the pavement system would significantly decrease the tensile strain at the bottom of the asphalt layer increasing the fatigue life of the pavement structure. This enhancement could contribute to the shifting of the location of the maximum tensile strain as Figure 2.1 indicates. The contribution of the cement treated base in the pavement structure can be associated with the improvement in the tensile stress distribution capacity of the base layer. Consequently, the cement treated layer provides a more efficient load bearing capacity compared to unbound systems. Additionally, the author found that the deflections in the pavement structure significantly decreased as the stiffness of the base layer increased. In addition, the fatigue cracking potential in asphalt layer is significantly minimized due the stabilized layers performance in the multi-system. These conclusions were based on pavement design models and not directly on laboratory characterization of fatigue

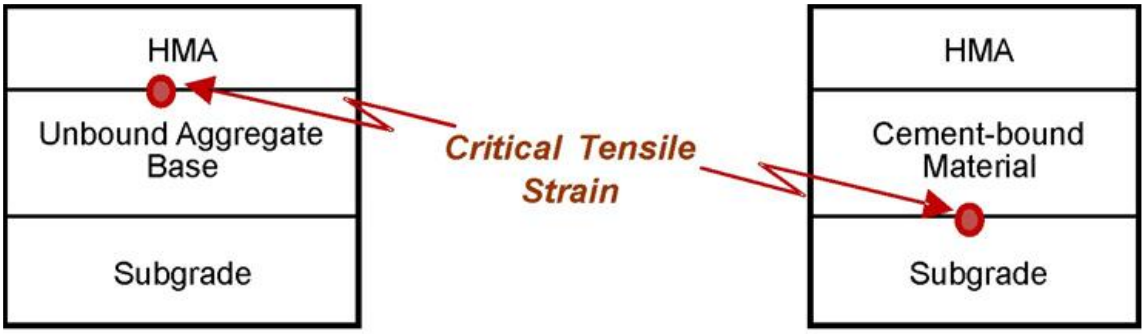

Figure 2.1: Shift in Critical Strain Location from Traditional Flexible Pavement to Pavement with Cement-Treated Base (Flintsch et al. 2008).

Li et al. (1999) studied the improvement in terms of fatigue performance properties and failure modes of asphalt pavements with soil-cement bases. For this study, failure conditions for cracking were defined as 5 m/m2 over fifty percent of the loaded area and a significant reduction in the base layer modulus. The authors discovered that placing a stone crack relief layer between the cement treated base and the asphalt layer significantly increased the fatigue life of the pavement structure by a factor of five to six.

Yan et al (2011) studied the fatigue life of stabilized materials at several stress states and cement contents. The data demonstrated a high variability in the results, primarily accredited to low cement content, deterioration of external particles, variability in strength values, and loss of moisture during testing period. In addition, the fatigue life was significantly influenced by the stress ratios acting in the specimens of lower cement content.

Mahasantipiya (2000) studied the variation of the modulus of cement treated bases calculated in laboratory specimens and field cored specimens. The author explained that the variations were due to different environmental circumstances between laboratory and field conditions. Additionally, the layering analysis of pavement structures when using cement treated bases presented a reduction of the stresses and strains at the bottom of asphalt layer and top of the sub grade compared to pavement structures with ordinary unbound aggregate bases (UABs). Therefore, the author concluded that the life of pavements using cement treated base layers was increased compared to traditional pavements.

Khoury and Zaman (2007) studied the durability of the specimens influenced by stabilization on different materials using cement, fly ash and bed ash as stabilizer binders. The authors found that the resilient modulus decreases by increasing the number of freeze thaw cycles. To describe this phenomenon, the authors explained that the micro fractures that develop

between binder and particles during freezing and a remarkable increase in moisture content during the thawing process were the reasons for a notable decreasing in the resilient modulus with environmental cycles such as freeze thaw. Figure 2.2 shows the resilient modulus reduction as the number of F-T (freeze-thaw) cycles increases for all permutations in their study.

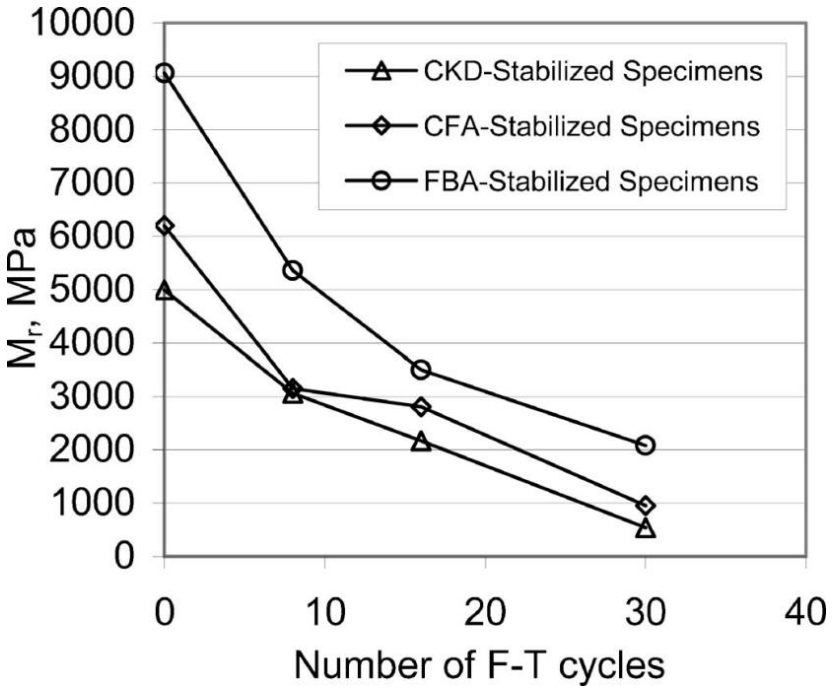

Figure 2.2: Variation of Resilient Modulus with Freezing and Thawing Cycles (Khoury and Zaman 2007).

Puppala et al. (2011) studied the determination of resilient modulus in stabilized materials by changing the confinement pressure. They discovered that the resilient modulus is less sensitive to the variation of the confinement pressure due the improvement in stiffness properties by stabilizing the material.

Sobhan and Das (2007) studied the durability of soil-cement treated systems against fatigue fracture. For this study, the specimens were subjected to a flexural test using four-point bending beam test at a load frequency of 2 Hz under constant sinusoidal load amplitude on beams of 6 x 6 x 30 inch (152 x 152 x 762 mm) dimensions. The authors noted that the

endurance limit for fatigue failure for stabilized systems increases to 53 percent of its maximum strength evidently demonstrating similar strength as other cementations materials. The damage ratio derived from the dissipated energy was used to characterize the fatigue performance of the cementation materials as Figure 2.3 illustrates. The authors concluded that the decision to implement rehabilitation of pavement structures might be based on using the damage ratio in the laboratory fatigue test.

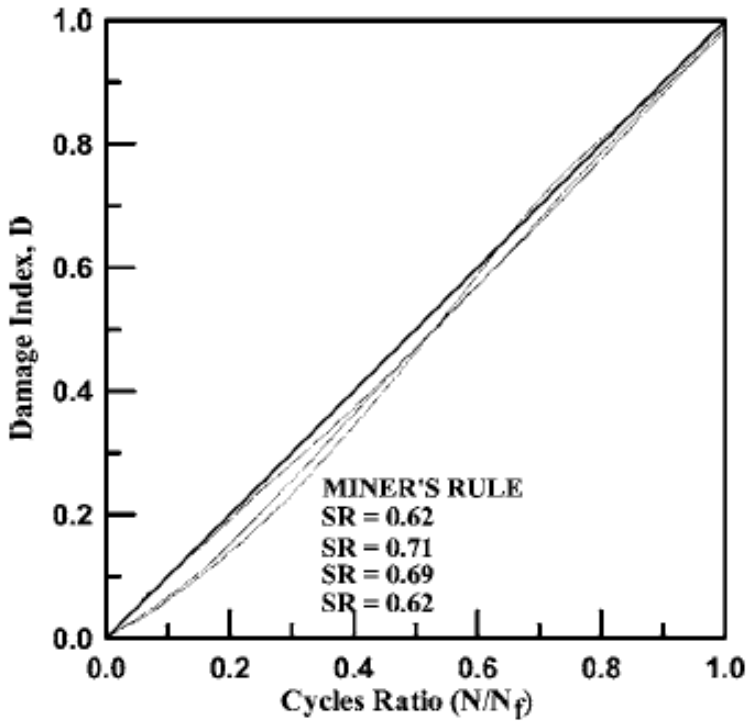

Figure 2.3: Variation of Damage Index with Cycles Ratio (Sobhan and Das 2007).

Arnold et al. (2012) studied the determination of the flexural strength, modulus and fatigue properties of stabilized materials using the four-point bending fatigue beam test. He highly recommended the compaction of the mixes using a mold by applying repeated impacts using a hummer. Referring to strength measurements, the beams were subjected to a loading rate of 1 mm/min or 3.3 kN per minute until the specimens failed. For modulus determination, 100

load cycles were applied. In terms of fatigue performance, at least 1 million of cyclic loads were applied or until failure specimen was observed.

Papapcostas and Alderson (2013) studied the estimation of flexural strength, breaking strength and flexural modulus for cemented materials. The materials included in this study were Portland Cement (PC), lateritic gravel, weathered granite, calcrete, ferricete and metagreywacke. The test procedures of this study consisted of flexural test methods such as flexural strength and flexural modulus testing. For flexural beam, test specimens of 100 x 100 x 400 mm were used for easier handling and test preparation as shown in Figure 2.4. The authors developed a model based on the data collected that correlates the material properties of the flexural strength and breaking strength. Based on the model results, the cement content was the most significant factor that influences the strength results. They also mentioned that enough data exist to establish a relationship between the UCS and the flexural modulus.

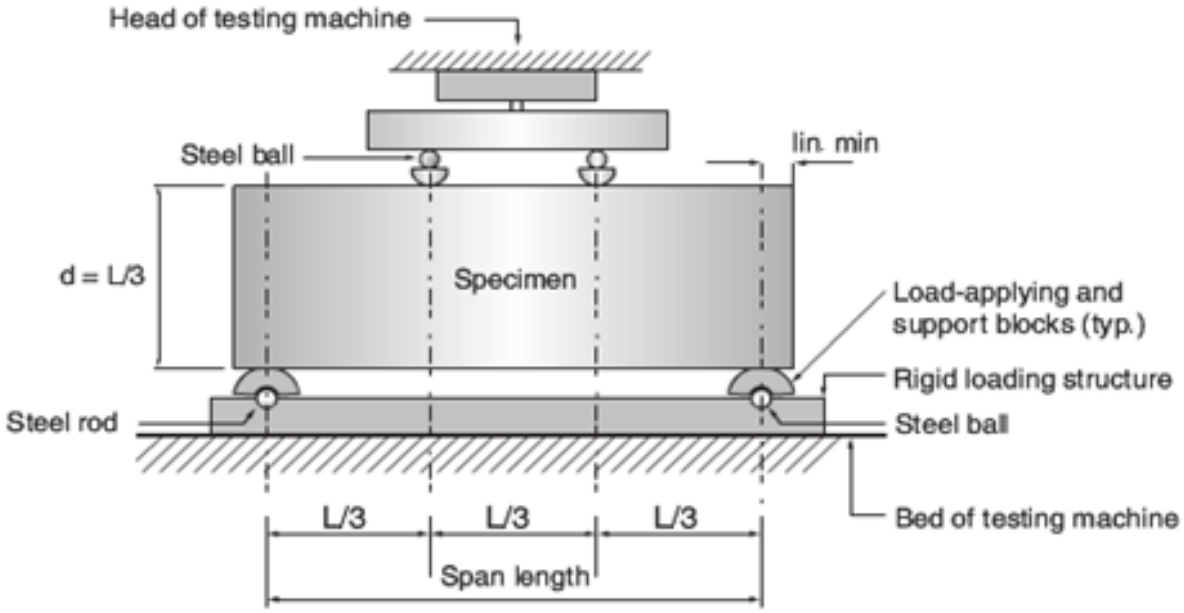

Figure 2.4: Cross-sectional view of flexural beam testing apparatus (Papapcostas and Alderson 2013).

Majumder et al. (1990) studied the fatigue life of stabilized systems executing several flexural fatigue tests using a four-point loading test. For this study, the load was applied in repetitions consisted of on-load and off-loads cycles of 0.27 seconds over beam specimens with 4 x 4 x 20 in (101 x 101 x 508 mm) dimensions. The load cycles were applied until rapid and brittle failure was observed. Based on the results, the authors developed relationships between the fatigue life and stress ratio acting on the specimens. Figure 2.5 shows that the cement-stabilized materials with laterite aggregates demonstrated higher fatigue life when compared to systems with gravel and doloreite aggregate types. For all permutations, the fatigue life was reduced significantly when the stress ratios increase clearly demonstrating an inverse relationship.

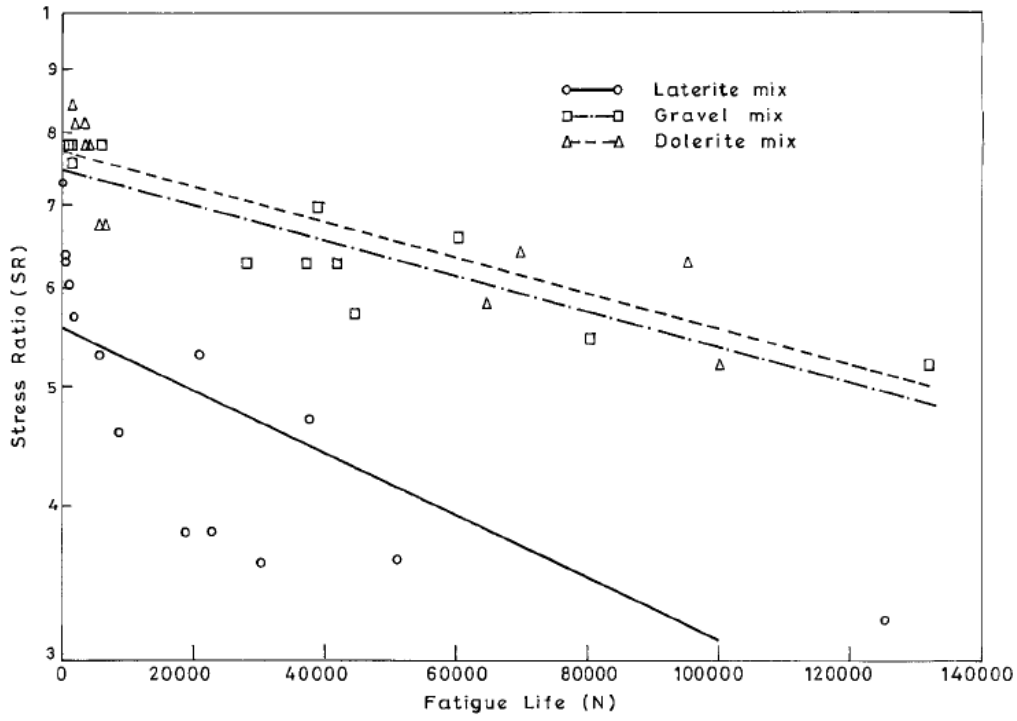

Figure 2.5: Fatigue life of cement treated mixes versus stress ratio (Majumder et al. 1999).

Paul and Gnanendran (2012) studied the characterization of stabilized granular bases using the flexural beam test and the influence of rate loading on the results. The materials used in

this study consisted of well-graded sandy gravel with a portion of fines based on Unified Soil Classification System (USCS). The material used for stabilization at 1% and 3% were blend cement and fly ash due the low potential of shrinkage/cracking potential and also for economic reasons. The authors remarked in the report that after 28 days of curing time, the specimens containing 1% of stabilizer were damaged more than once during removal from the mold. The authors applied monotonic load/displacement of 1.2 mm/min as per ASTM D1663 until failure fracture was developed in the beams. However, the specimens failed in just a few second and the authors concluded that such specifications are not suitable for lightly stabilized materials. After applying different rate values, a rate of 0.5 mm/min was selected for the testing protocol of this study. Figure 2.6 shows the schematic representation of the test set up. The results of the flexural testing are given in Table 2.1.

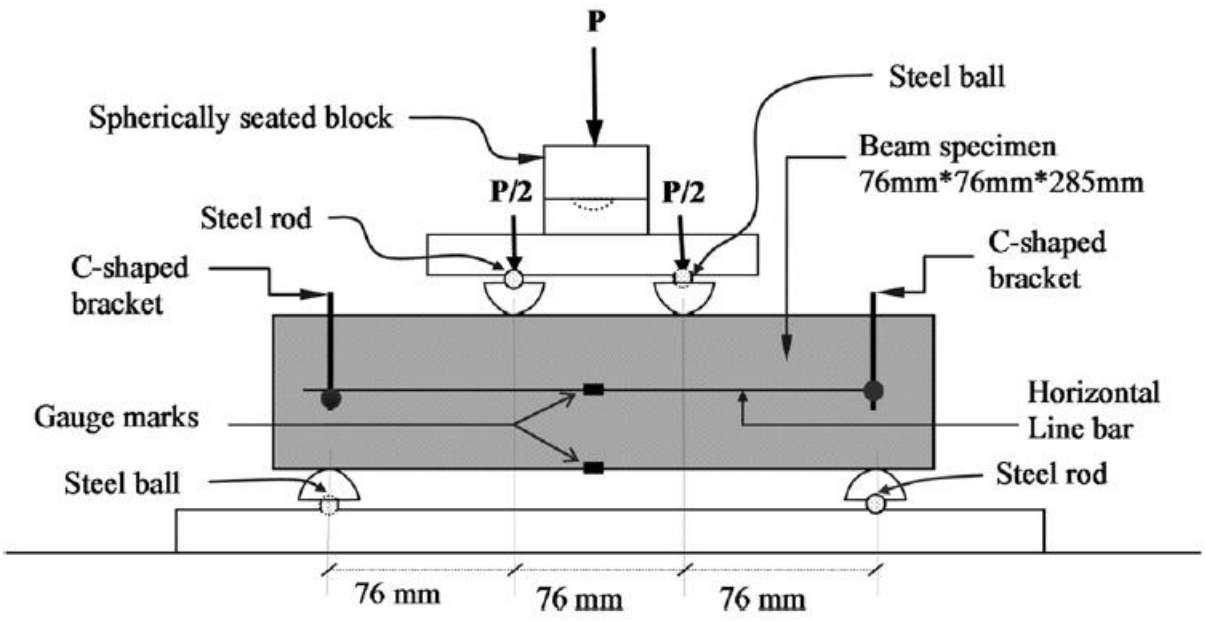

Figure 2.6: Schematic diagram of flexural testing setup (Paul and Gnanendran 2012).

Table 2.1: Flexural properties of lightly stabilized materials and comparison of variations in flexural testing (Paul and Gnanendran 2012).

		Flexural Strength M_R		Static Stiffness modulus E		Breaking strain ε_f	
Parent material	BC (%)	Mean (MPa)	CoV (%)	Mean (MPa)	CoV (%)	Mean (MPa)	CoV (%)
CLM	1.0	0.10	4.0	203	7.1	1020	16.7
	1.5	0.25	11.9	1620	7.8	270	12.3
	2.0	0.33	8.4	2040	12.1	216	8.3
	3.0	0.50	6.4	2507	5.7	214	15.2
QRM	1.0	0.10	-	159	-	1720	-
	1.5	0.63	1.4	2642	17.4	322	21.2
	2.0	0.85	8.1	4408	18.4	235	13.2
	3.0	1.17	6.7	5466	4.3	237	12.8

The results confirmed an improvement in flexural strength and static stiffness as binder content increased for both materials. However, the breaking strain decreased as cement content increased. Finally, the authors concluded that this test might not be practical for lightly stabilized materials due the unavailability of equipment and staff during testing and specimen preparation.

Zhou et al. (2010) characterize cement treated material based on the UCS test, free-free resonant column (RC) test and modulus of rupture ordinarily determined with the flexural beam load test. The specimens were prepared using 2%, 3% and 4% cement contents. The results of this study demonstrated an improvement of UCS and modulus or rupture values as cement content increase as Table 2.2 indicates.

Table 2.2: Summary of all results (Zhou et al. 2010).

Cement Content (%)	Seismic Modulus (ksi)		7-day UCS (psi)	28-day MR (psi)
	Day 3	Day 7		
2% Cement - A	939.3	1011.3	316.7	67.5
2% Cement - B	964.8	1008.9	329.4	74.2
2% Cement - C	927.8	1089.4	306.1	75.8
3% Cement - A	982.7	1151.5	429.9	90.0
3% Cement - B	928.6	1095.6	440.6	93.3
3% Cement - C	942.7	1235.1	457.2	94.2
4% Cement - A	987.6	1239.2	586.0	117.5
4% Cement - B	963.2	1245.6	582.1	118.3
4% Cement - C	1012.5	1401.1	606.5	116.7

Scullion et al. (2008) developed input values for a mechanistic-empirical pavement design analysis by characterizing material properties of cement treated materials. The material properties characterized in this study were resilient modulus, modulus of rupture and Poisson ratio. The results indicated that the resilient modulus is approximately fifty percent of the modulus measured using seismic devices. The authors used three different methods to measure the modulus in the laboratory namely the seismic modulus test, dynamic modulus test and the resilient modulus test. The authors concluded that the frequency of loading did not have significant effect on the modulus as shown in Figure 2.7. This is an indication that the cement treated bases behave as an elastic material under cyclic loading. Therefore, the dynamic modulus and the resilient modulus are the same modulus and they can be used as an input to the design analysis. Table 2.3 compares the three test approaches used in their study. The seismic modulus test is the cheapest and fastest test to establish a measurement of the modulus in stabilized systems. Based on a case study where two different materials were subjected to the seismic modulus test, the results showed that this test offers a realistic alternative test procedure for

characterizing the stiffness properties of stabilized systems. The authors also developed a relationship between the UCS test and the resilient modulus based on very limited data.

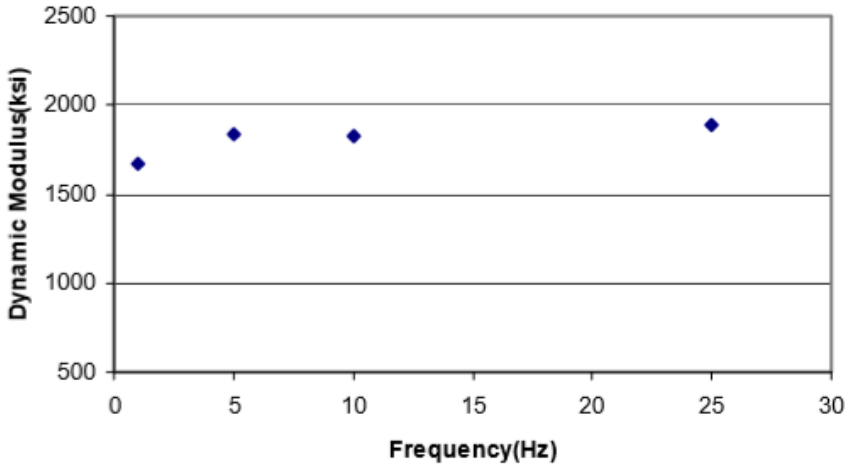

Figure 2.7: Dynamic Moduli at different frequencies Scullion et al. (2008).

Table 2.3: Comparison of Three Moduli Test Methods Scullion et al. (2008).

	Seismic Modulus Test	Dynamic Modulus Test	Resilient Modulus Test
Equipment Cost	$5,000	$40,000	$350,000
Testing Time	3 minutes	40 minutes	30 minutes
Sample Capping	No capping	Capping	Capping
Coefficient of Variation @ 28 day	7%	7%	10%

Mbaraga et al (2013) studied how the beam span/depth ratio was influenced by the geometry and aggregate particle size. The material selected in this study was crushed gravel rock at three cement contents of 2%, 3 % and 6%. The aggregate particles size used included P_{max} 19.00 mm and P_{max} 13.20 mm. The specimens were subjected to monotonic loading condition with a strain-controlled rate of 0.025 mm/second using a four-point bending beam and testing until failure. The deflections were measured using 20 mm Linear Variable Differential Transformer (LVDT) located at the mid-span of the beam. The specimens had spans of 300 mm and 450 mm of span. The author used the flexural strength and the elastic moduli to characterize

the cement stabilized material. The results provided in Figure 2.8 clearly show an improvement in terms of flexural strength when the stabilizer content increases. Additionally, beams with P_{max} 19.00 mm demonstrated lower R^2 value, which could be attributed to the use of large particles in a small beam.

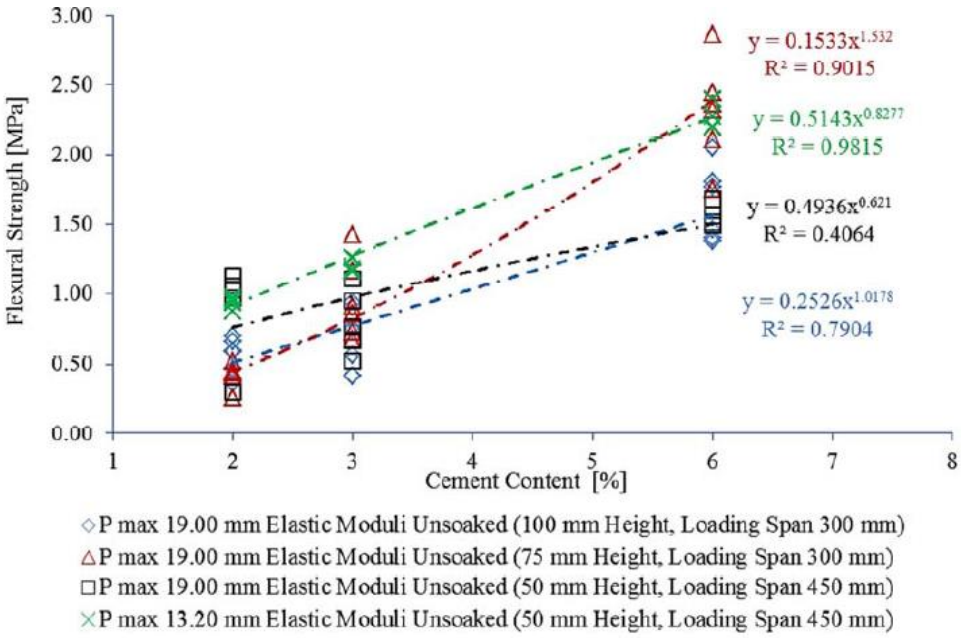

Figure 2.8: Flexural strength versus cement content (Mbaraga et al. 2013).

Figure 2.9 shows the relationship between the elastic modulus and cement content. The use of large particles in small beams also causes reduction of the elastic modulus as Figure 2.9 demonstrates. This significant reduction may be attributed to the creation of weakness zones between the large particles compared to beams with smaller particles. The beams with the highest span/depth ratio demonstrated a lower shear stress capacity compared to those with lower span/depth ratio. In this case, the beam with the lowest ratio (of nine) showed the lowest shear stress capacity. Therefore, the authors concluded that the use of large aggregate size in small beams contributes to a reduction of flexural strength and elastic modulus. The author suggested using smaller aggregate particles of P_{max} 20.00 mm on beams with 60 mm or less height.

Additionally, they suggested using a span/depth ratio of nine or above to reduce shear stresses in the beam. Finally, developing correction factors should be incorporated for reliable results.

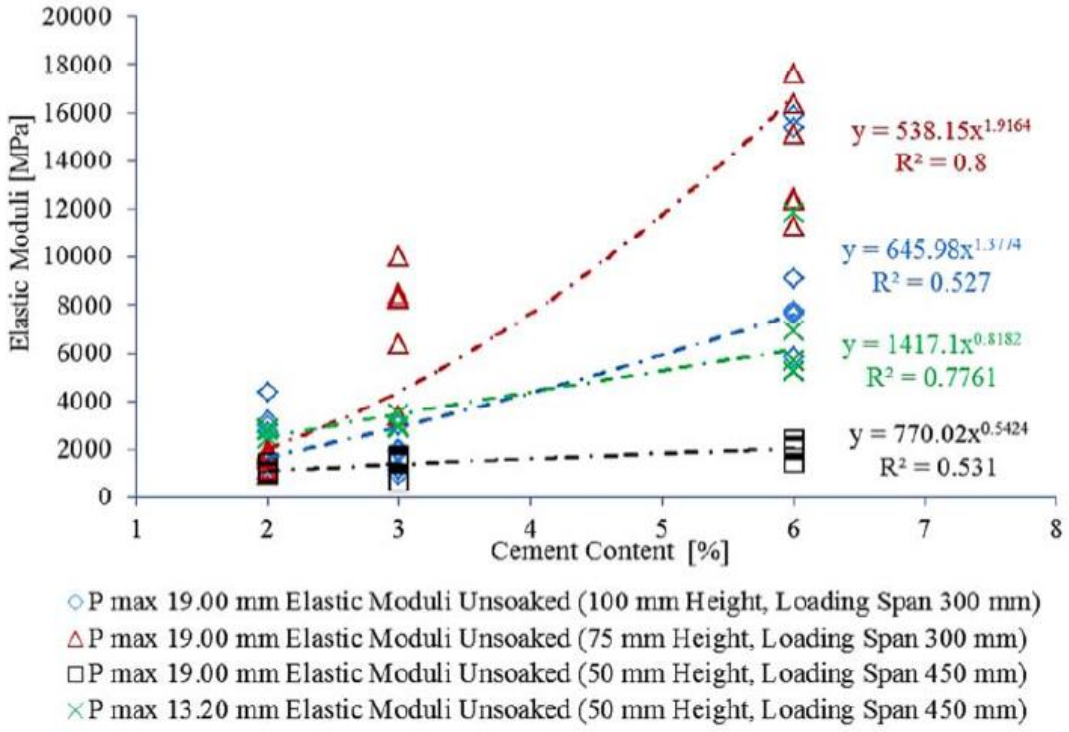

Figure 2.9: Elastic moduli versus cement content (Mbaraga et al. 2013).

Khalid (2000) used both the beam fatigue test and the Indirect Diametrical Tension (IDT) test to compare five different materials. For this study, the author defined failure when the stiffness properties of the specimens were reduced to a small percentage of their initial values. Based on this definition, the author concluded that performing the bending test at 20 degrees Celsius and 5 Hz is equivalent to performing the diametrical test at 12 degrees Celsius and 0.67 Hz for all permutations of the experiment. The results of the study are shown in Figures 2.10 and 2.11 where the tensile strain for each cycle decreased as the number of cycles increase for all materials.

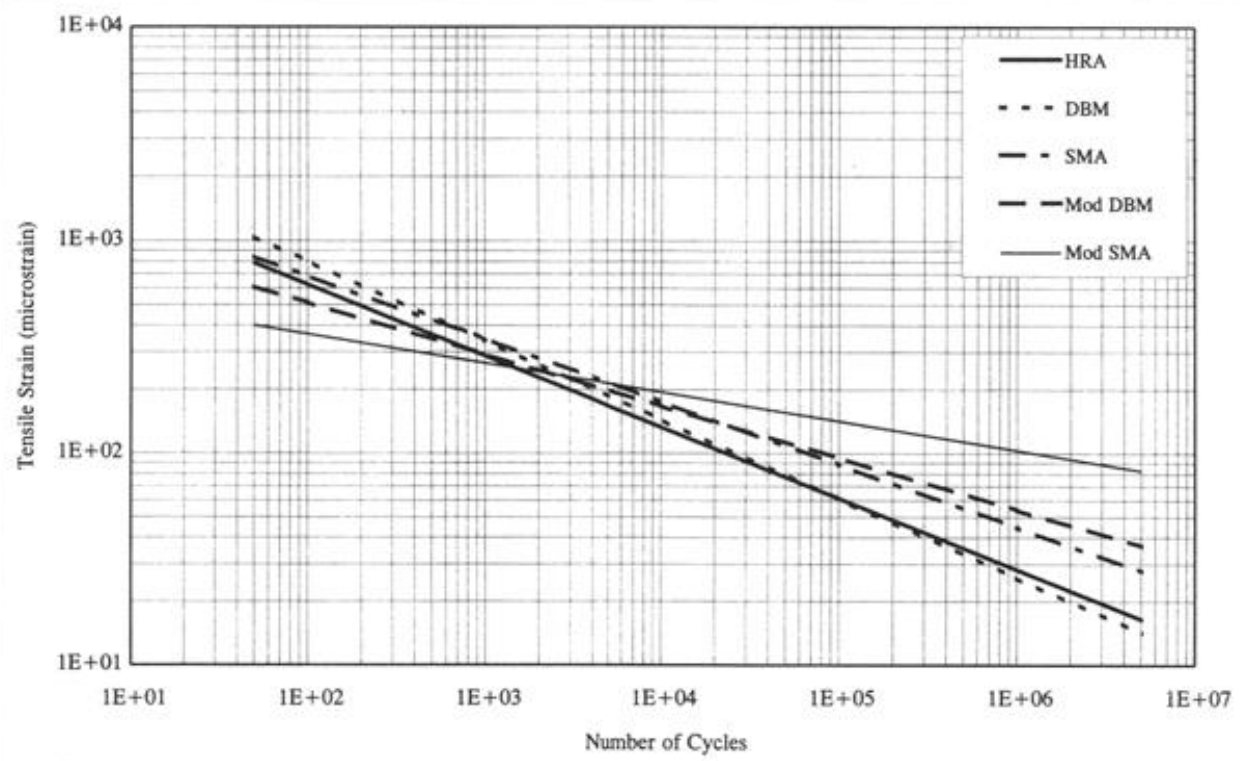

Figure 2.10: Fatigue relationship for five mixtures from indirect tensile fatigue (Khalid 2000).

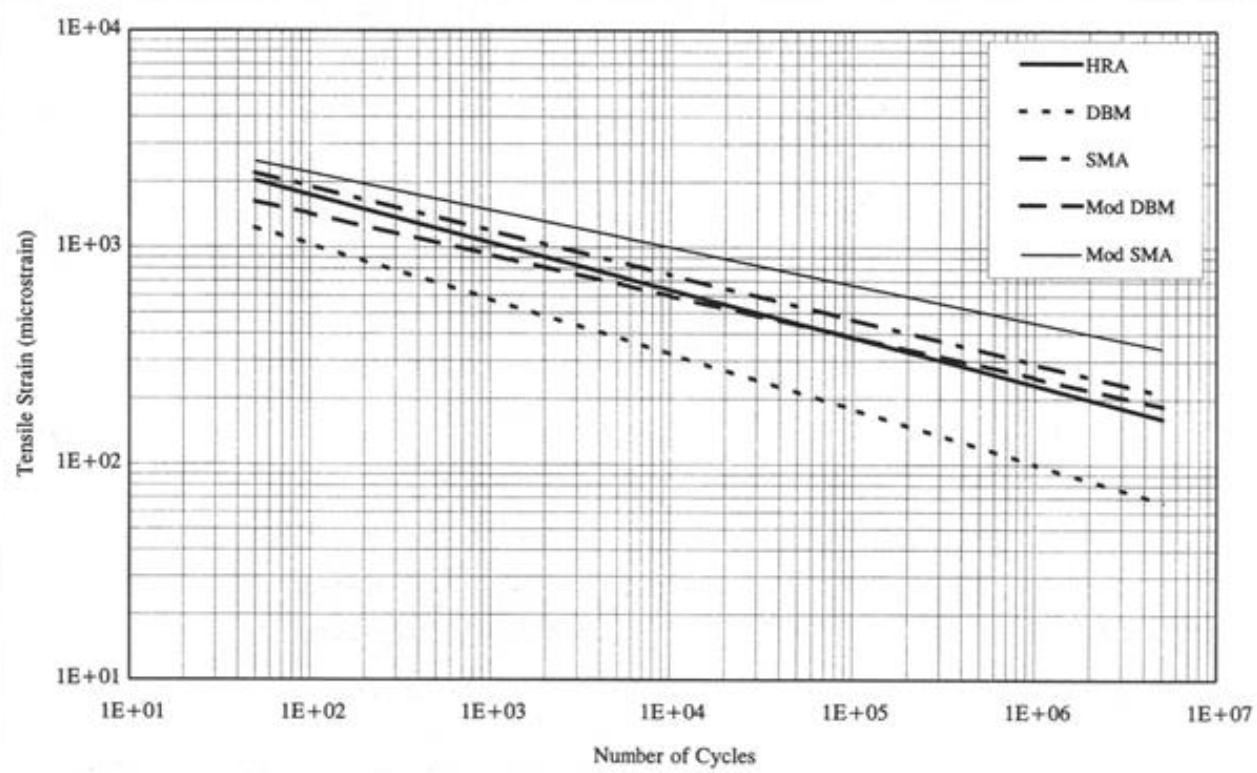

Figure 2.11: Fatigue relationship for five mixtures from indirect tensile fatigue (Khalid 2000).

Based on the data collected from this study, the author developed a pavement model in order to illustrate the important role of fatigue relationships and to confirm the data results originated in the beam fatigue test and diametrical fatigue test. Table 2.4 explains the results obtained from this model where the author concluded that the diametrical test was an appropriate quality control test in terms of mix design and repeatability of proper results. However, the equivalence ratios between the bending beam and diametrical test are significantly low; therefore, the author mentioned that the diametrical test is not appropriate for pavement design.

Table 2.4: Fatigue lives form flexural and diametrical fatigue tests and their equivalence ratios (Khalid 2000).

Mix Type	Maximum Tensile Strain (με)	Flexural Fatigue Life	Diametrical Fatigue Life	Equivalence Ratio (%)
HRA	210	1.57E-06	2553	0.2
DBM	212	5.38E-04	3538	7
SMA	203	6.21E-06	6055	0.1
Mod DBM	210	2.56E-06	3884	0.2
Mod SMA	204	9.87E-06	6952	0.04

Gnanedran and Piratheepan (2008) developed a study where the Indirect Diametrical Test (IDT) method was used as a substitute to the bending beam test for characterization of stiffness properties of stabilized materials. The authors decided to use slag-lime as stabilizer material because it did not develop shrinkage and cracking potential in the specimens. Figure 2.12 illustrates the preparation of the IDT using two LVDTs attached to Perspex strips that measure horizontal deformations.

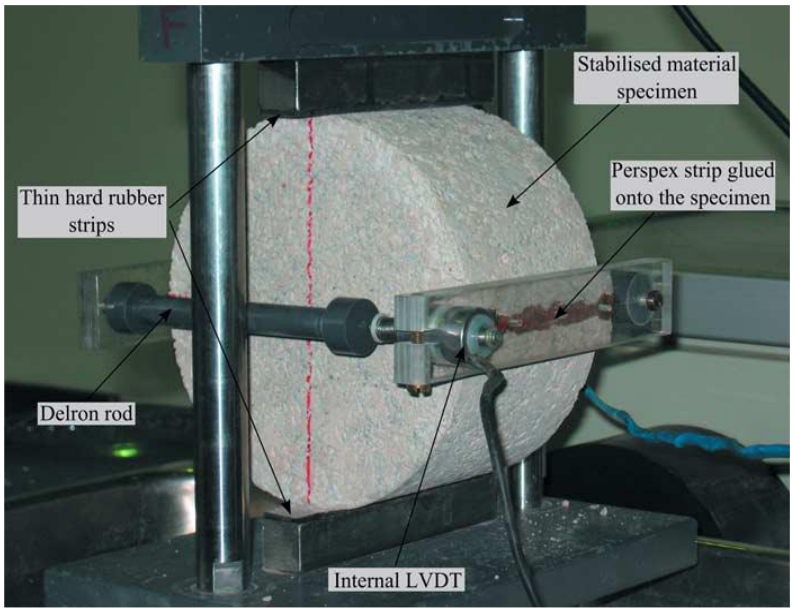

Figure 2.12: Modifications for Horizontal Deformation Measurement (Gnanendran and Piratheepan, 2008).

The goal of this test was to determine the static stiffness modulus (SSM) and the dynamic stiffness modulus (DSM). The SSM was calculated from monotonic loading conditions with a vertical induced deformation of 1 mm/min. The DSM was determined from repeated cyclic loading condition with a 3 Hz frequency sinusoidal loading criteria. The authors defined fatigue failure by two conditions, stiffness reduction by 50 percent of its initial value and by the energy ratio method. The authors found that SSM and DSM were not affected by the moisture content however, both were affected by the binder content as Figures 2.13 and 2.14 demonstrate. Finally, the authors mentioned that this IDT was appropriate for properly characterizing stabilized materials in terms of strength, stiffness modulus and fatigue performance properties. Consequently, empirical relations were developed to correlate the fatigue life of stabilized materials based on monotonic IDT procedure.

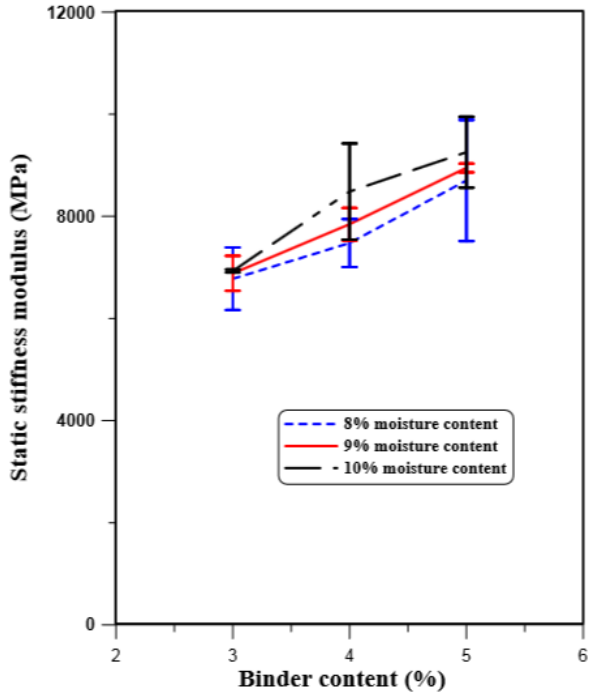

Figure 2.13: Variation of static stiffness modulus versus content (Gnanendran and Piratheepan 2008).

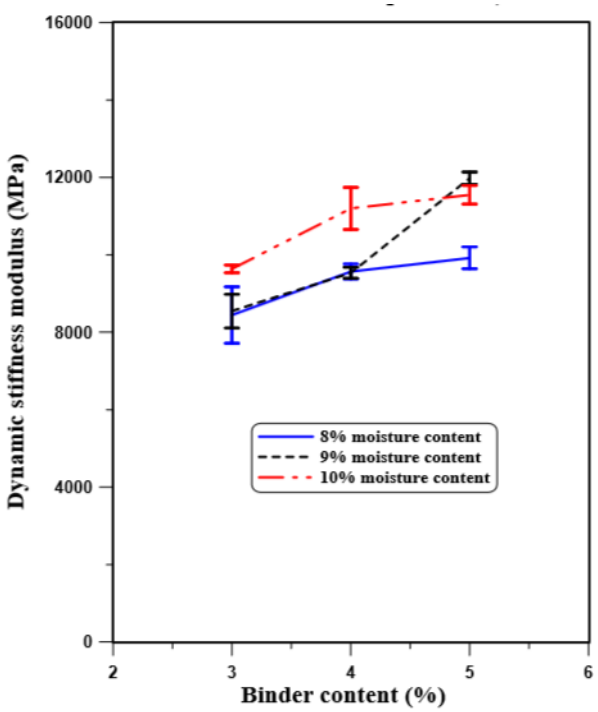

Figure 2.14: Variation of dynamic stiffness modulus versus content (Gnanendran and Piratheepan 2008).

Piratheepan et al (2010) used the UCS test and indirect tensile testing to characterize slightly stabilized materials with internal displacement measurements. The author developed a linear correlation between the elastic moduli from the UCS and monotonic IDT strength results. Figure 2.15 illustrates the correlation developed where the IDT strength is 0.1119 times the UCS value. Based on the correlation developed in this study, the author suggested using the UCS test to estimate the IDT strength, SSM and DSM of stabilized materials since the UCS test is a relatively effortless test.

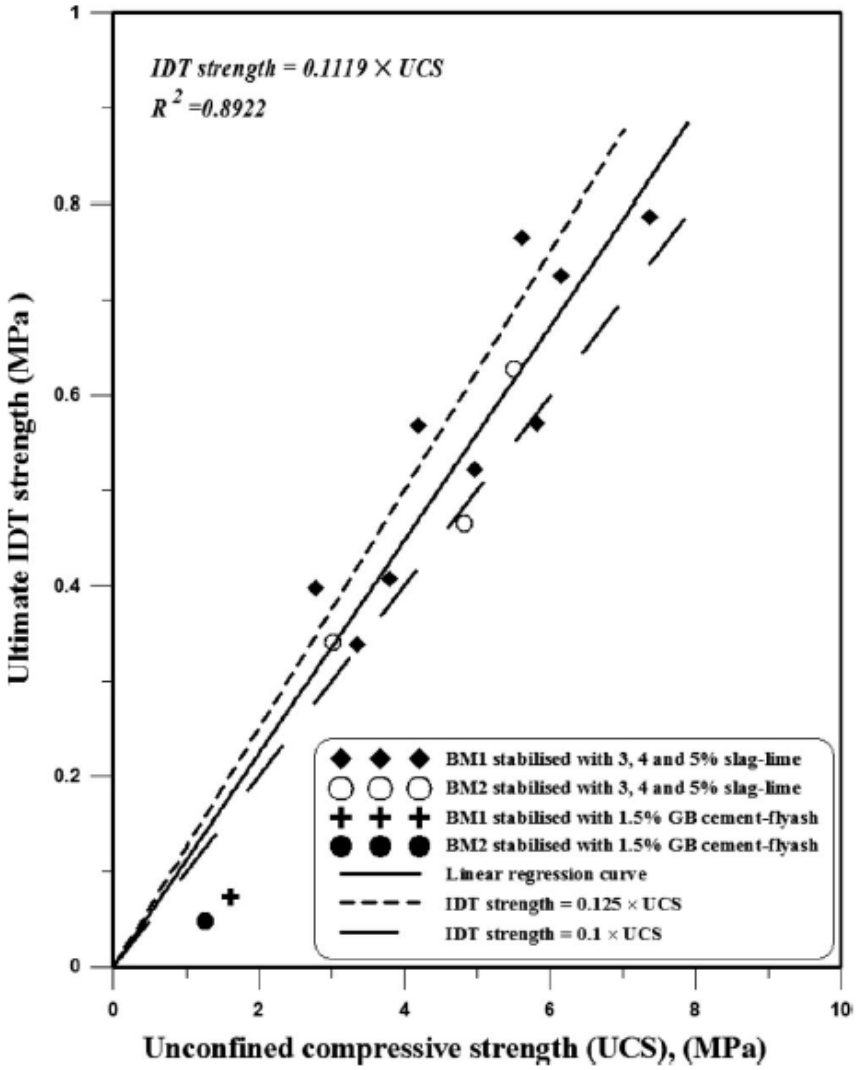

Figure 2.15: Variation of ultimate IDT strength versus UCS (Piratheepan et al. 2010).

Midgley and Yeo (2008) used the indirect tensile test as an alternative approach to characterize the fatigue properties of cement treated materials. The authors found a the gyratory compactor was appropriate for the preparation of laboratory indirect tensile specimens. Additionally, the authors found that this test was appropriated for testing materials of lower strength and stabilizer content (less than 5,000 MPa).

Scullion et al. (2012) suggested using smaller specimen test setup, which would take less time such as the Texas Gyratory Compactor and the IDT test. Using three road materials from Texas, the strength results of the UCS test and IDT test were compared in Figure 2.16. The authors found a better correlation between the UCS on 6 x 8 inch (152 x 203 mm) specimens compared to IDT results of 2 x 4 inch specimens. The use of UCS test was a suitable alternative since it can be completed in 7 days to obtain good results.

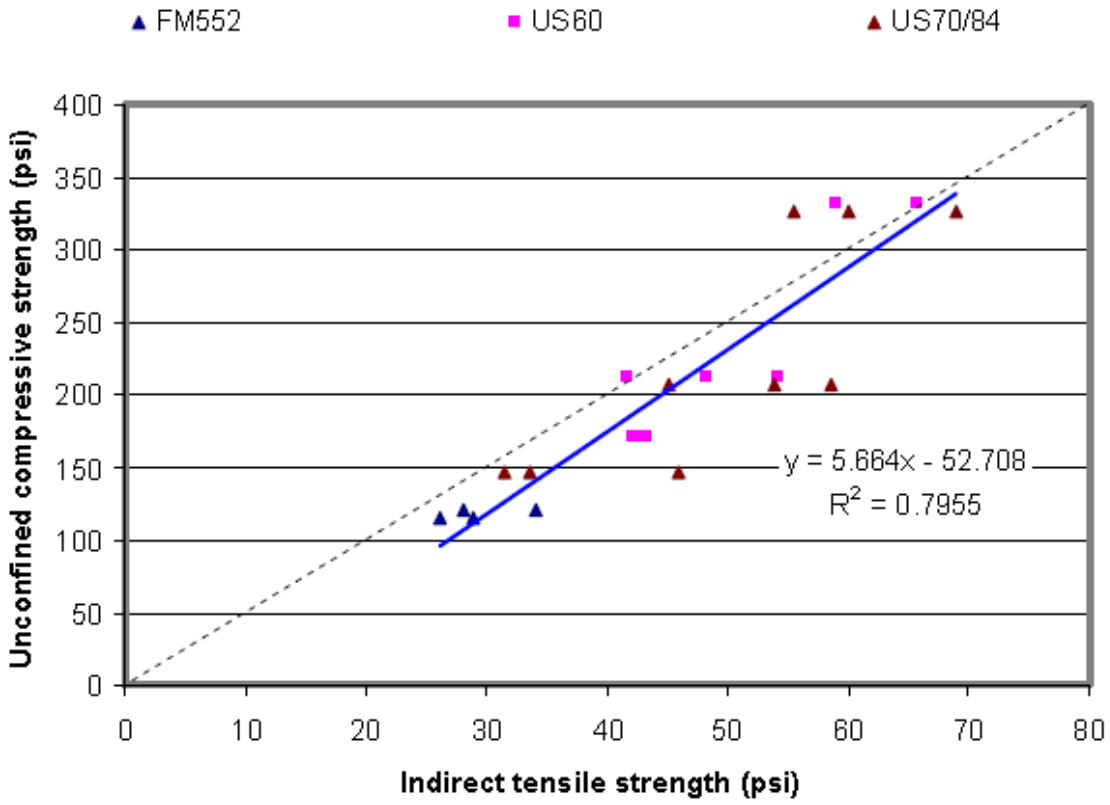

Figure 2.16: Relationship between UCS and IDT (Scullion et al. 2012).

Burns and Tillman (2006) studied the variation of the UCS value of cement treated materials with respect to fine content, cement content, mineralogy and freeze-thaw cycles. This study was conducted for the Virginia Department of Transportation. The aggregates selected in this study were mica, limestone, diabase and granite; which were tested at 3%, 4% 5% and 6%, cement content. The authors found that the aggregate mineralogy of the specimens significantly influenced the strength of the materials. Additionally, the strength of the materials increased as the cement content was incremented in the specimens.

Paul and Gnanendran (2012) developed a laboratory investigation to characterize lightly stabilized material using the UCS testing procedure. The materials selected were well-graded sandy gravels with a portion of fines based on USCS. The stabilizer materials consisted of slag lime and general-purpose cement with fly ash. The objective of this study was the determination of the stiffness modulus using axial deformation measurements to obtain stress-strain relationships. Figure 2.17 shows the schematic representation of the test set up.

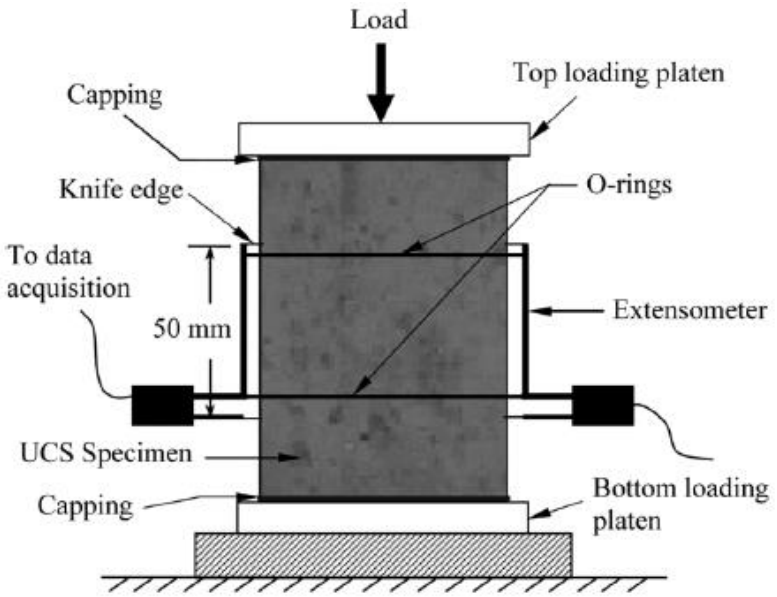

Figure 2.17: Schematic Diagram of the Axial Deformation Measurement Setup (Paul and Gnanendran 2012).

The authors used a five-parameter stress-strain equation to develop a mathematical model using the Ramberg-Osgood expression modified by Hill and Rasmussen presented in equation 2.2. The authors found that UCS has a linear increase with the stabilizer content for the specimens tested. Finally, they noted that the findings of this study were only applicable to the undamaged condition and that a wider range of materials and binders must be incorporated to validate the model developed.

$$\bar{\varepsilon} = \frac{\bar{\sigma}}{E_{0.2}} + \bar{\varepsilon}_{up}\left(\frac{\bar{\sigma}}{\bar{\sigma}_u}\right)^m \quad for\ \sigma > \sigma_{0.2} \tag{2.2}$$

where σ and ε are the transformed stress and strain.

White (2016) studied the influence of the degree of saturation on the UCS values for cement treated materials. The UCS values of unsaturated and saturated specimens increased with increasing cement content as Figure 2.18 illustrates. The average saturated UCS of the unbound materials varied between 0 and 60 psi. The average saturated UCS of stabilized materials varied between 44 and 287 psi at 4% cement content, 108 and 528 psi at t 8% cement content, and 162 and 709 psi at 12% cement content. The UCS of the saturated specimens was on average 1.5 times lower than of the unsaturated specimens.

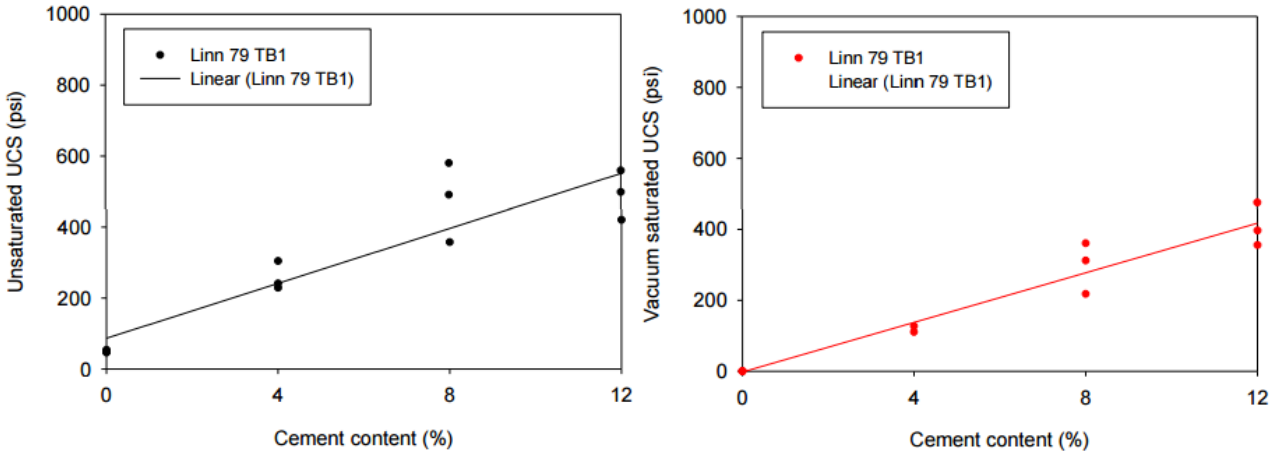

Figure 2.18: Unsaturated and Vacuum Saturated UCS vs. Cement Content (White 2016).

LABORATORY TESTING PROCEDURES FOR FATIGUE CHARACTERIZATION

These section supplies a detailed description of the laboratory testing procedures suggested for fatigue characterization of cement-stabilized materials. Based on the extensive literature search, the identified laboratory approaches in the current state of practice for characterization of cement-stabilized materials are resilient modulus, modulus of rupture, flexural beam fatigue test, FFRC test, IDT test, and UCS test

Resilient Modulus Test

The resilient modulus test varies according to the specimen size, compaction method, loading time, stress sequence, confinement pressure and the location of sensors. Gupta et al. (2007) indicate that the resilient moduli obtained with internal displacement measurements can be up to three times greater than when the displacement measurements are made outside of the confining cell. The specimens are subjected to cyclic loading to measure stress-strain relationships. The loading and unloading periods simulate the moving wheel load passing over the pavement. Figure 2.19 illustrates the schematic representation of the resilient modulus test. The relationship used to estimate the resilient modulus is as given in Equation 2.3.

$$Mr = k_1 P_a \left(\frac{\theta}{P_a}\right)^{k_2} \left(\frac{\tau_{oct}}{P_a} + 1\right)^{k_3} \quad (2.3)$$

Where:

Mr = Resilient Modulus

P_a = Atmospheric Pressure

θ = Bulk Stress

τ_{oct} = Octahedral Shear Stress

k_i= Fitting Parameters

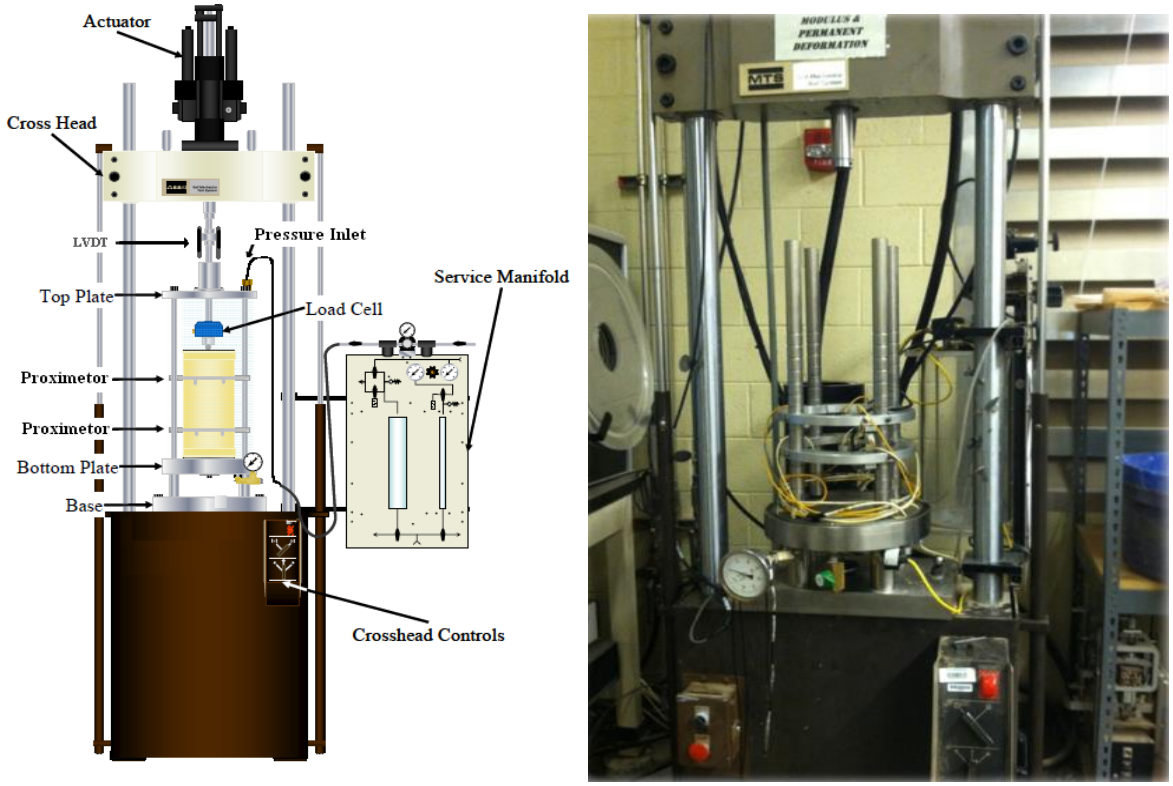

Figure 2.19**:** Resilient Modulus (M_r) Test set up.

Four Point Bending Beam Test

The modulus of rupture namely the flexural strength of a stabilized material is determined using the four-point bending beam test. This employs four-point loading bearing blocks to ensure that loads applied to the beam will be vertical to the face of the specimen. The load is applied using two bearing blocks to make sure the shear forces acting in the failure region are zero as Figure 2.20 shows. In general, the specimen beam size varies according to the agency specifications but usually it is 6 x 6 x 20 inch. The load protocol is a monotonic loading condition at a specified strain-controlled rate until the specimen develops failure. The equations used to determine the modulus of rupture values were presented in chapter 1.

Figure 2.20: Four-Point Bending Beam Test Set Up.

Free-Free Resonant Column (FFRC) Test

The free-free resonant column (FFRC) (Nazarian et al., 2003) method estimates the linear-elastic (low-strain) seismic modulus based on the determination of the fundamental resonant frequency of vibration of a specimen. The main components of the test setup are shown in Figure 2.21. An accelerometer is securely placed on top of the specimen, and the specimen is impacted with a hammer instrumented with a load cell. As an impulse load is applied to the specimen, seismic energy over a wide range of frequencies propagates within the specimen. Equation 2.4 is used to determine the seismic modulus, E_{FFRC},

$$E_{FFRC} = \rho(2f_L L)^2 \quad (2.4)$$

Where:

E_{FFRC} = Seismic Modulus

ρ = Specimen Density

f_L = Resonant Frequency

L = Specimen Length

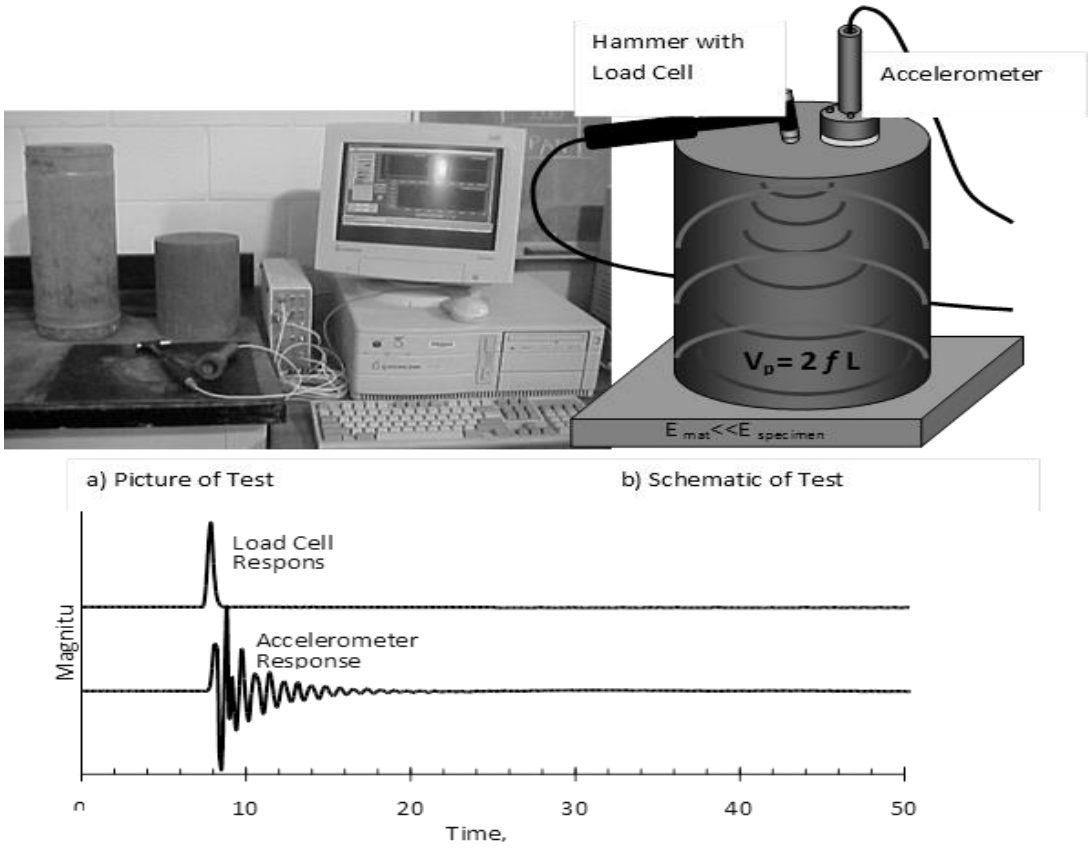

Figure 2.21: Free-Free Resonant Column (FFRC) Test Setup.

Indirect Diametrical Tensile (IDT) Test

In general, the indirect tensile test set up is similar to the traditionally used set up for asphalt mixtures as shown in Figure 2.22. However, appropriate loading rates, specimen geometry, and deformation measurements need to be modified accordingly to measure the stress-strain response of the stabilized granular materials. The monotonic or static tensile test aims at measuring the tensile strength at constant displacement. Assuming plane stress conditions, the split tensile strength can be calculated using the relation given in Equation 2.5. For the repeated load indirect tensile test, percentages of the maximum load under the monotonic conditions are applied. The stress or strain ratio and the number of cycles can be used to determine the fatigue parameters for a particular type of mix.

$$\sigma_t = \frac{2p}{\pi dt} \quad (2.5)$$

Where:

σ_t = Tensile Strength

p = Load at Failure

d = Specimen Diameter

t = Specimen Thickness

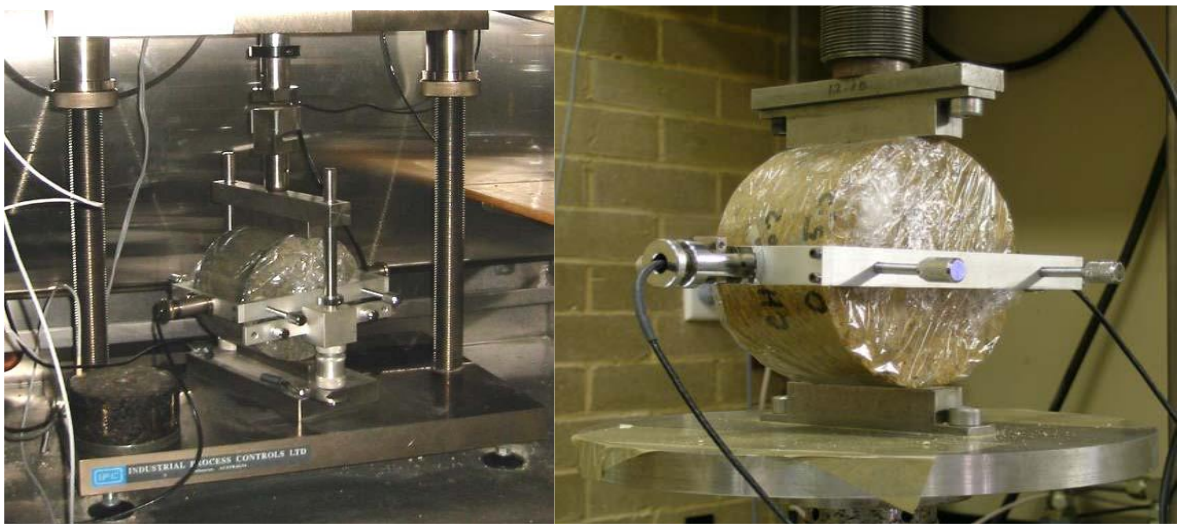

Figure 2.22: Indirect Tensile Setup for Strength and Fatigue Testing (Midgley and Yeo 2008).

Unconfined Compressive Strength (UCS) Test

This procedure is a destructive test where the vertical compressive stress is the major principal stress and the other two principal stresses are zero, in other words there is not any confinement pressure around the specimen. The application of a compressive stress is only along the longitudinal axis. The cylindrical specimens are loaded by a strain-controlled rate until failure takes place. The parameter measured is the maximum axial compressive stress that a material can tolerate. Figure 2.23 shows the specimen failure after the application of the axial loading. Moreover, the test assumes that there is no loss of moisture during the test, which is performed quickly therefore, no rubber membrane is necessary to cover the specimen. The UCS

is defined as the ratio of failure load to the cross sectional area of the sample as given in Equation 2.6.

$$q_u = \frac{P}{A_c} \tag{2.6}$$

Where:

q_u= Unconfined Compressive Strength

P = Load at Failure

A_c = Corrected Area at Failure

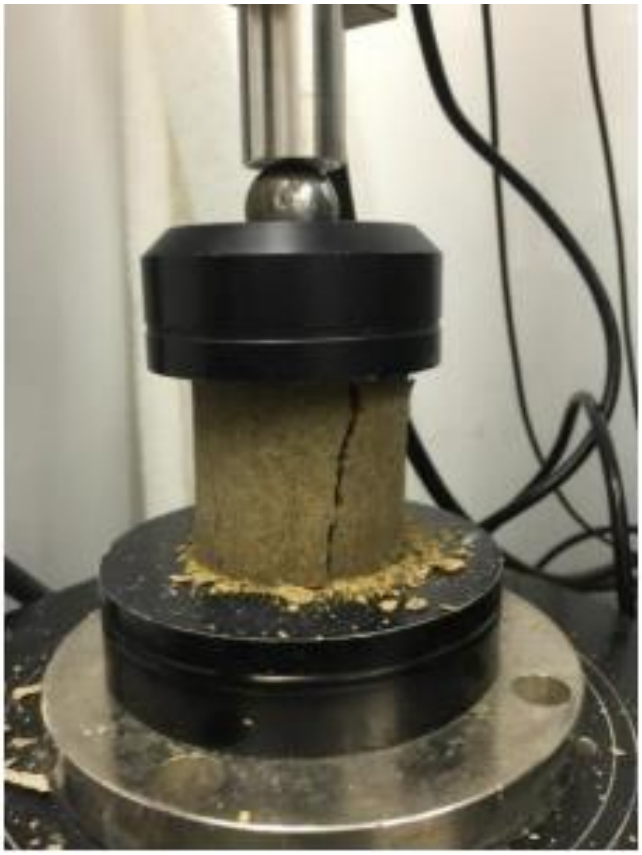

Figure 2.23: Specimen failure after UCS Test (White 2016).

Table 2.5 provides a summary of the mentioned laboratory testing protocols. According to the authors of previous investigations, each of the testing protocols developed include their own advantages and limitations.

Table 2.5: Summary of test methods for characterization of stabilized materials.

Test	Purpose	Sample Size	Loading Pattern	Failure Criteria	Advantages	Limitations
UCS	Strength	6 x 8 in.	Biaxial	Until failure	Ease of use, availability of equipment	Tensile and compressive parameters varies
IDT	Strength	*4 x 6 in.	Axial	Until failure	Ease of use, availability of equipment	Few Correlations of IDT strength
M_{rup}	Strength	6 x 6 x 20 in	Four Point	Until Failure	Simulates loading field conditions	Failure of specimens due to self-weight
Mr	Modulus	6 x 8 in.	Axial	Stress sequence	Provides stiffness information of a material under traffic loading condition	Time consuming, measurement errors and unavailability of equipment
FFRC	Modulus	No restrictions	Impact	NA	Easy to use, test results can be related to those from field modulus tests	Unavailability of equipment
IDT Fatigue	Modulus and Fatigue properties	*4 x 6 in.	Biaxial	50 - 60 % reduction in modulus	Provides stiffness information of a material under traffic loading condition	Large measurement variation, time consuming
Flexural Beam Fatigue		*6 x 6 x 20 in.	Four point		Relatively large measurement variation	Time consuming, failure of specimens due to self-weight and unavailability of equipment

*****Specimen dimension vary with agency; UCS: Unconfined Compressive Strength; IDT: Indirect Tensile; M_{rup}: Modulus of Rupture; M_r: Resilient Modulus; FFRC: Free Free Resonant Column

The majority of the studies suggest the integration of the bending beam test in the characterization protocol. This test is suitable to provide valuable results in terms of the tensile characteristics of cement treated materials. However, there are several practical and theoretical discrepancies associated with the implementation of the bending beam test to the stabilized materials. These concerns are more crucial and sensible at low amounts of stabilizer in the materials systems. Based on technical discrepancies, the specimens have a tendency to develop

considerable damage during sample preparation and transportation to the execution of the test. Additionally, the theoretical assumption of linear stress-distributions is a source of uncertainly in the results that may not appropriate for charactering the fatigue performance of stabilized materials. Additionally, the UCS test has been implemented by many researchers in order to predict the fatigue performance based on compressive parameters even if the compressive and tensile characteristic are dissimilar each other. Conversely, the Indirect Diametrical Tensile test, also known as the split tension test, is an excellent candidate to replace ordinary methods in the laboratory. Such a test does not present technical concerns and the specimen dimensions are considerably reduced compared to the beam dimensions of the four-point bending beam test. Therefore, an experiment matrix containing both compressive and tensile testing procedures is necessary to distinguish the differences of stabilized materials subjected to compressive and tensile loading conditions.

Chapter 3: Methodology and Testing

INTRODUCTION

The use of cement treated base layers is a common technique implemented by several US departments of transportation. However, the material mineralogy and environmental conditions vary from state to state. Therefore, the alternative testing protocol proposed by this study should have the potential to be adapted for stabilized materials with different cement content and several mineralogy types that are subjected to moisture content variations.

This chapter provides the material selection criterion, specimen curing conditioning, testing procedures and specimen preparation in order to develop an experiment matrix whose data can validate the developed testing protocol for the use of fatigue characterization of stabilized materials.

MATERIAL CRITERIA

The determination of the material diversity for this study was derived from a survey presented in Appendix A. This survey was created with the intention of clarifying the parameters used in base layers including aggregate mineralogy, cement content and gradation. The survey was sent to eighteen Texas Department of Transportation (TxDOT) districts with twenty responses received where two districts submitted multiple responses. In such cases, the responses were clarified through contacting the districts for supplementary information. This section will provide the survey results and the criteria for the determination of material selection for the study.

Significance of Soil Stabilization

The results presented in Figure 3.1 indicate that all the eighteen Districts have used soil stabilization on previous projects related to pavement. The results demonstrated that eleven Districts responded they “often” and seven responded they “sometimes” used soil stabilization, however is it important to note that no district responded that they never used soil stabilization. This demonstrates the significance of the use of this technique in the pavement design.

Figure 3.2 illustrates the number of projects that have been performed in the past year plus future projects that are schedule in each district. The San Antonio district has the highest amount of pavement projects regarding soil stabilization followed by Bryan, Paris and Fort Worth. Since there are a significant number of future projects concerning soil stabilization, it is very important to mention that a new approach is urgently needed to properly characterize the stabilized materials.

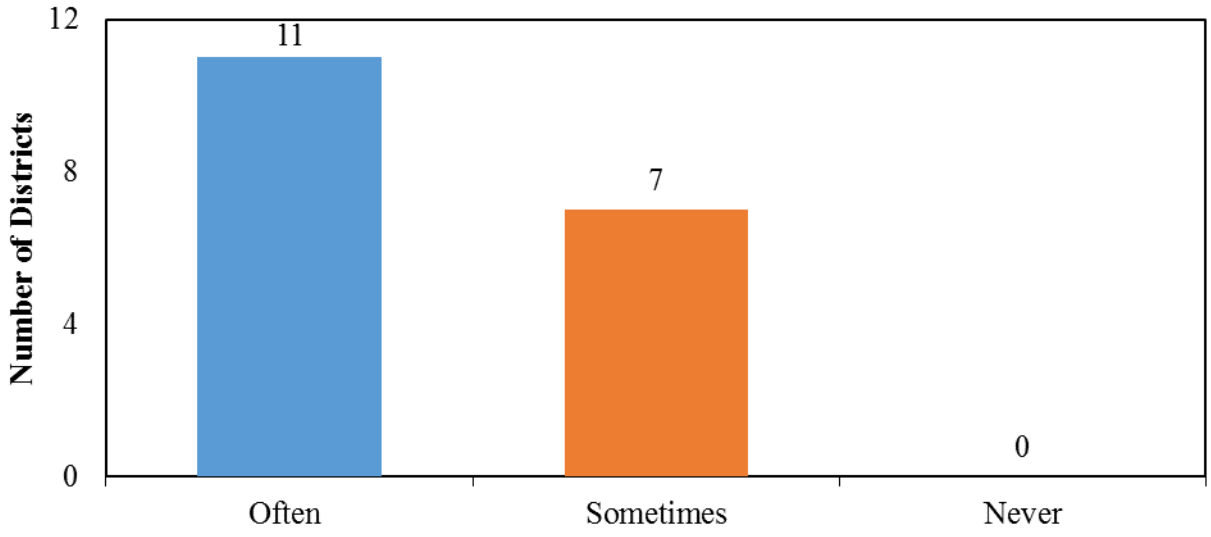

Figure 3.1: Use of Portland cement to Stabilize Base Layers in the District.

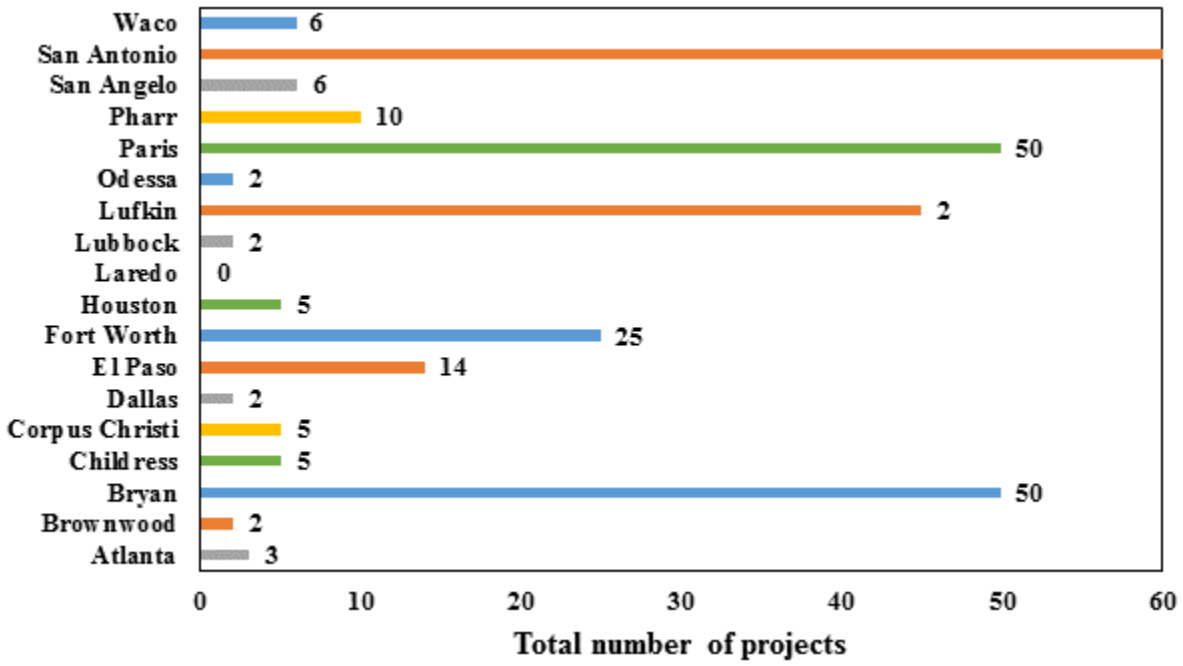

Figure 3.2: Estimated Number of projects that have been completed in the last 5 years or are scheduled in the near future.

Determination of Cement Content

Figure 3.3 indicates the range of gravimetric cement content used for base layers in soil stabilization. The cement content used for all districts ranges from two to five percent. The results show that 3 percent is the most common percentage, followed by 2 percent. In addition, 69 percent of the Districts are using low cement content such as 2 and 3 percent. However, the traditional four-point bending beam test has significant discrepancies with specimens treated with low percentages of cement in the mix. Therefore, this is another indication of the necessity of a practical testing protocol for stabilized specimens especially at low cement content. Figure 3.4 shows the cement content used for each District where clearly most of districts are using low stabilizer content and no district is using a cement content above five percent.

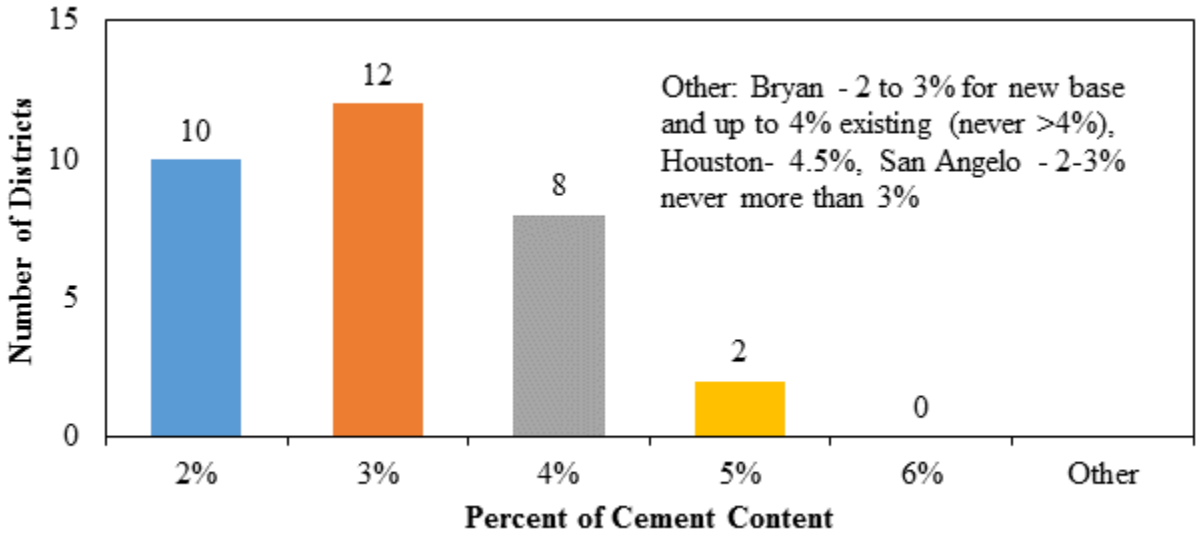

Figure 3.3: Percentage of Cement Content Typically used for Stabilization of Base Layers.

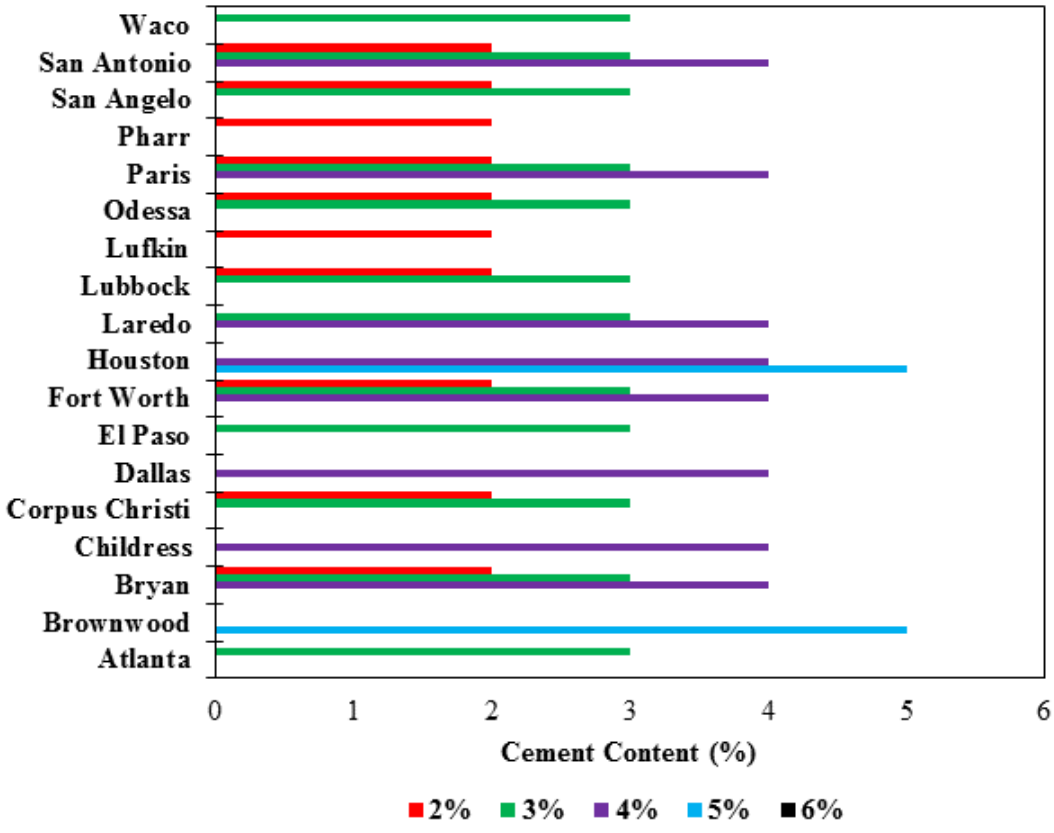

Figure 3.4: Percentage of Cement Content Typically used for Stabilization by District.

The criteria selected for the determination of the stabilizer amount added to the base layer is not the same for all districts. Figure 3.5 indicates that the selection is primarily based on laboratory testing followed by local experience from previously designed projects. It is important to note that 66 percent of the districts are not using a laboratory testing protocol to determine the most favorable cement content for a determined pavement project. Ten of the eighteen districts declared that they follow a "strength based" requirement indicated in Figure 3.6. Several districts, such as El Paso, San Antonio, and Waco, specify a strength requirement of 150 psi (1.03 MPa) on the Unconfined Compressive Strength (UCS) with 80 percent retained strength. Other districts such as Atlanta, Fort Worth, Lubbock, Odessa, and Paris have a requirement of 300-psi (2.07 MPa) strength on UCS as criteria. In addition, Bryan has 210-psi (1.44 MPa) strength requirement at 85% retained strength. Bryan District reported that they do not stabilize the base layer when the sulfate content is higher than 3000 ppm or the organic content is higher than 1 percent. This is important information that should be considered by those locations having problems with high sulfate and organic content in the soil.

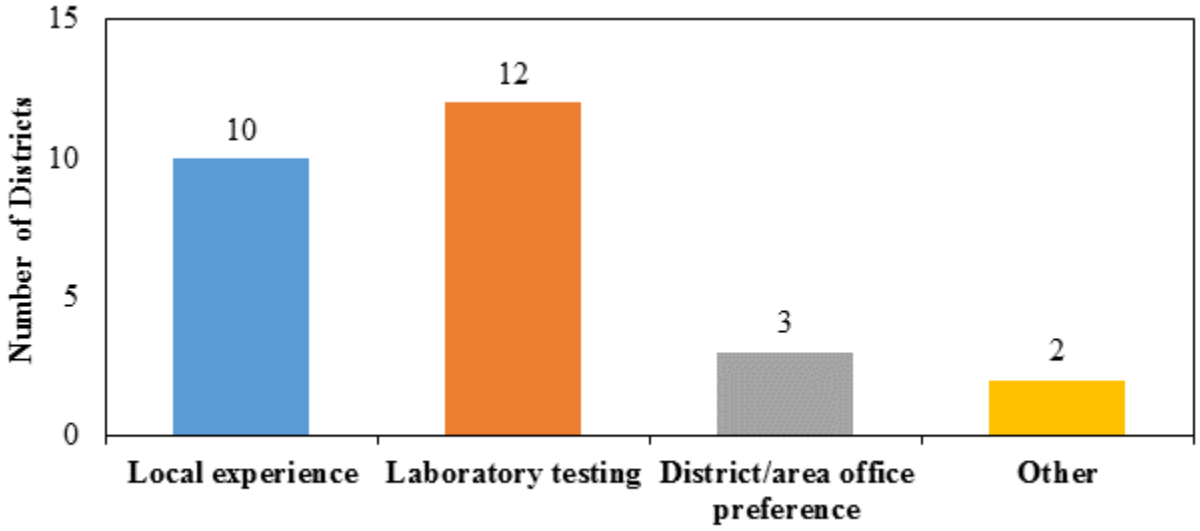

Figure 3.5: Basis of Selection of the Percentage of Cement Content.

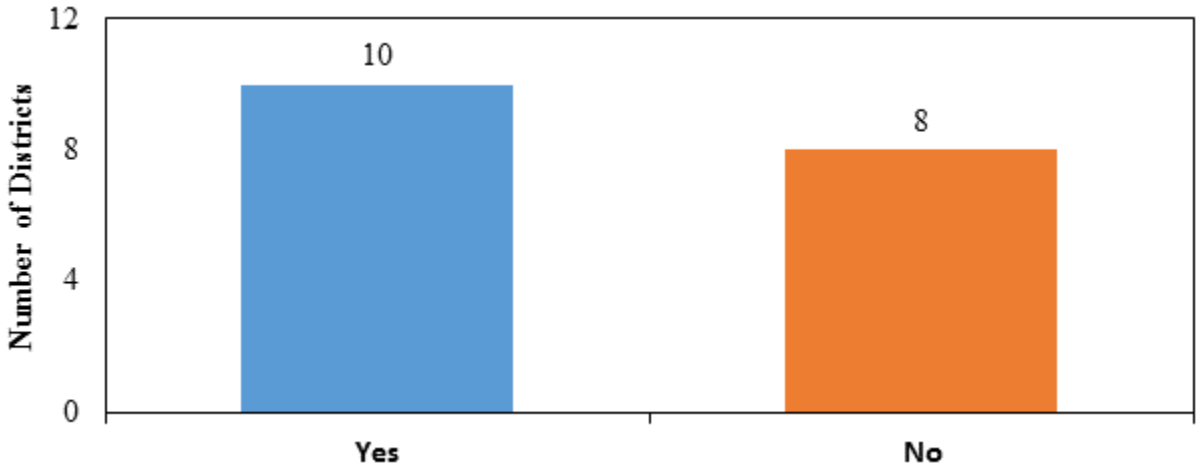

Figure 3.6: Strength Requirements for Cement Stabilized Base Used by Districts.

Determination of Aggregate Selection

Another important parameter required for this study was the type of aggregates and material sources selected for stabilization of base layers. Figure 3.7 demonstrates that most districts are using limestone and gravel as the predominant aggregate type in the base layers. Six of the examined districts reported that they utilize non-conventional aggregates such as sandstone, iron ore, recycled crushed concrete and caliche. The aggregate type used by the districts are listed in Table 3.1

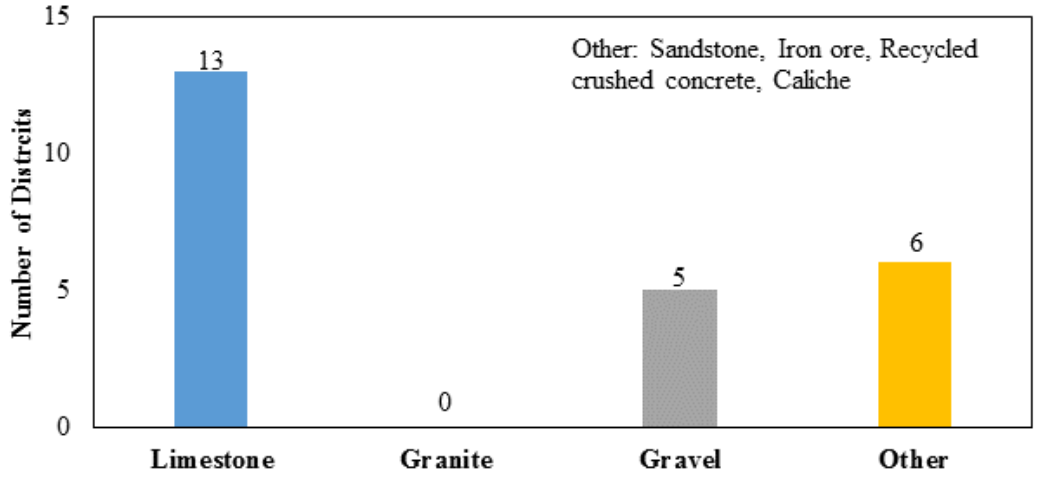

Figure 3.7: Most Common Aggregate Types used for Cement Stabilized Base Layers.

Table 3.1: List of Districts and Quarries Used.

District	Quarry
Atlanta	Sandstone & Iron Ore
Brownwood	Vulcan BWD & Eastland
Bryan	Usual Flexbase suppliers
Childress	Zack Burkett
Corpus Christi	Calica (Yucatan) Beckman
El Paso	McKelligon Canyon or Ned Finney
Fort Worth	Bridgeport
Houston	Zack Burkett
Lubbock	Local quarries
Odessa	Local Pits
Lufkin	Hanson Perch Hill
Paris	Martin Marietta & Smith Buste Sandstone
Pharr	Fordyce Showers
San Angelo	Job Specific US83 Real Co.
San Antonio	Lonestar, Vulcan, Martin Marietta, S&J, Colorado Materials, South Texas Chapman's
Waco	A number of sources

Determination of Gradation Parameters

Finally, particle size distribution is the last parameter needed in terms of material selection for the purpose of this study. Figure 3.8 indicates that the majority of the districts are using Grade 4 and Grade 2 in the stabilized base layers. Just two districts reported using Grade 1 and no district is using Grade 3 for stabilized base layers.

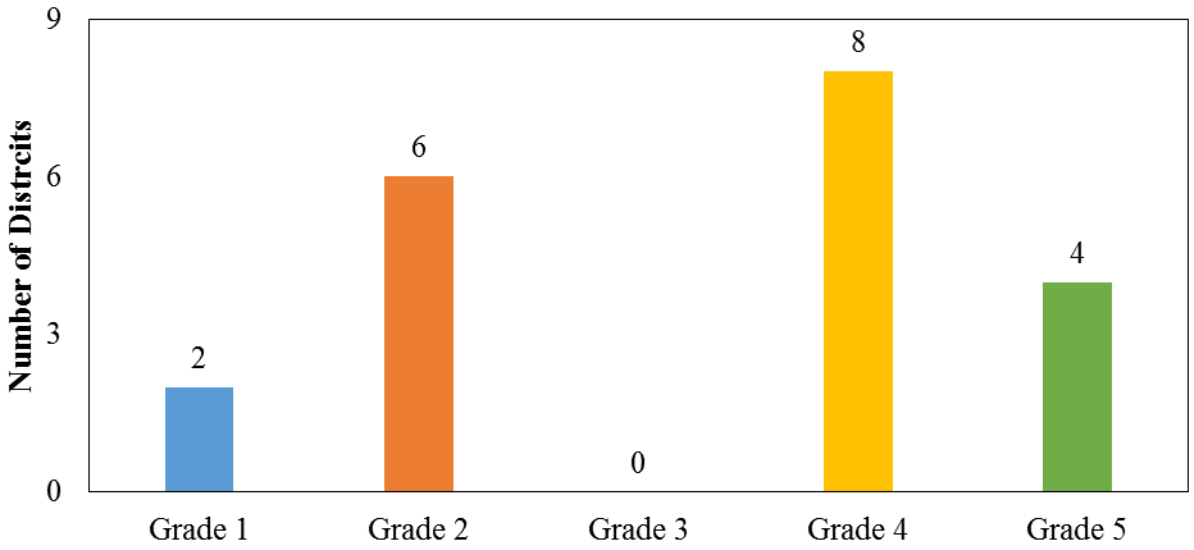

Figure 3.8: Grade Selected as per Item 275 that is Most Frequently used for Cement Stabilized Base Layers in Texas.

MATERIAL SELECTION

The criteria considered in the material selection for aggregate type and source was based on the mineralogy frequently used, number of stabilization projects and the geographical distribution. Given that the proposed testing protocol in this study should be inclusive of all mineralogy types across the US, more than one aggregate type should be selected to account for the influence of mineralogical properties of aggregate on the pozzolanic reactions during the cement stabilization process. For this reason, the aggregate types selected for this study are limestone, sandstone and gravel since most of districts reported the frequent use of these particular aggregate types in base layers. The aggregate source selection was based on the number of future projects where San Antonio is the district with the highest number of soil stabilization projects. Additionally, gravel sourced from Pharr and sandstone from the Paris districts were incorporated to the material selection of this study. Finally, the last criteria factor taken into consideration for the material selection was the geological distribution of selected aggregate sources. This decisive factor was considered to account for the variety of the

mineralogy properties and environmental conditions across the state of Texas. As a result, limestone materials sourced from the El Paso and San Antonio districts were selected in this study in order to prove that the engineering properties of El Paso and San Antonio materials can behave differently. The geographical distribution of the material sources is presented in Figure 3.9.

Figure 3.9: Geographical Distribution of Selected Aggregate Sources.

In conclusion, the survey results were considered in the selection process for a better recognition of the current state of the practice and realization of soil stabilization in the field. After the analysis of the responses, four materials were incorporated in this study. Additionally, one gradation such as Grade 4 based on item 247 according to TxDOT specification for flexible bases was integrated in this study given that it is the gradation most used by the districts. The testing protocol developed in this study should be applicable to specimens at low and high cement content consequently; all cement contents used by the districts were incorporated in this

study. Table 3.2 provides a summary of the material selection for the purpose and significance of this study.

Table 3.2: Determination of Materials and Cement Content.

Material Selected	Range of Cement Selected	Grade Selected
El Paso (Limestone)	2%-5%	Grade 4
San Antonio (Limestone)	2%-5%	Grade 4
Pharr (Gravel)	2%-5%	Grade 4
Paris (Sandstone)	2%-5%	Grade 4

SPECIMEN CURING CONDITIONING

The specimen conditioning has a significant importance in this study because the testing protocol implemented in this study should be applicable to specimens subjected to moisture variation. In many cases, the stabilized base layers of pavements are subjected to moisture intrusion. Consequently, it is important to incorporate a moisture susceptibility testinging to identify the influence of moisture ingress on the mechanical properties of the stabilized materials. Therefore, the specimens were subjected to two moisture conditions namely a 7-day moist cured and a 10-day capillary Soak-Tube Suction Test (TST). For the 7-day moist cured condition, the specimens will be introduced in a temperature-controlled chamber with at least 95 percent relative humidity for seven consecutive days. For TST specimens, according to the specification procedure Tex-144-E (draft) the specimens should be placed on porous stones in a tub of water at ambient temperature and then subjected to capillary moisture intrusion during ten consecutive days. Figure 3.10 illustrates the schematic representation of the TST specimen curing condition.

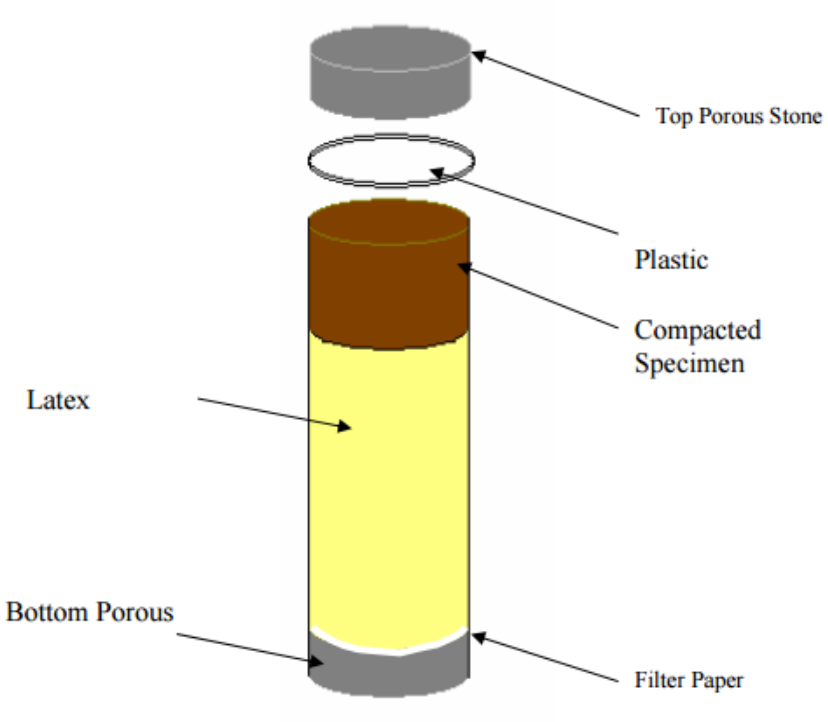

Figure 3.10: Specimen Assembly for Tube Suction Testing (Tex-144-E Draft).

The main motivation for the inclusion of the capillary soak curing condition in the experiment was to recognize the sensitivity of the aggregates to attract and move moisture inside the void structure. The data obtained from both specimen conditions will provide important information to identify the potential to degrade the stiffness properties of the stabilized materials and consequently compromise the durability of the pavement structure.

MATERIAL TESTING

The selection of the test procedures utilized in this study was founded on the current state of practice for characterization of stabilized materials presented in Chapter 2. The laboratory testing procedures incorporated were included to identify a practical alternative testing protocol to characterize the fatigue performance of stabilized materials. According to the purpose of this study, performing the four-point bending beam test is extremely difficult especially for lightly

stabilized materials and the results tend to be inaccurate and non-repeatable therefore this test was discarded. This following section provides a detailed description of the testing protocols utilized in this study in order to characterize the fatigue performance of cement treated materials.

Unconfined Compressive Strength (UCS) Test

Many researchers have suggested the use of UCS test to characterize the fatigue performance of stabilized materials. However, the compressive and tensile characteristics of stabilized materials can be significantly different from each other. Therefore, the UCS test has been incorporated into the experiment design primarily to recognize the unconfined compressive strength, compressive strain-stress relationships, degree of non-linearity, and a ultimately different measure of modulus This destructive test was imposed at a rate of 1 mm/min until specimens of 6 x 12 inch (152 x 305 mm) developed failure. The results were analyzed to identify the contribution of the cement content. The information obtained was incorporated in the database for supplementary post processing and trend analysis of the data. Figure 3.11 illustrates the protocol developed for the execution of the UCS test in the study.

Submaximal Modulus Test

The submaximal modulus test was incorporated into the experiment design to examine the resilient behavior and the permanent deformation of the materials under compressive cyclic loads at different cement contents. The specimens were subjected to 5,000 load repetitions at three levels 20, 40 and 60 percent of the UCS values. The cycle durations consisted of 0.1 sec of loading condition and 0.9 sec of rest period with a total of 1 sec per cycle. Vertical deformations were recorded using four proximeters attached to the specimens as Figure 3.12 demonstrates. Figure 3.13 shows the protocol for the implementation of the submaximal modulus test in the study.

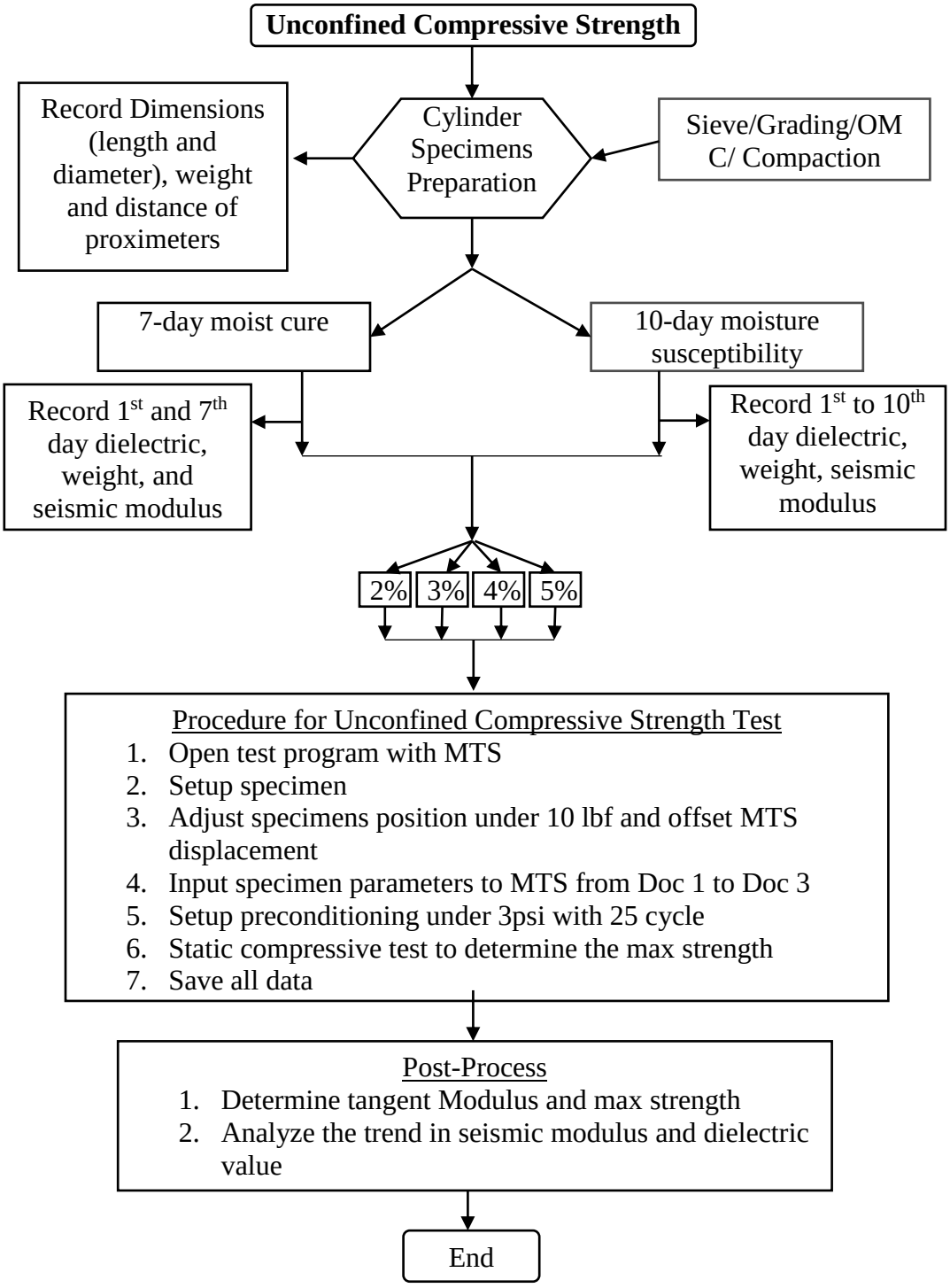

Figure 3.11: Unconfined Compressive Strength Test Procedure.

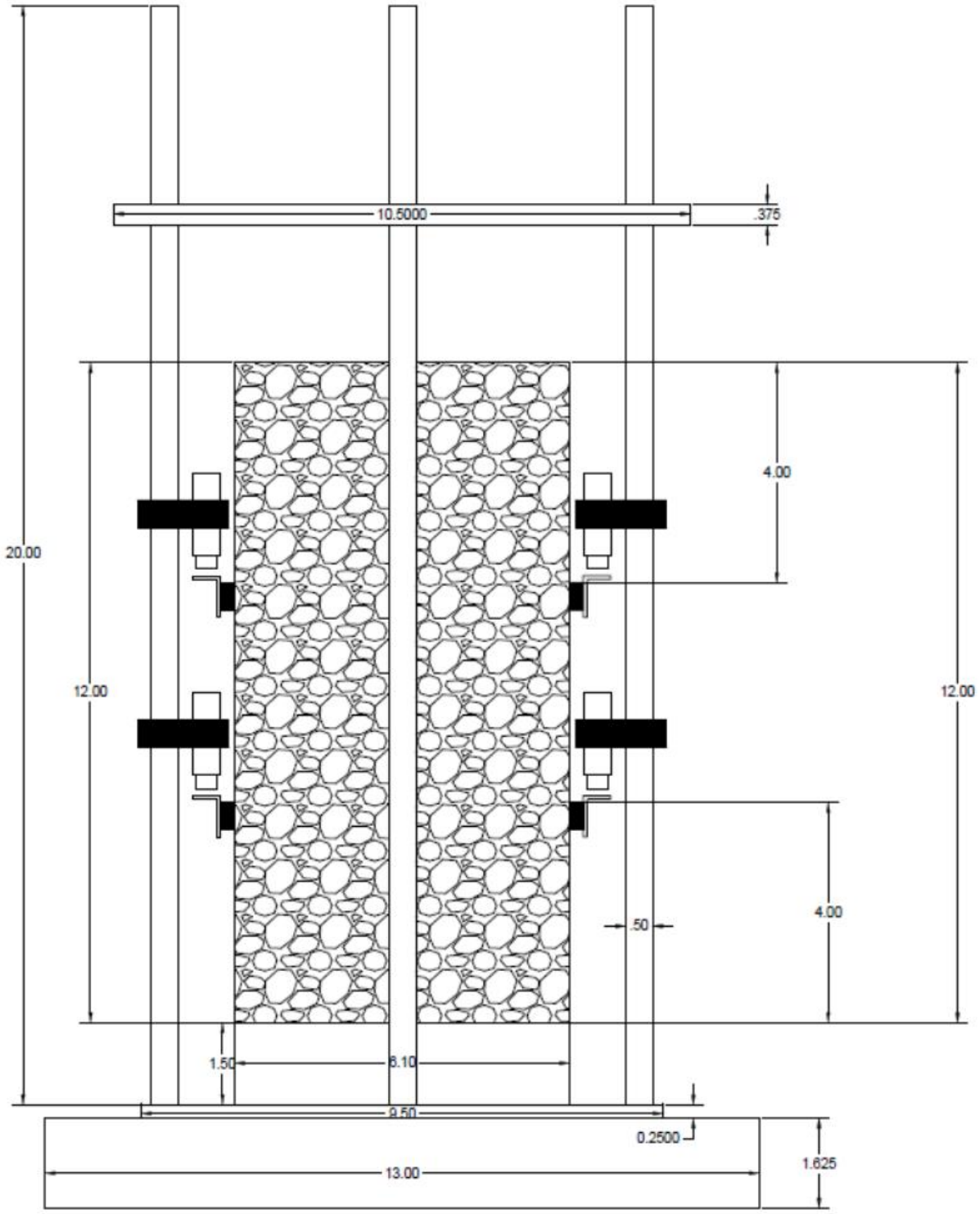

Figure 3.12: Submaximal Dimensions.

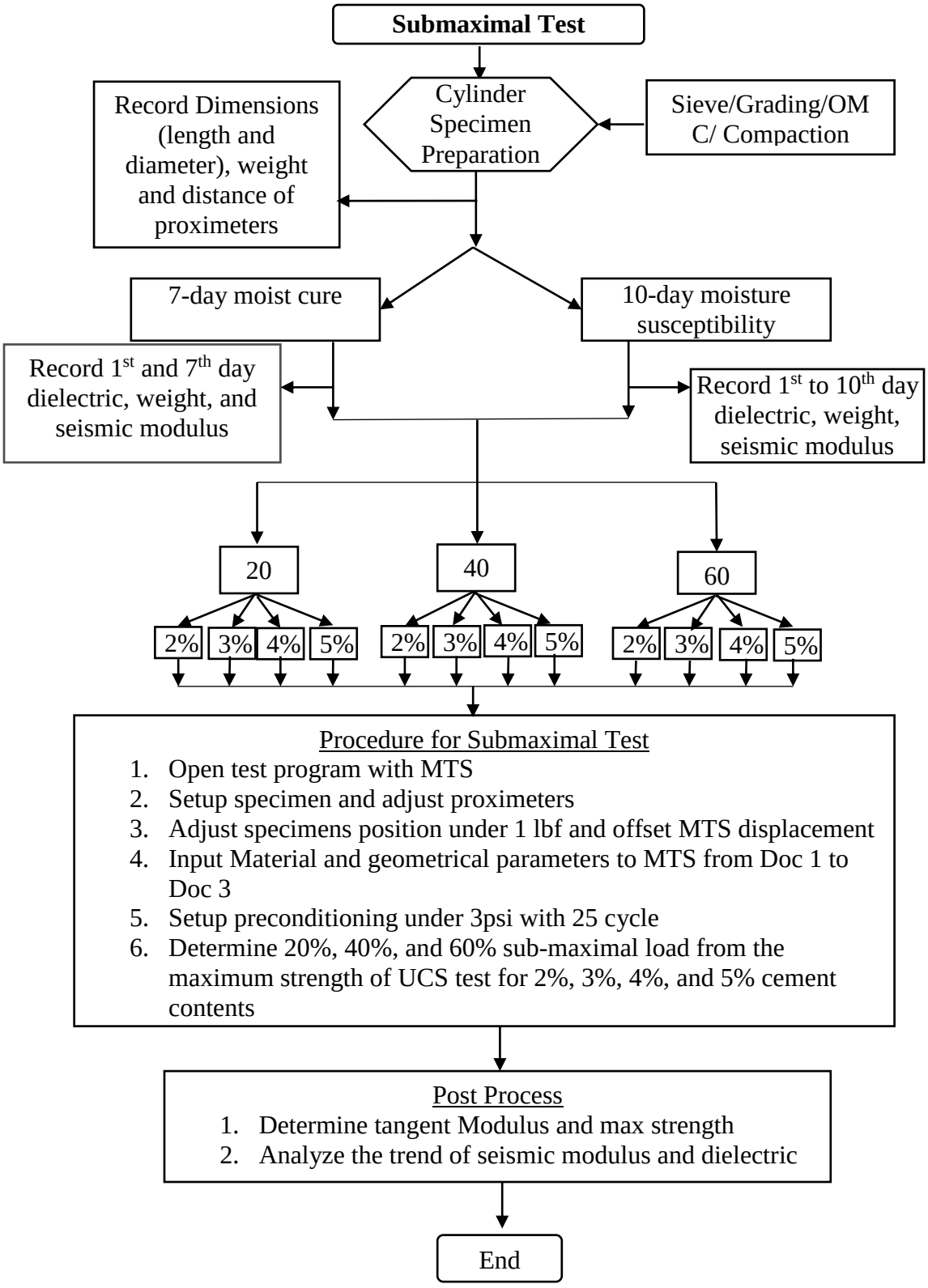

Figure 3.13: Submaximal Modulus Test Procedure.

Static Indirect Diametrical Tensile (S-IDT) Test

Originally developed for concrete and asphalt testing, the static Indirect Diametrical Tensile (IDT) test is an excellent candidate for identifying the tensile properties of stabilized materials. This test provides a measure of the tensile strength of specimens subjected to different cement contents. This indirect test was imposed at a rate of 1 mm/min until cylindrical specimens of 6 x 4.5 inch (152 x 114 mm) developed failure. This test provided valuable information on the materials in relation to the tensile strength, tensile strain-stress relationships, degree of non-linearity, and measures of modulus such as tangent and secant modulus at peak strength. The validation of the implementation of this test to recognize the tensile properties of stabilized materials in the laboratory depends on the trend analysis of the processed data results. Figure 3.14 illustrates the testing protocol created for the execution of this test in the laboratory.

Dynamic Indirect Diametrical Tensile (D-IDT) Test

Additionally, a new variation of the IDT was developed for this study in order to verify the tensional performance of the cement stabilized materials subjected to tensile cyclic load. This test was developed and incorporated into the study so that it could provide information on the horizontal deformation of stabilized materials. Similar to the concept presented in the Submaximal Modulus test, the static IDT test results were used as a benchmark to determine the loading magnitude in the dynamic IDT test. In other words, after determining the IDT strength of each variant of the experiment design, a percentage of the static IDT strength was applied for 50,000 load cycles. The selected levels of the cyclic loads were 20, 40 and 60 percent of the static IDT strength. Figure 3.15 provides a schematic representation of the test set up. The horizontal deformations were measured using two LVDTs attached to aluminum brackets that

were placed on the specimens. The testing protocol developed for this dynamic test is presented in Figure 3.16.

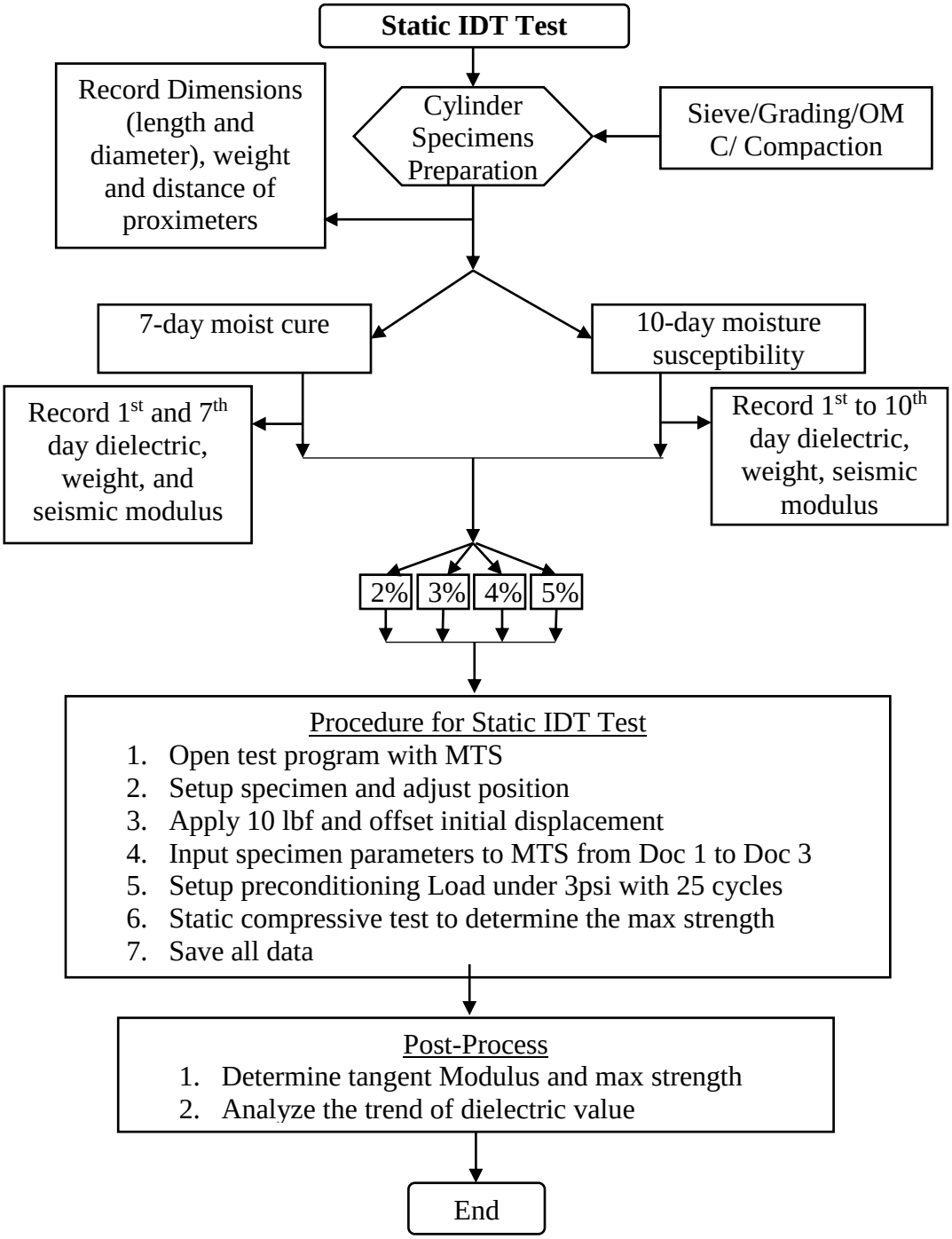

Figure 3.14: Static Indirect Diametrical Test (IDT) Procedure.

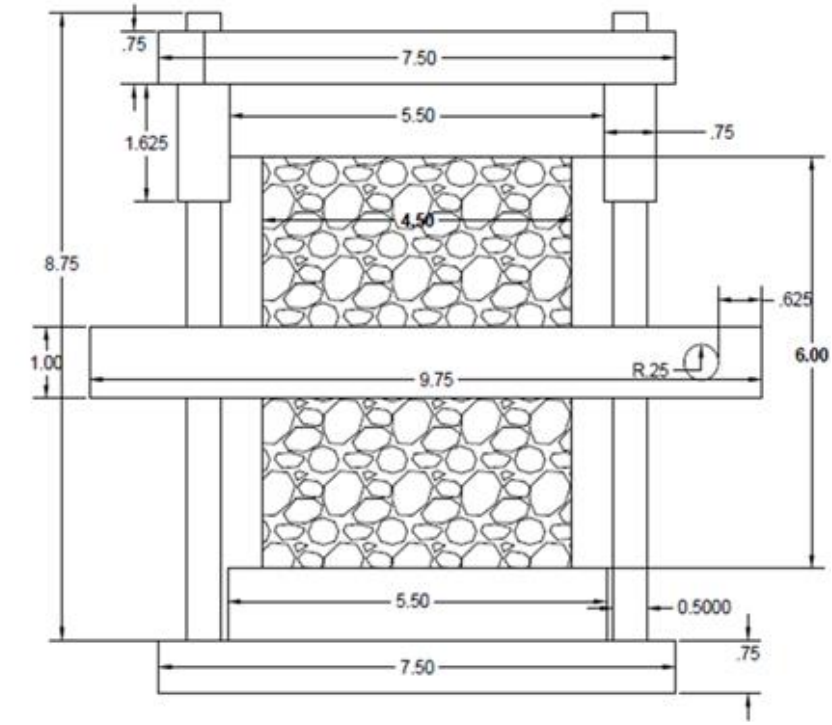

(a)

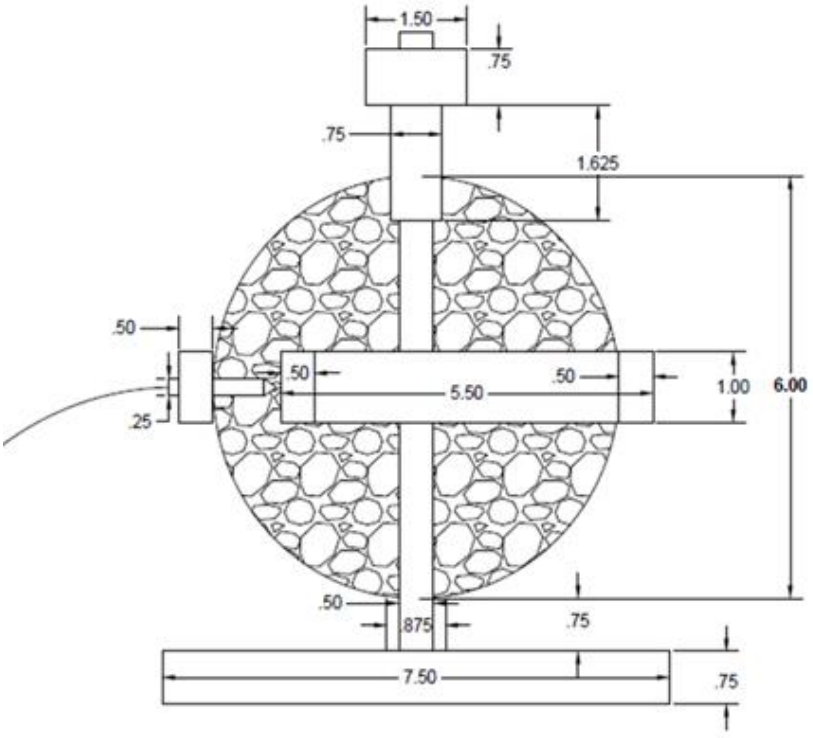

(b)

Figure 3.15: Indirect Diametrical Test Setup (a) Front View (b) Side View.

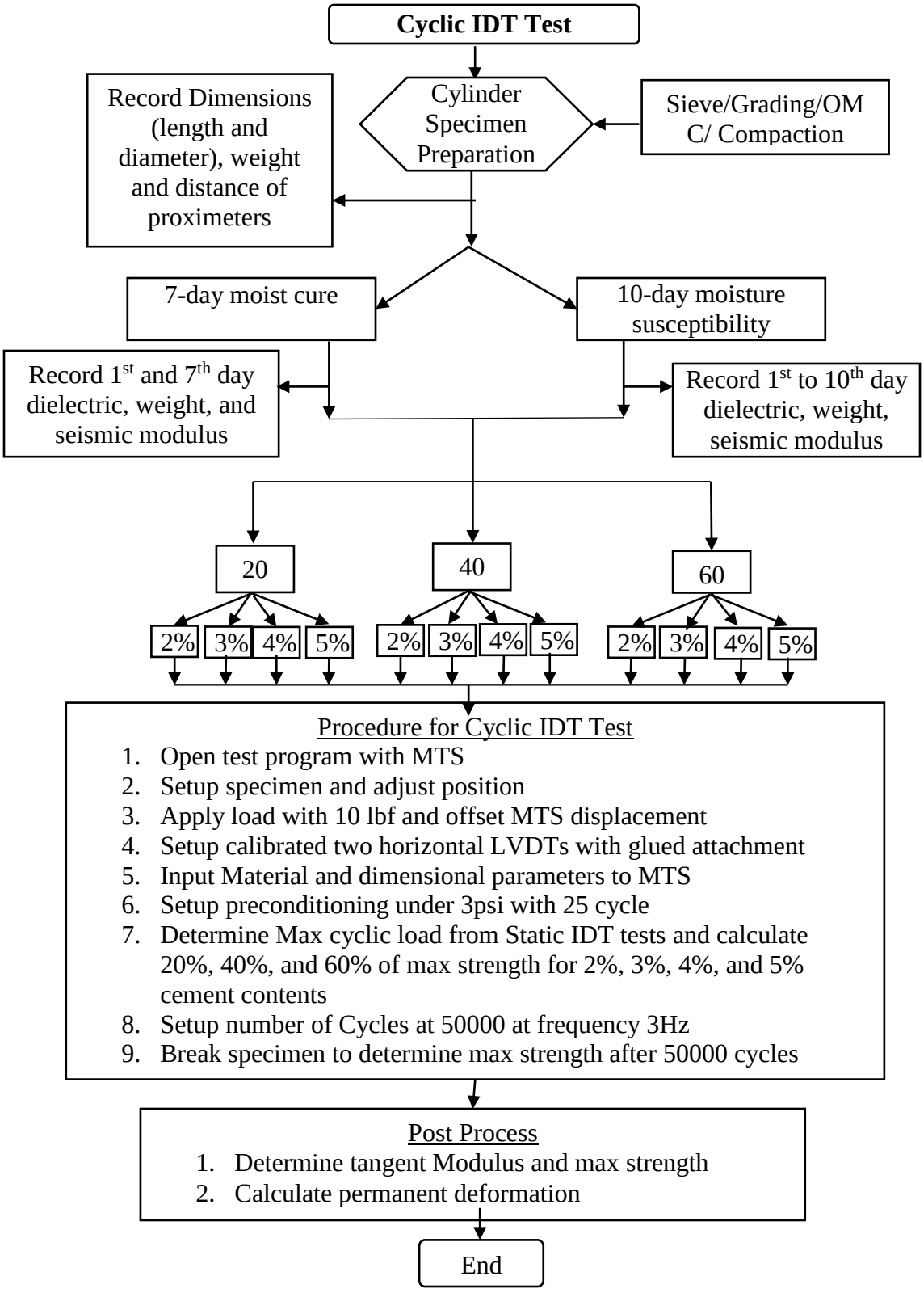

Figure 3.16: Dynamic Indirect Diametrical Test (IDT) Procedure.

Dielectric Value Test

The TST specimens produced in this experiment design were subjected to a moisture susceptibility test created for this study. In order to determine the moisture susceptibility of the stabilized materials, the moisture was measured by tracking the variations of the dielectric constants using a Rainbow dielectric constant meter in the laboratory. The variation in the dielectric values is an indication of the varying in the moisture content within the specimens. Therefore, monitoring the dielectric values at the top of the specimens provided valuable information on the affinity of the specimen to absorb and transport moisture through the pore structure. Additionally, the dielectric values provided a measure of the variation of the moisture consumption during the pozzolanic reactions in the specimens. The dielectric values of the TST specimens was measured every day for 10 consecutive days at five different points at the top of the specimen. The locations of measurements are presented in Figure 3.17. This testing procedure provided information related to the affinity of the specimens to transport moisture within the pore structure.

Figure 3.17: Dielectric Value Test Setup.

Free-Free Resonant Column (FFRC) Test

Finally, the last test procedure incorporated into the experiment design for 6 x 12 inch (152 x 205 mm) specimens was the Free-Free Resonant Column test based on Tex-148-E (draft). Resonant frequencies were propagated into the specimens and the small strain modulus values of the stabilized materials were computed using the principle of wave propagation. Figure 3.18 demonstrates the process of FFRC tests in this study. The daily continuous measurement of the seismic modulus values during 10 days provided supplementary information related to the improvement of stiffness properties as pozzolanic reactions took place within the specimens. Similarly, the seismic modulus test provided important information on the favorable or deleterious effect of moisture intrusion on the mechanical performance of the stabilized systems.

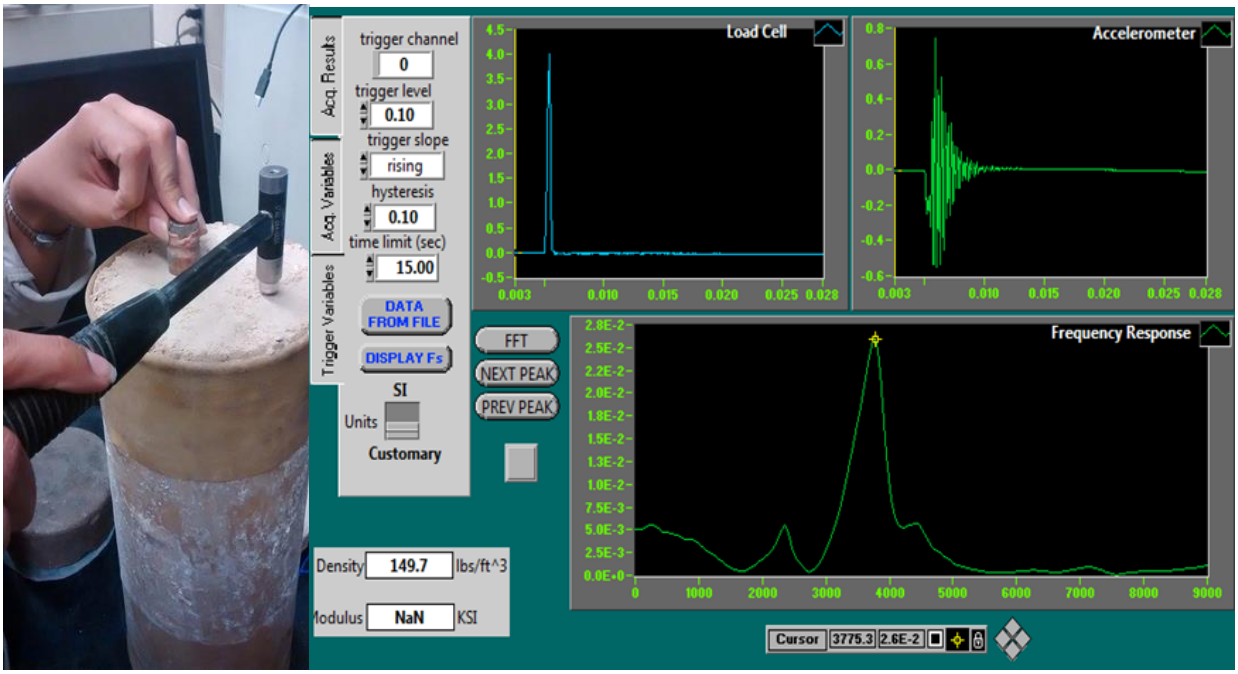

Figure 3.18: FFRC Test Setup and Software Output.

EXPERIMENT MATRIX

The experiment testing design created for this study consists of four materials at four different cement contents, one gradation, two curing conditions and six testing procedures to fully characterize the contributions of aggregate type, cement content and curing condition on the mechanical performance of the stabilized specimens. Two non-destructive procedures namely dielectric constant test and seismic modulus test were incorporated to daily verify the moisture susceptibility and the improvement or degrading in stiffness properties as the curing time increased. Additionally, four destructive tests were incorporated to distinguish the compressive and tensile behavior of stabilized materials under monotonic and cyclic loading conditions. Table 3.3 summarizes the laboratory testing protocols and material selection.

Table 3.3: Laboratory tests and Materials Selection.

	Aggregate Type															
	El Paso Limestone				Phar Gravel				Paris Sandstone				San Antonio Limestone			
	Cement Content (%)															
	2%	3%	4%	5%	2%	3%	4%	5%	2%	3%	4%	5%	2%	3%	4%	5%
Unconfined Compressive Strength (UCS)	√	√	√	√	√	√	√	√	√	√	√	√	√	√	√	√
Submaximal Test	√	√	√	√	√	√	√	√	√	√	√	√	√	√	√	√
Static Indirect Diametrical Tensile Test (S-IDT)	√	√	√	√	√	√	√	√	√	√	√	√	√	√	√	√
Dynamic Indirect Diametrical Tensile Test (D-IDT)	√	√	√	√	√	√	√	√	√	√	√	√	√	√	√	√
Dilective Value Test	√	√	√	√	√	√	√	√	√	√	√	√	√	√	√	√
Free-Free Resonant Coloumn (FFRC)	√	√	√	√	√	√	√	√	√	√	√	√	√	√	√	√

Table 3.4 represents a detailed introduction of the established experiment matrix for the purpose of this study. More than 500 specimens were subjected to various destructive laboratory tests. The dielectric constant test was imposed on more of 130 specimens for TST curing conditioning.

Table 3.4: Experiment Design.

			Aggregate Type															
			El Paso Limestone				***San Antonio*** Limestone				***Pharr*** Gravel				***Paris*** Sandstone			
			Cement Content (%)															
			2	3	4	5	2	3	4	5	2	3	4	5	2	3	4	5
7 Day Moist Cured	**UCS Test**		X	X	X	X	X	X	X	X	X	X	X	X	X	X	X	X
	Submaximal Modulus	@ 20% UCS	X	X	X	X	X	X	X	X	X	X	X	X	X	X	X	X
		@ 40% UCS	X	X	X	X	X	X	X	X	X	X	X	X	X	X	X	X
		@ 60% UCS	X	X	X	X	X	X	X	X	X	X	X	X	X	X	X	X
	Static IDT Test		X	X	X	X	X	X	X	X	X	X	X	X	X	X	X	X
	Dynamic IDT Test	@ 20% Strength	X	X	X	X	X	X	X	X	X	X	X	X	X	X	X	X
		@ 40% Strength	X	X	X	X	X	X	X	X	X	X	X	X	X	X	X	X
		@ 60% Strength	X	X	X	X	X	X	X	X	X	X	X	X	X	X	X	X
TST	**UCS Test**		X	X	X	X	X	X	X	X	X	X	X	X	X	X	X	X
	Submaximal Modulus	@ 20% UCS	X	X	X	X	X	X	X	X	X	X	X	X	X	X	X	X
		@ 40% UCS	X	X	X	X	X	X	X	X	X	X	X	X	X	X	X	X
		@ 60% UCS	X	X	X	X	X	X	X	X	X	X	X	X	X	X	X	X
	Static IDT Test		X	X	X	X	X	X	X	X	X	X	X	X	X	X	X	X
	Dynamic IDT Test	@ 20% Strength	X	X	X	X	X	X	X	X	X	X	X	X	X	X	X	X
		@ 40% Strength	X	X	X	X	X	X	X	X	X	X	X	X	X	X	X	X
		@ 60% Strength	X	X	X	X	X	X	X	X	X	X	X	X	X	X	X	X

SPECIMEN PREPARATION

This section provides a detailed explanation of the techniques selected in terms of specimen preparation for this study. Primary un-stabilized specimens were prepared in accordance with Tex-101-E part II for the moisture-density analysis. Moisture and density relationships were established based on the Tex-113-E specification. All specimens for this study were compacted at optimum moisture content of virgin materials. However, the water content was adjusted according to incremental cement content in the mixes based on the Tex-120-E specification. In other words, the water content was incremented by 0.25 percent for every

percent of cement added to the virgin materials. Two different sample sizes were incorporated based on the testing procedures. The dimensions of the specimen for the UCS and submaximal modulus tests were 6 x 12 inch (152 x 305 mm). These specimens were compacted in six layers applying an energy effort of 750 ft-lb per layer. Specimen dimensions for the Static IDT and Dynamic IDT were 6 x 4.5 inch (152 x 114 mm). These specimens were compacted in three layers with 50 blows per layer using a 10 lb. hummer and 18 in drop. In order to achieve an enhanced uniform cement hydration and cement distribution in specimens of 6 x 4.5 inch, the water and cement were combined independently and then mixed with the virgin aggregates. Figure 3.19 shows the modified procedure of the sample preparation on 6 x 4.5 inch specimens before compaction.

Figure 3.19: Specimen preparation.

In conclusion, this chapter has presented the criteria for the material selection section and its significance to the purpose of this study. The survey results confirmed the requirement of a new testing protocol to properly characterize the tensile properties of stabilized materials. The IDT test applied to stabilized materials could be a suitable alternative whose validation will be influenced by the testing results of the study. In addition, several laboratory-testing procedures were presented where the stabilized specimens were subjected to compressive and tensile loading conditions.

Chapter 4: Laboratory Testing Results

INTRODUCTION

This chapter presents the laboratory test results based on the experiment matrix developed in Chapter 3. The performance of stabilized specimens subjected to compressive and tensile loading protocols was categorized based on the different aggregate mineralogy and stabilizer content.

GRADATION RESULTS

The particle size distribution selected for this study was based on the most common particle size distribution used in stabilized base layers. Therefore, according to the survey results presented in Chapter 2, the particle size distributions selected for this study were based on the Item 247 grade 4. Figure 4.1 illustrates the particle size distribution for the materials selected.

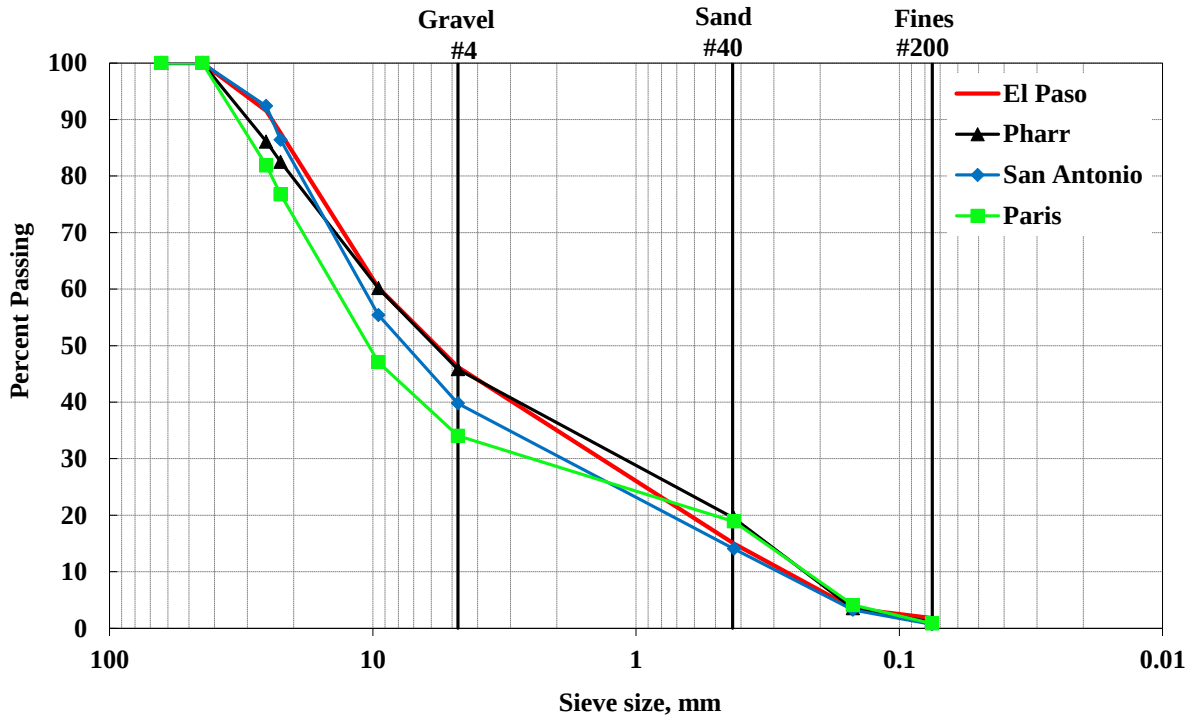

Figure 4.1: Particle Size Distributions of Aggregate Materials.

MOISTURE DENSITY RESULTS

The specimens prepared in this study were compacted at optimum moisture content of virgin materials. In order to determine the optimum moisture content of each material, graded virgin materials were compacted using Tex-113-E specifications to prepare cylindrical specimens. Additionally, the Moisture and Density (MD) curves were determined based on Tex-113-E, the curves are presented in Figure 4.2. Table 4.1 provides a detailed summary of the MD results.

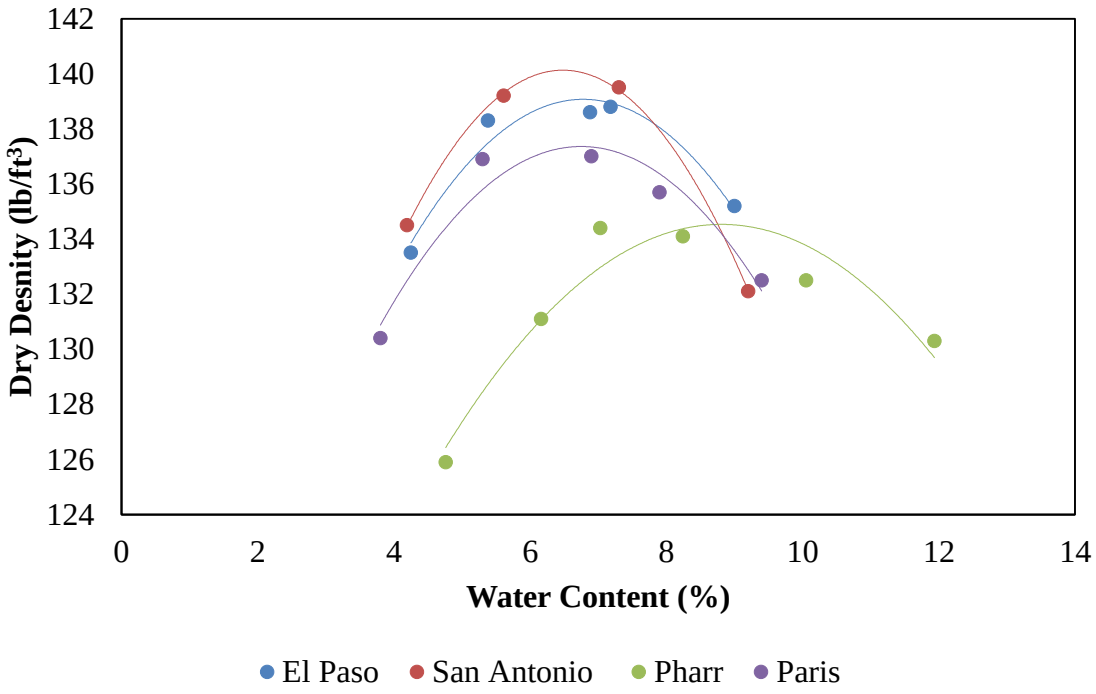

Figure 4.2: Moisture-Density Curves.

Table 4.1: Moisture-Density Test Results.

Material	OMC (%)	Max Dry Density (lb./ft^3)
El Paso	6.8	139.1
San Antonio	6.5	140.1
Pharr	8.8	134.5
Paris	6.8	137.4

UNCONFINED COMPRESSIVE STRENGTH (UCS) TEST

The UCS test was performed on 6 x 12 inch (152 x 305 mm) stabilized specimens at ambient temperature with an imposed deformation rate of 1 mm/min until the specimens developed failure. Figure 4.3 illustrates a set of stabilized specimen subjected to this strain-controlled test after fracture. Shear cracking failure was observed in all the specimens subjected to this test as Figure 4.3 illustrates.

Figure 4.3: El Paso Specimen after Failure in the UCS Test.

Figure 4.4 shows the compressive stress-strain relationships of Paris materials subjected to 7-day moist cured condition. The results clearly demonstrate an improvement in compressive strength properties as cement content increases within the specimens. Besides the compressive strength, several measures of modulus, such as tangent and secant modulus can be extracted from the stress-strain relationships. Based on Figure 4.4, the tangent modulus, secant modulus and the degree of non-linearity are also influenced by the cement content. This is an indication of the favorable effect that soil stabilization has on the specimens. Similarly, Figure 4.5 presents the compressive strain-stress relationships of Paris specimens subjected to TST curing condition.

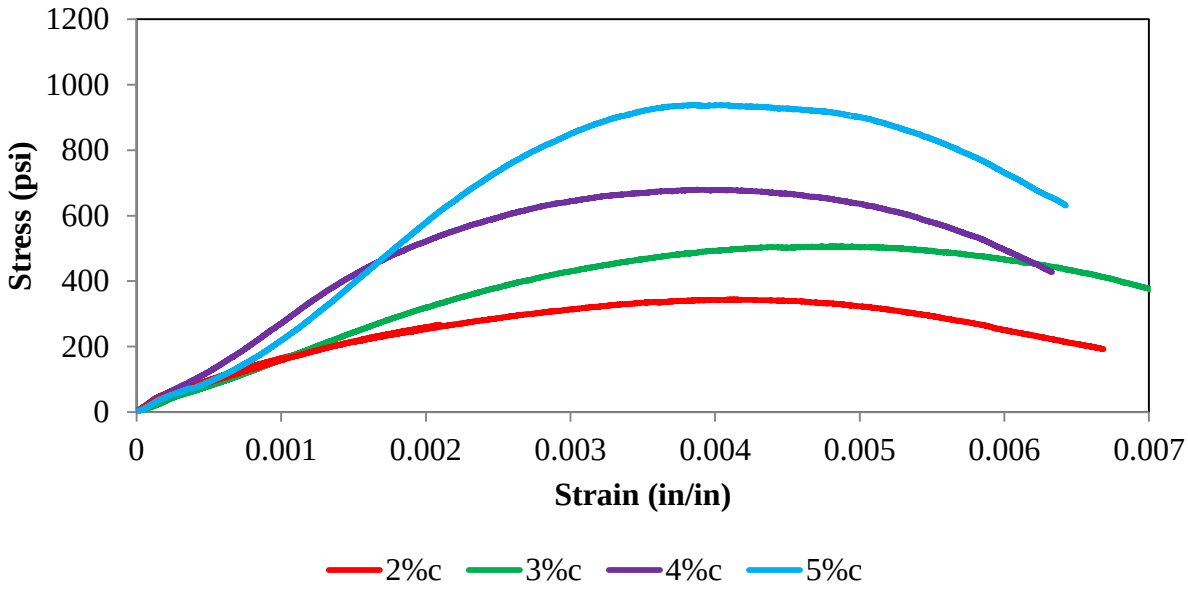

Figure 4.4: UCS Results for Paris Materials for 7-day Moist Cured Specimens.

In both results, similar trends are observed where the cement content increases the stiffness properties of Paris specimens.

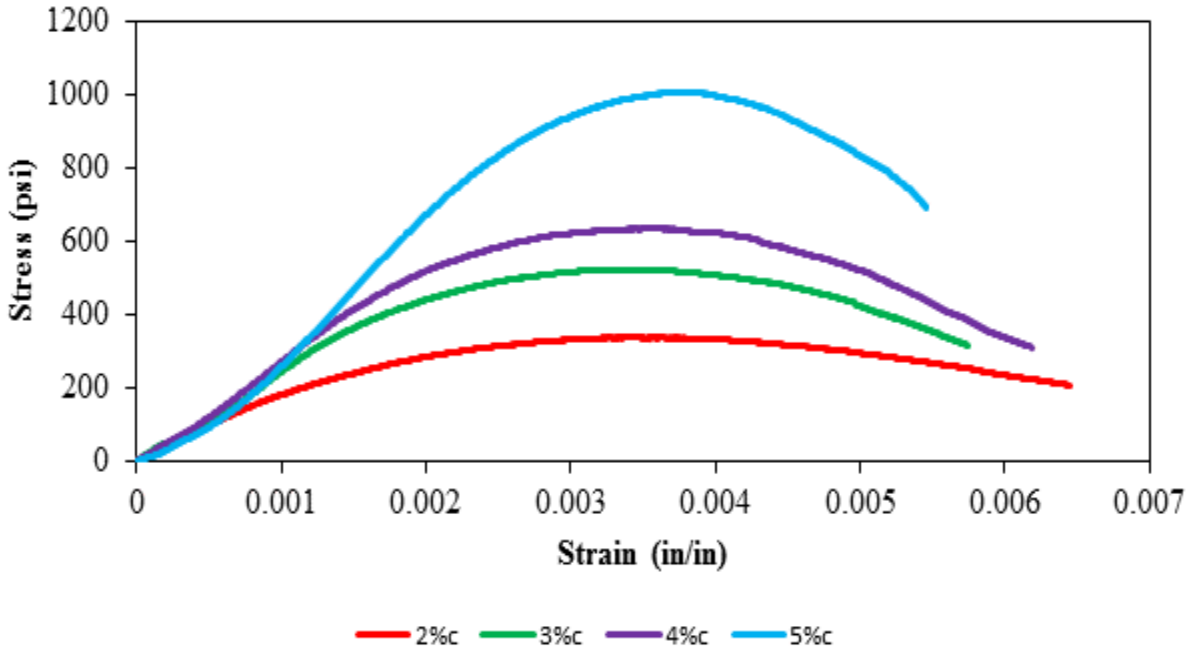

Figure 4.5: Paris Stress vs. Strain Curve for 10-Day Capillary Soak Specimens.

The laboratory results of the UCS values for specimens subjected to the 7-day moist cured condition are presented in Figure 4.6. The ascending nature of the trend lines is a notable indication of the favorable effect of soil stabilization for all the materials presented in the experiment design. The strength values do not have the same magnitude for all materials. Paris and El Paso specimens have the highest strength values and Pharr specimens have the lowest values. The rate of improvement is represented by the slope of the trend curves in the results. Moreover, the El Paso material trend curve exhibited a parabolic increase as cement content increased compared to Pharr material whose trend curve showed an asymptotic behavior as cement content increased.

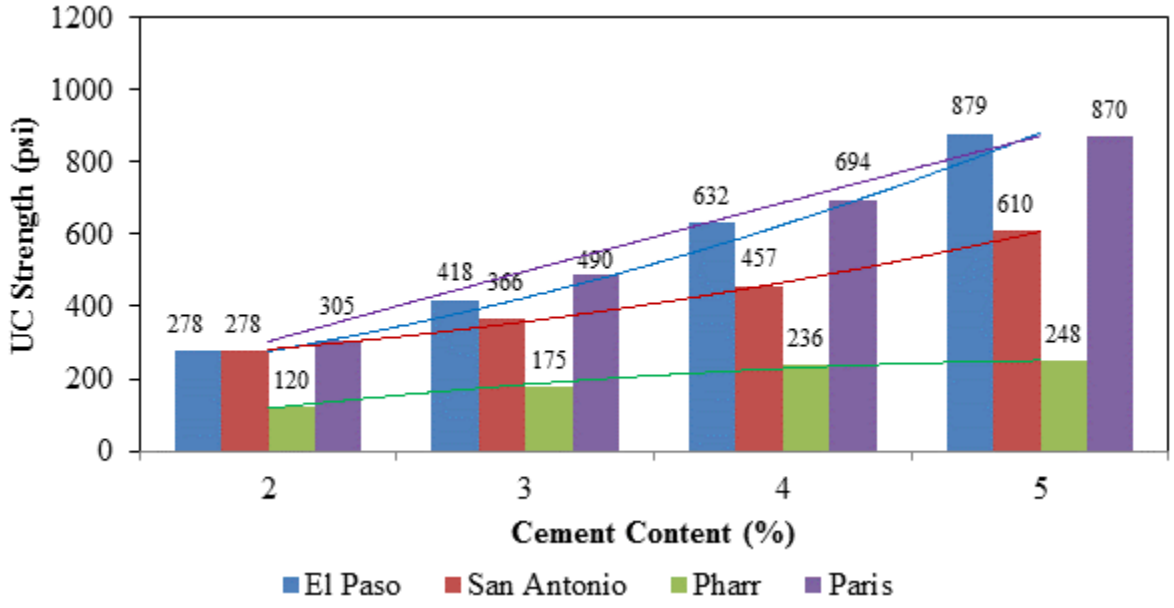

Figure 4.6: Unconfined Compressive Strength Results for 7-day Moist Cured Specimens.

Figure 4.7 illustrates the UCS values for specimens subjected to TST curing conditions. Similar trends are observed in specimens subjected to moisture intrusion for all variantions in the experiment design. The strength values are not the same especially for specimens at 4 and 5

percent. However, the difference in compressive strength values do not vary significantly particularly in specimens at 2 and 3 percent.

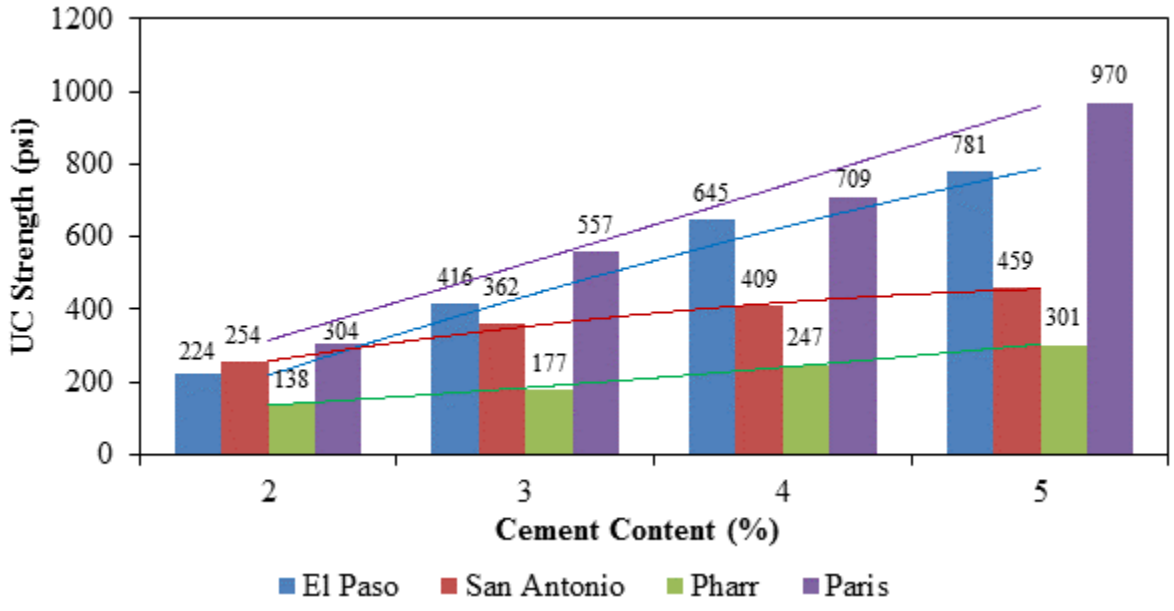

Figure 4.7: Unconfined Compressive Strength Results for 10-Day Capillary Soak Specimens.

The percentage of compressive strength improvement with increasing cement content on the specimens of the 7-day moist cured and TST curing conditions are presented in Figure 4.8 and 4.9 respectively. The percentages were calculated based on the difference with the lowest stabilizer content in the specimens (2 percent). An important observation from Figures 4.8 and 4.9 is the important role of the aggregate mineralogy in the process of the pozzolanic reactions within the specimens. These trend curves can be utilized for the selection of the optimum cement content for the stabilization of foundations in general. In addition, increasing cement content from two to three percent for Pharr specimens improves the strength by 47 percent. However, increasing from four to five percent cement content for Pharr materials only increases the strength by 10 percent.

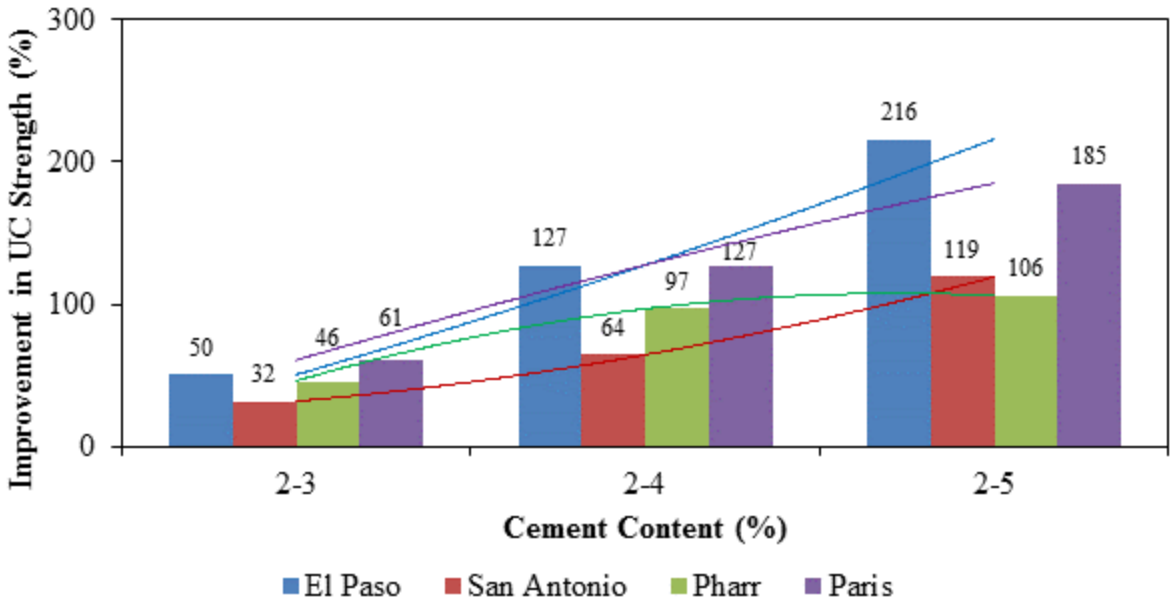

Figure 4.8: Improvements in Unconfined Compressive Strength for 7-day Moist Cured Specimens.

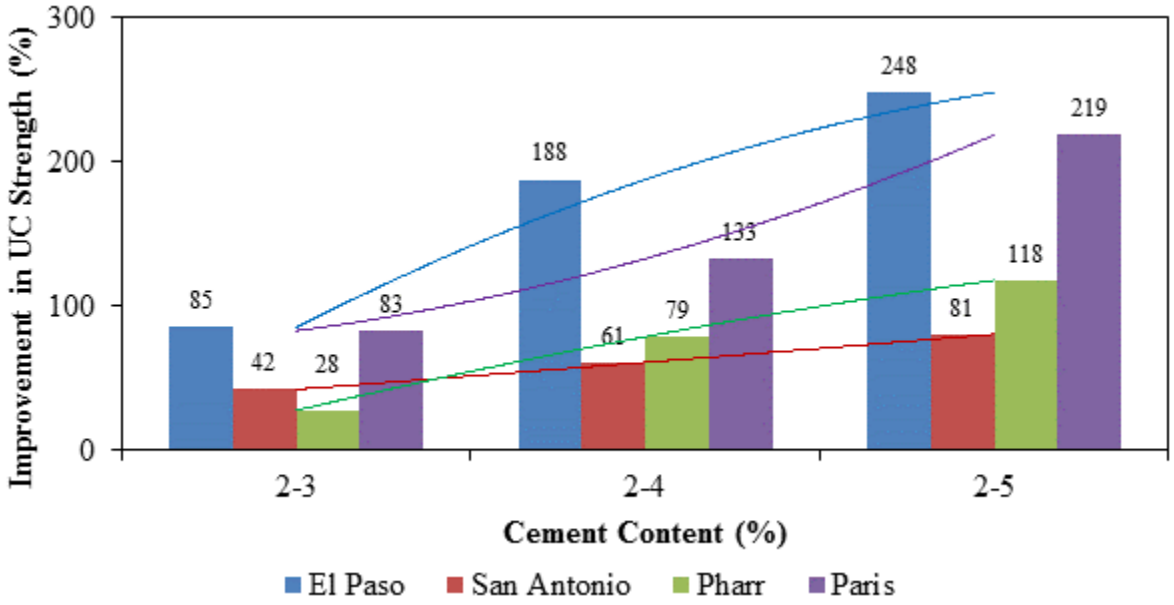

Figure 4.9: Improvements in Unconfined Compressive Strength for 10-Day Capillary Soak Specimens.

An important parameter determined from the compressive stress-strain relationships is the tangent modulus of the fractured specimens. Figure 4.10 shows the tangent modulus values and the trend lines for specimens subjected to the 7-day moist cured condition.

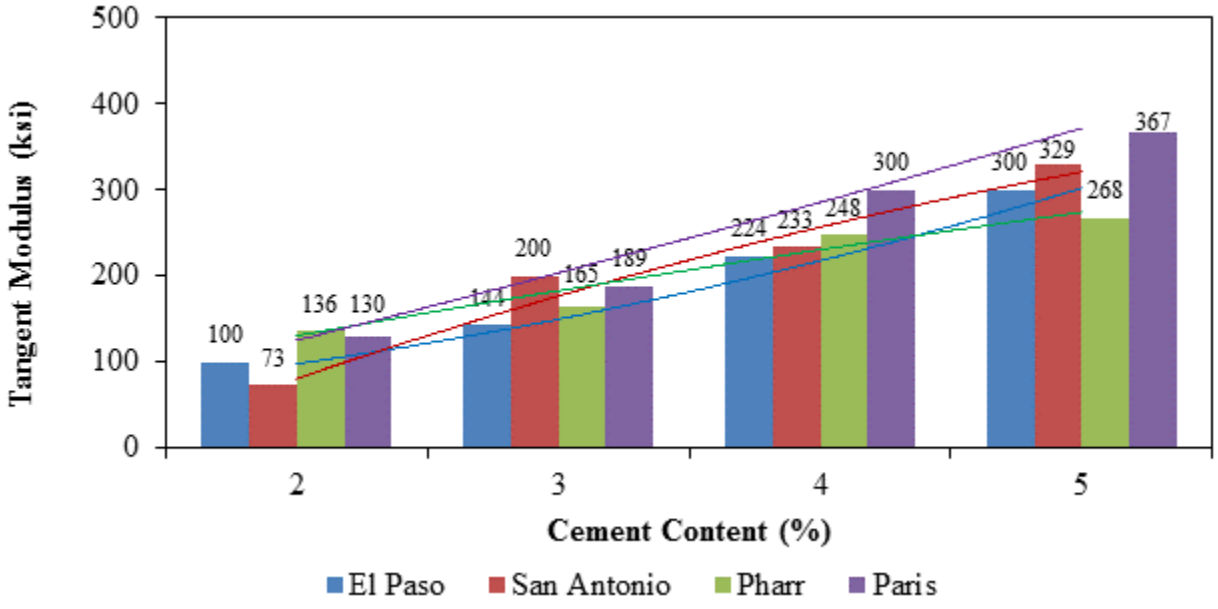

Figure 4.10: Tangent Modulus for 7-day Moist Cured Specimens.

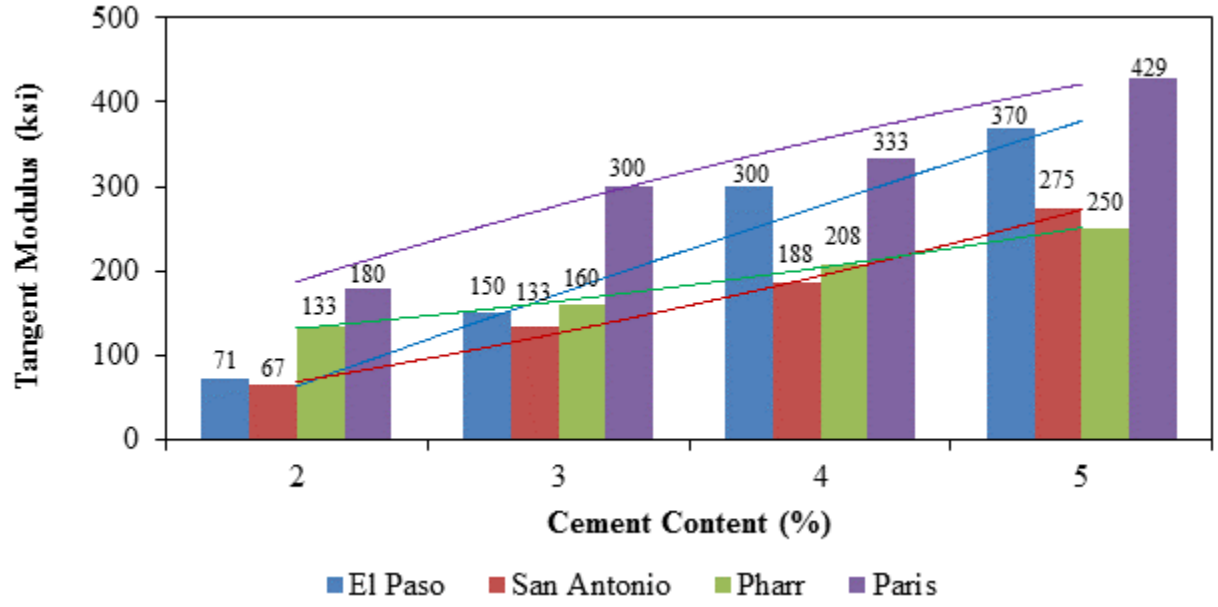

Figure 4.11: Tangent Modulus for 10-Day Capillary Soak Specimens.

Obviously, the modulus values increased as cement content increased for all permutations of the study. This tangent modulus was measured from the linear portion of the undamaged small-strain portion or elastic region. Again, this is an indication of the increase in stiffness properties due to the soil stabilization process. Then modulus values and trends for specimens subjected to TST conditions observed in Figure 4.11 show similar results.

The degree of non-linearity is another significant parameter obtained from the compressive strain-stress relationships. Figure 4.12 and 4.13 illustrates the results for specimens prepared according to the 7-day moist cured and TST curing conditions respectively. The trends show that all variants of the study become linear as cement content increases. This is another indication of the positive effect of increasing cement content in the specimens. However, the degree of non-linearity is lower for specimens subjected to the TST condition than specimens subjected to the 7-day moist cure condition.

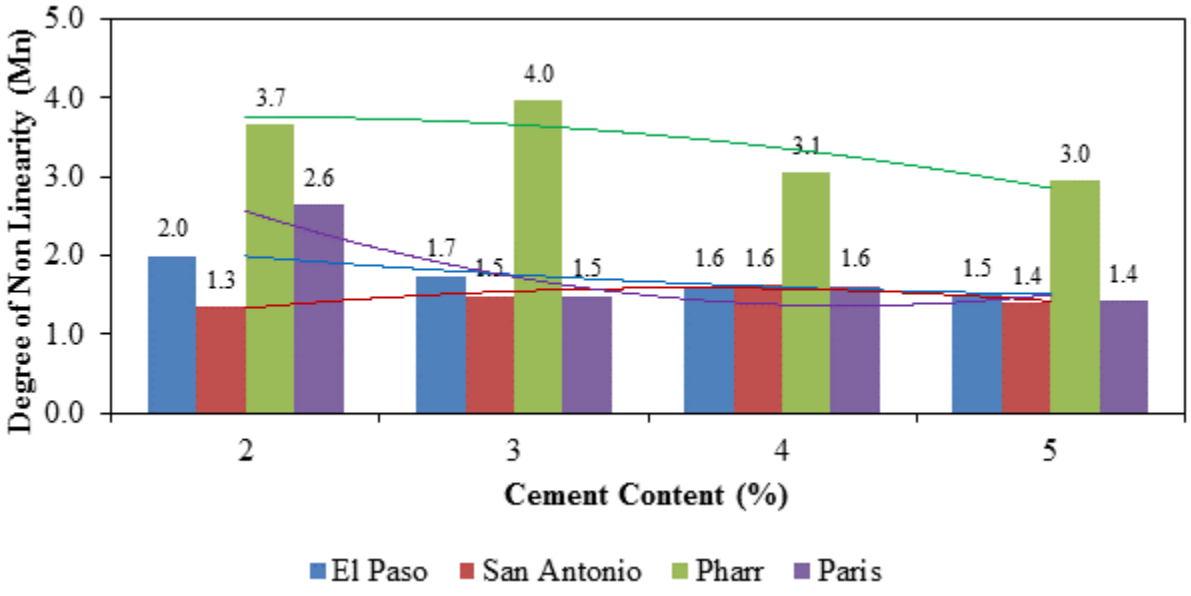

Figure 4.12: Degree of non-linearity for 7-day Moist Cured Specimens.

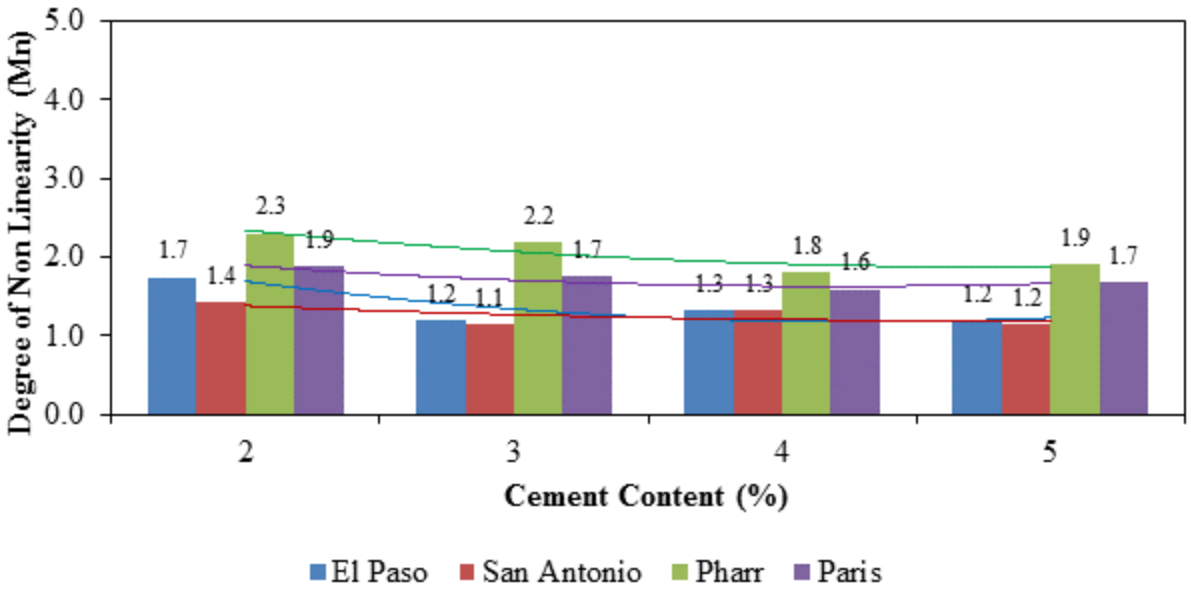

Figure 4.13: Degree of non-linearity for 10-Day Capillary Soak Specimens.

The last parameter obtained in this study from the UCS test is the strain at failure of stabilized specimens. Usually, the strain at failure is an indication of the stiffness and flexibility parameters of the specimens. Figure 4.14 provides the strain at failure of specimens with the 7-day moist cured condition. The trends show a decreasing strain failure value as the specimens' cement content increases. The results indicate that the specimens become more rigid or less flexible as cement content increases. San Antonio and Pharr specimens show a decrease in flexibility at higher cement content compared to El Paso and Paris specimens. Figure 4.15 illustrates the results for TST specimens where the same trends are observed.

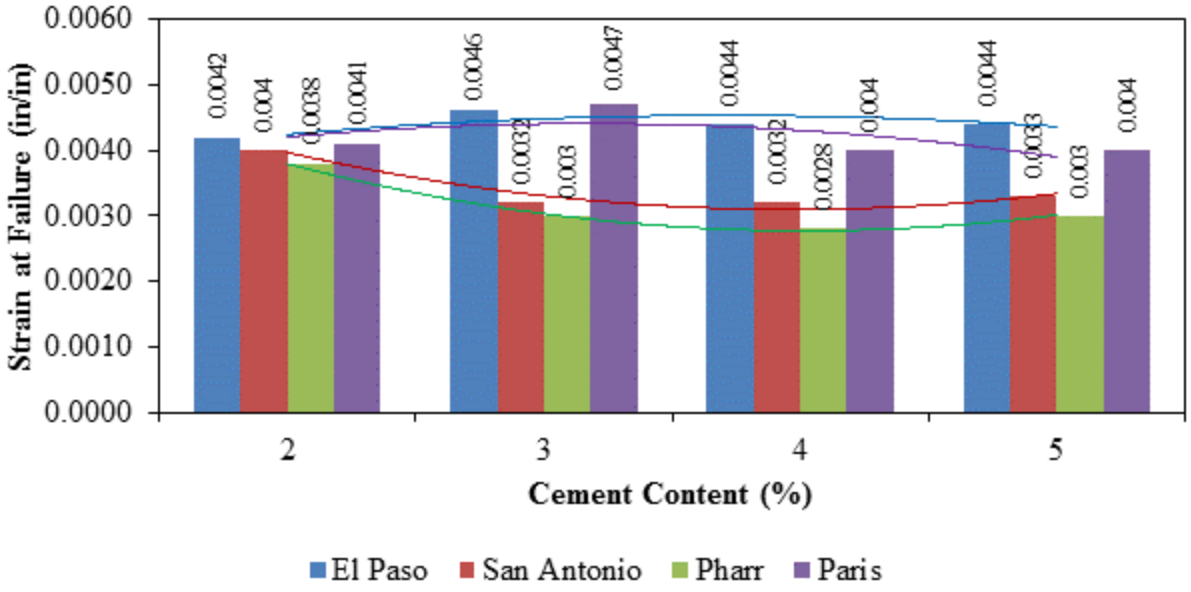

Figure 4.14: Strain at Failure for 7-day Moist Cure Specimens.

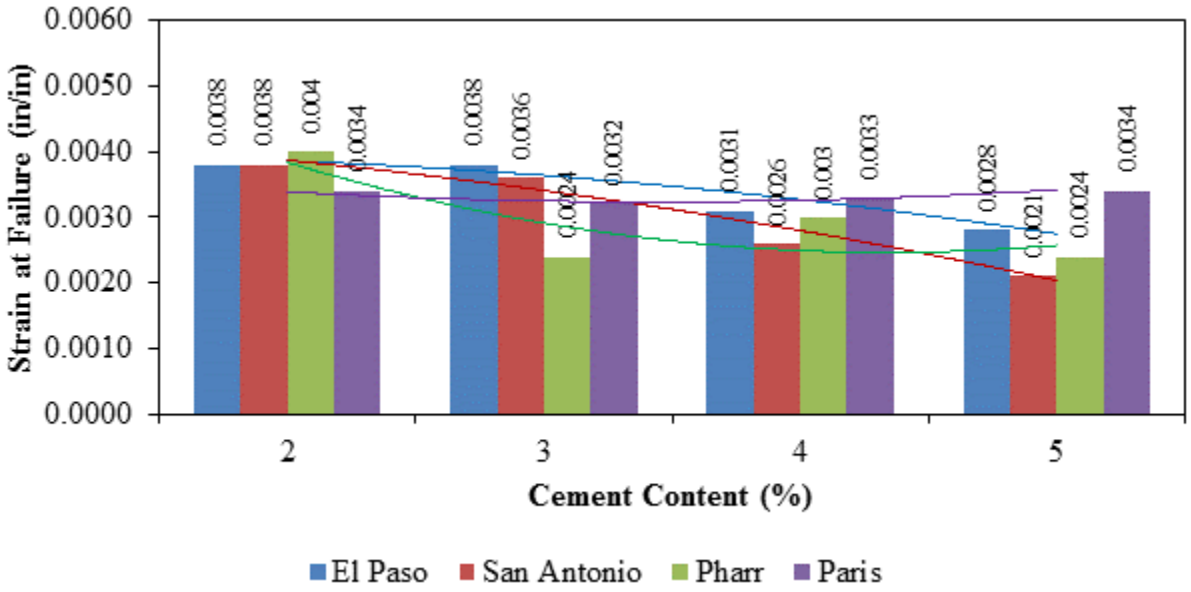

Figure 4.15: Strain at Failure for 10-Day Capillary Soak Specimens.

STATIC INDIRECT DIAMETRICAL (S-IDT) TEST

The static IDT test was performed on 6 x 4.5 inch (152 x 114 mm) stabilized specimens at ambient temperature with an imposed deformation rate of 1 mm/min until the specimens developed failure. The specimens subjected to this test always demonstrated a straight crack failure along the loading supports as Figure 4.16 illustrates. This test was induced on stabilized specimens without technical difficulty related to the stabilizer content and curing condition. This section presents the laboratory results of the static IDT test for the 7-day moist cure and TST specimens.

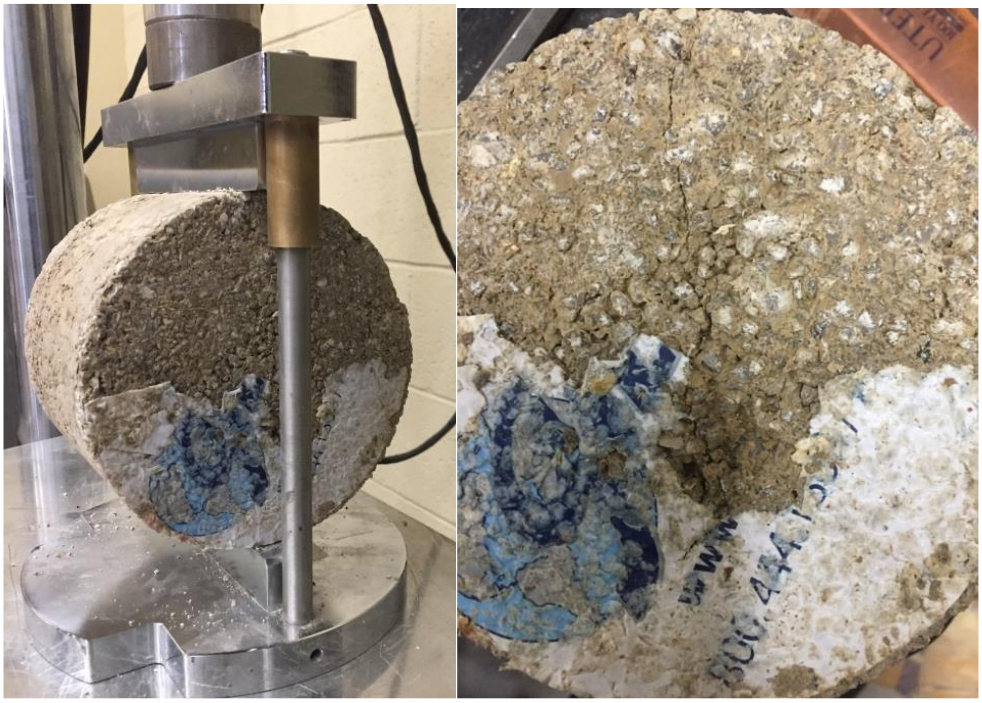

Figure 4.16: El Paso Specimen Failure after Static IDT Test.

Figure 4.17 represents the IDT values for specimens subjected to the 7-day moist cured procedure where the increment of the IDT strength values with increasing cement content for all permutations in this study is an indication of the favorable effect of stabilizer content on the tensile properties. However, the rate of increase in the IDT values was not similar as indicated by

the trend lines in figure 4.17. Similar to the UCS results presented in previous section, El Paso limestone benefited most from the increase in the cement content. Conversely, the rate of improvement in the tensile strength of siliceous gravel from Pharr district with increasing cement content was lower as indicated by trend lines in figure 4.17.

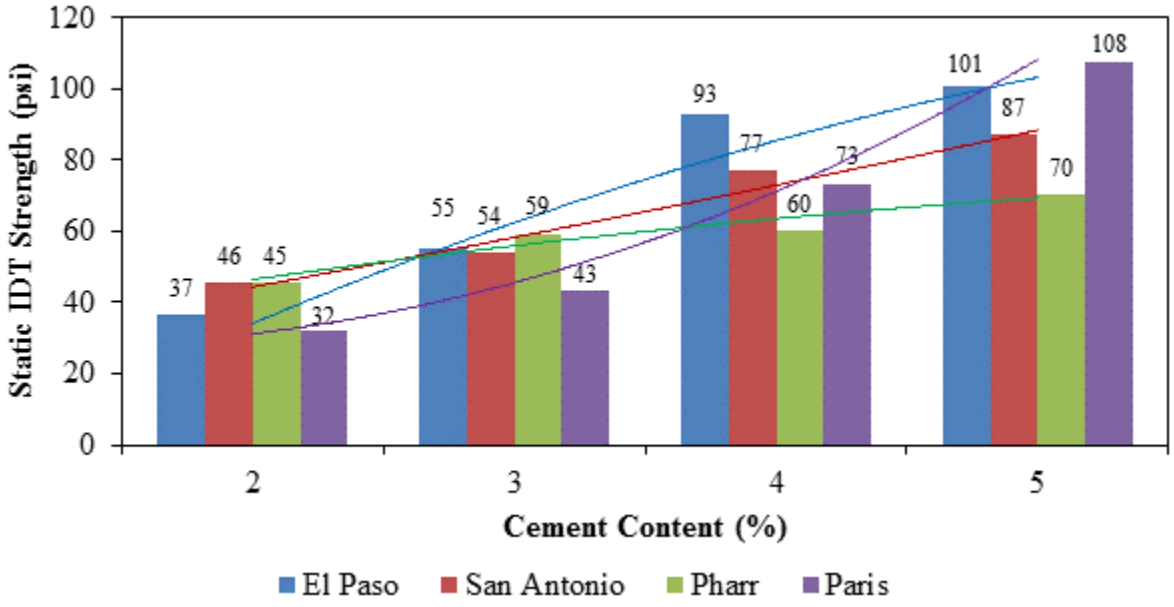

Figure 4.17: Static IDT Test Results for 7-day Moist Cured Specimens.

Figure 4.18 presents the laboratory results for the static IDT performed on the TST specimens. The trend lines follow a similar pattern as in the 7-day moist cure specimens. A comparison of the results presented in figures 4.17 and 4.18 reveals the deleterious influence of moisture in degrading the tensile stiffness of the stabilized specimen.

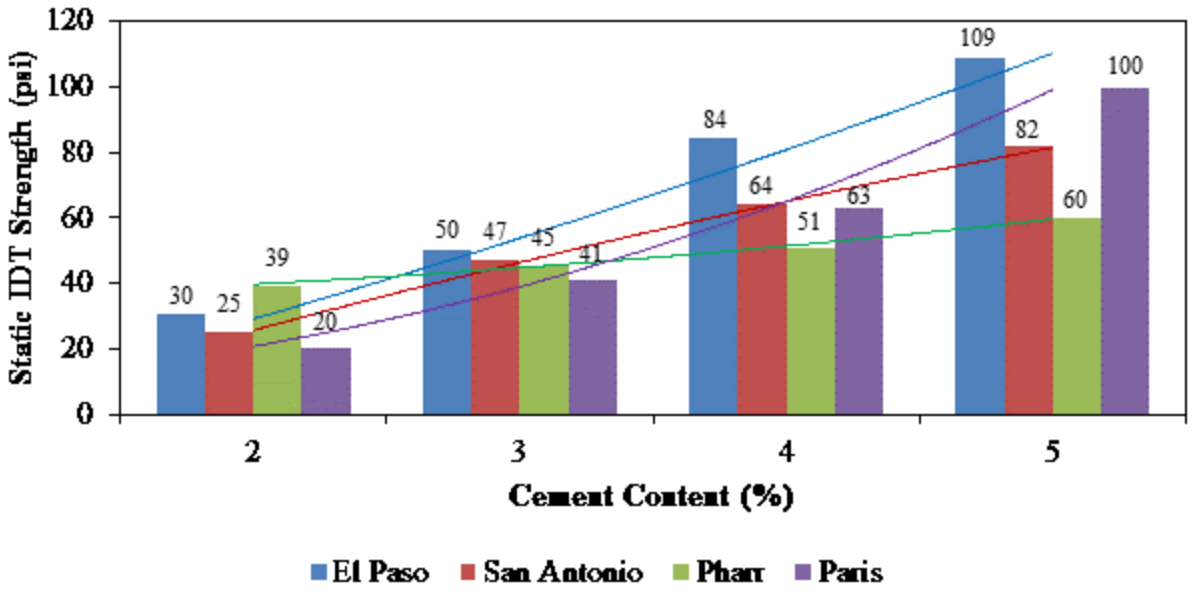

Figure 4.18: Static IDT Test Results 10-Day Capillary Soak Specimens.

Figure 4.19 and 4.20 represent the improvement in tensile strength for the 7-day moist cure and 10-day capillary soaked (TST) specimens, respectively. A notable observation in these plots is the significant underperformance of Pharr materials at high stabilizer contents compared to other materials in the experiment. The underperformance of Pharr materials is more pronounced in the TST results presented in figure 4.20. For instance, the tensile strength of Paris samples improved by 397 percent, by increasing the cement content from 2 to 5 percent, while Pharr specimens showed only an improvement of 52 percent. Again, Paris material benefited the most in terms of tensile strength improvement by incrementing cement content in the specimens.

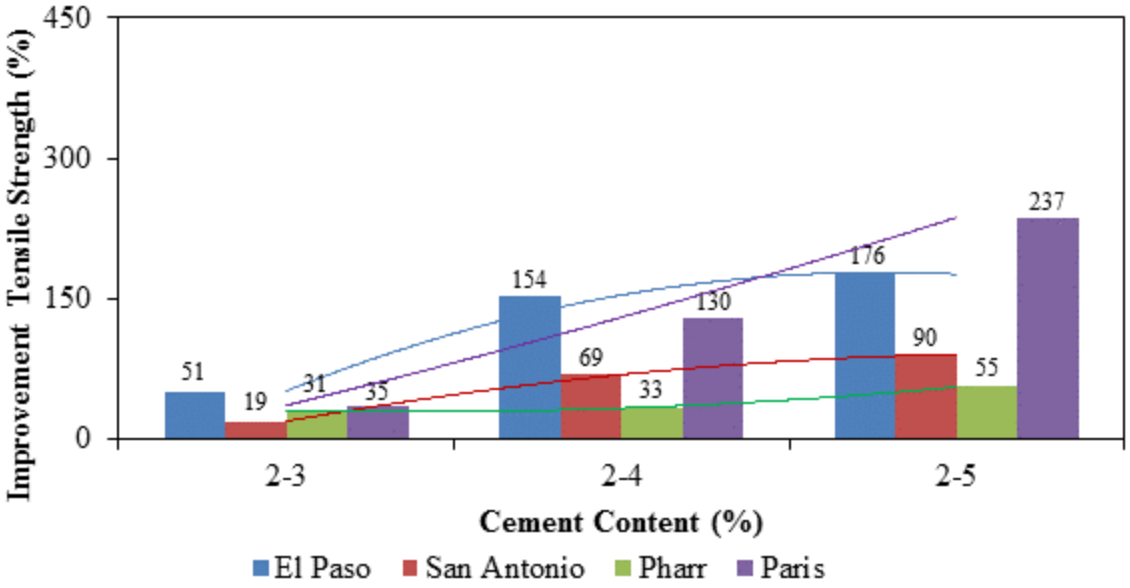

Figure 4.19: Tensile Strength Improvement for 7-day Moist Cure Specimens.

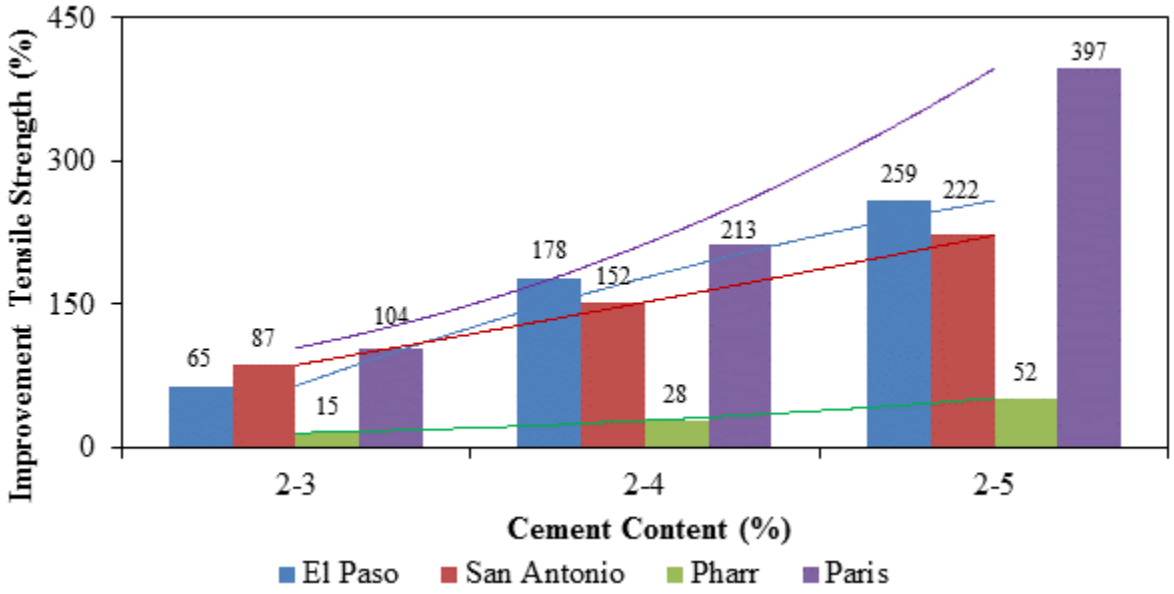

Figure 4.20: Tensile Strength Improvement for 10-Day Capillary Soak Specimens.

Figures 4.21 and 4.22 represents the tangent modulus values calculated based on the tensile stress-strain curves using the 7-day moist cure and TST specimens respectively. As

expected, the trend lines increase when cement content increases. However, the tangent modulus values do not vary significantly in the four materials presented in the experiment.

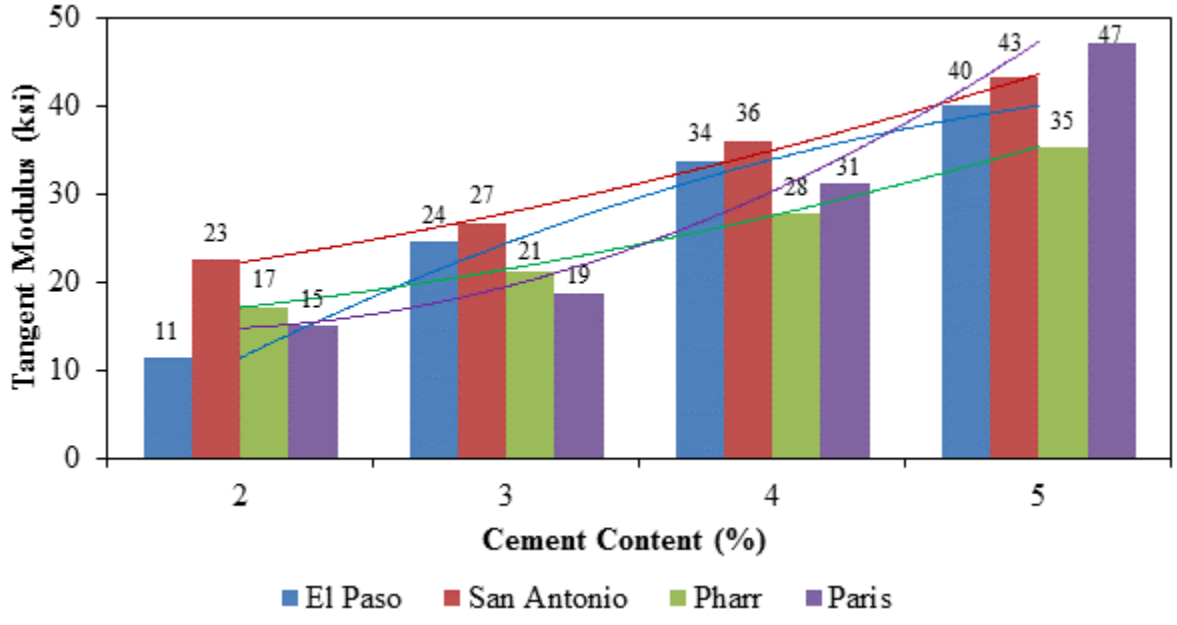

Figure 4.21: Tangent Modulus for 7-Day Moist Cured Specimens.

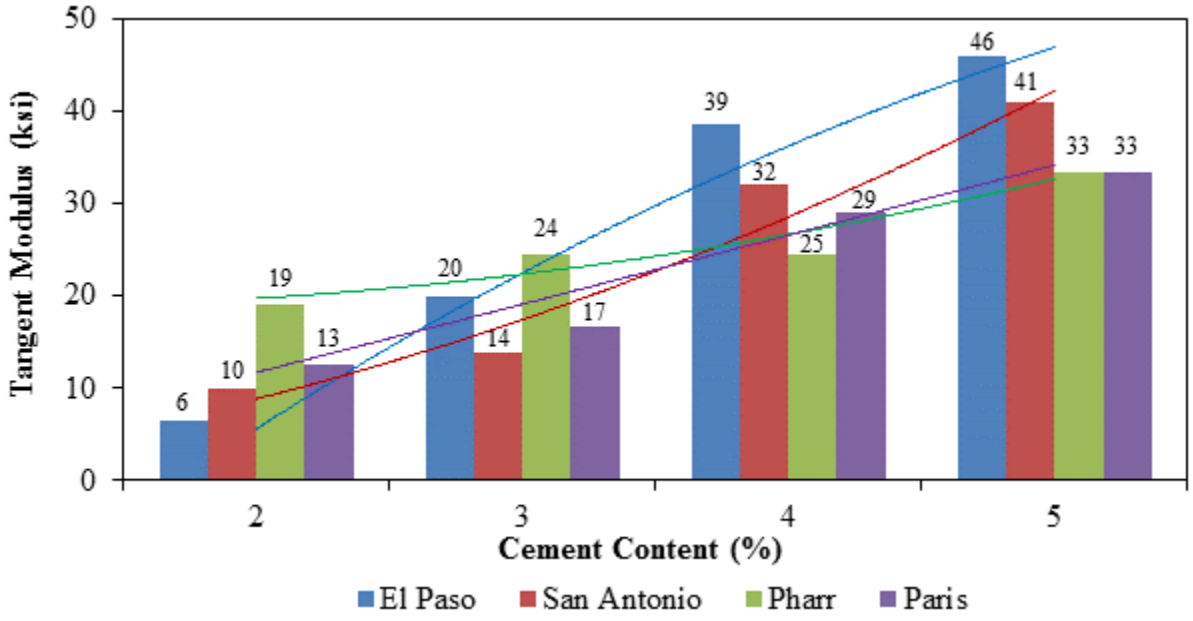

Figure 4.22: Tangent Modulus for 10-Day Capillary Soak Specimens.

Another significant result derived from the static IDT was the measurement of the degree of the non-linearity of the stabilized specimens. The results presented in figures 4.23 and 4.24 clearly indicate a more linear behavior for stabilized specimens subjected to tensile load compared to compressive load. In addition, the degree of non-linearity stays similarly constant for all stabilizer contents, except for Paris specimens where the degree of non-linearity decreases as cement content increases. It is important to mention that the IDT test implemented for stabilized materials properly captures the increment in tensile strength as cement content increases for all variants. Additionally, the behavior of stabilized specimens subjected to the IDT test is significantly linear with respect to the stabilizer content and mineralogy type. This could be an indication of the validation of the use of the IDT test on stabilized specimens to properly characterize tensile properties such as fatigue performance.

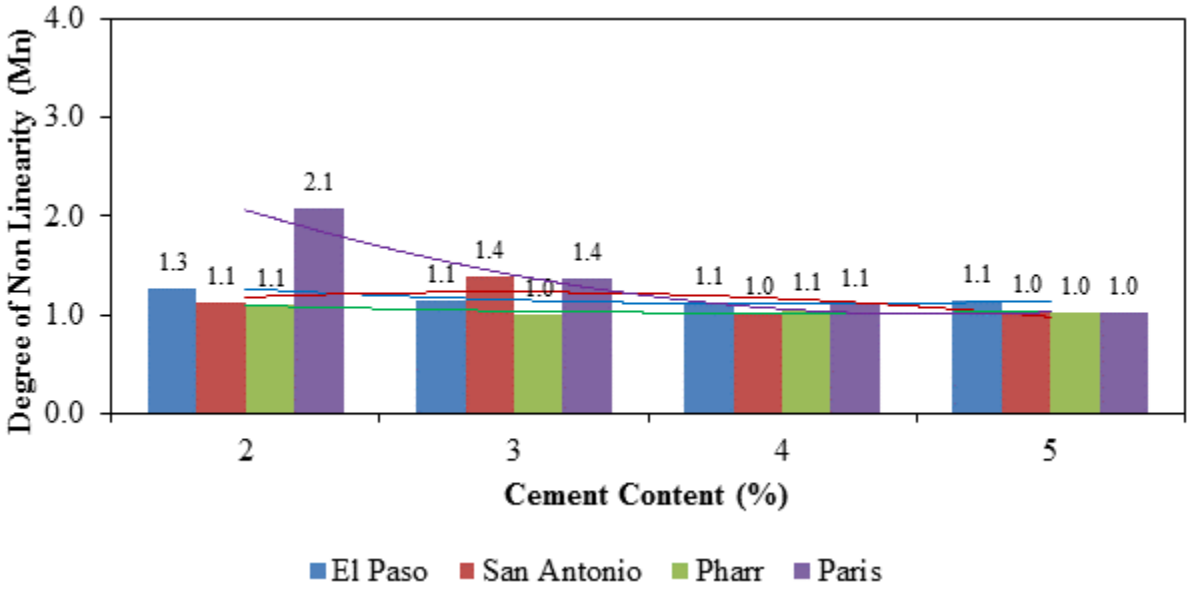

Figure 4.23: Degree of Non-linearity for 7-day Moist Cure Specimens.

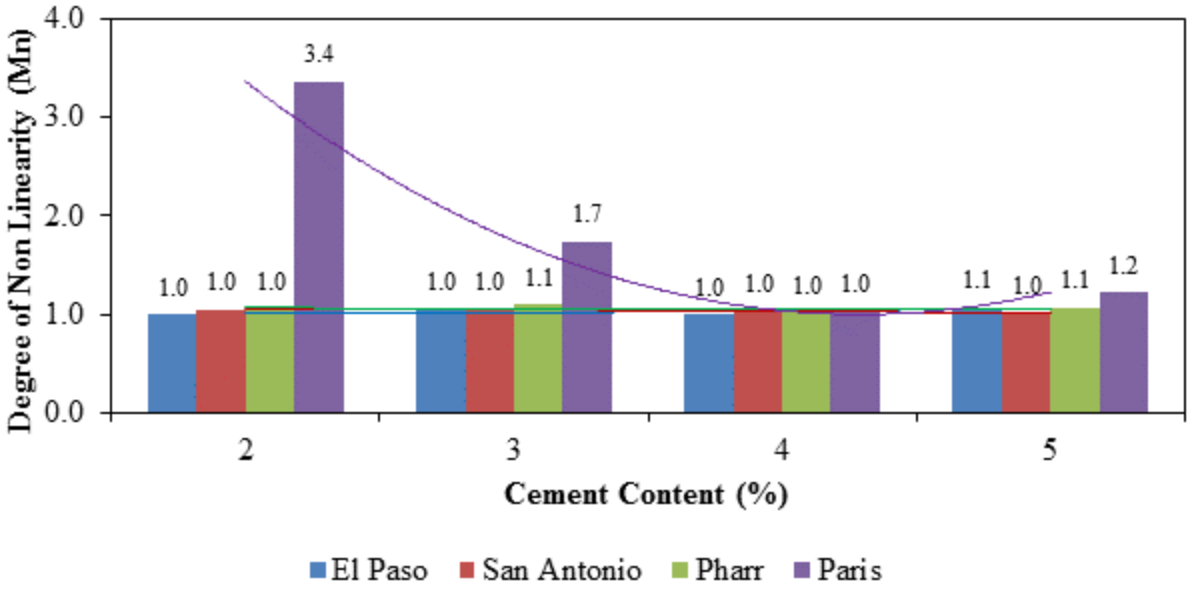

Figure 4.24: Degree of Non-linearity for 10-Day Capillary Soak Specimens.

Characteristics of Tensile Behavior

Compressive behavior and tensile behavior of the stabilized specimens were independently presented and discussed in previous sections of this study. The simultaneous improvements in tensile and compressive behavior of stabilized systems can be seen in figure 4.25. As shown in this plot, the orthogonal improvements of strength are anisotropic for all variants. This is more pronounced for Pharr materials that show nearly twice the rate of improvement of strengths in compression as compared to strength gain in tension. The compressive and tensile improvements are not the same with different cement contents. The degree of non-linearity also changes significantly from compressive and tensile loading procedures. According to the findings of this study, it is not recommended to use compressive procedures such as UCS test to characterize the tensile characteristics of stabilized specimens.

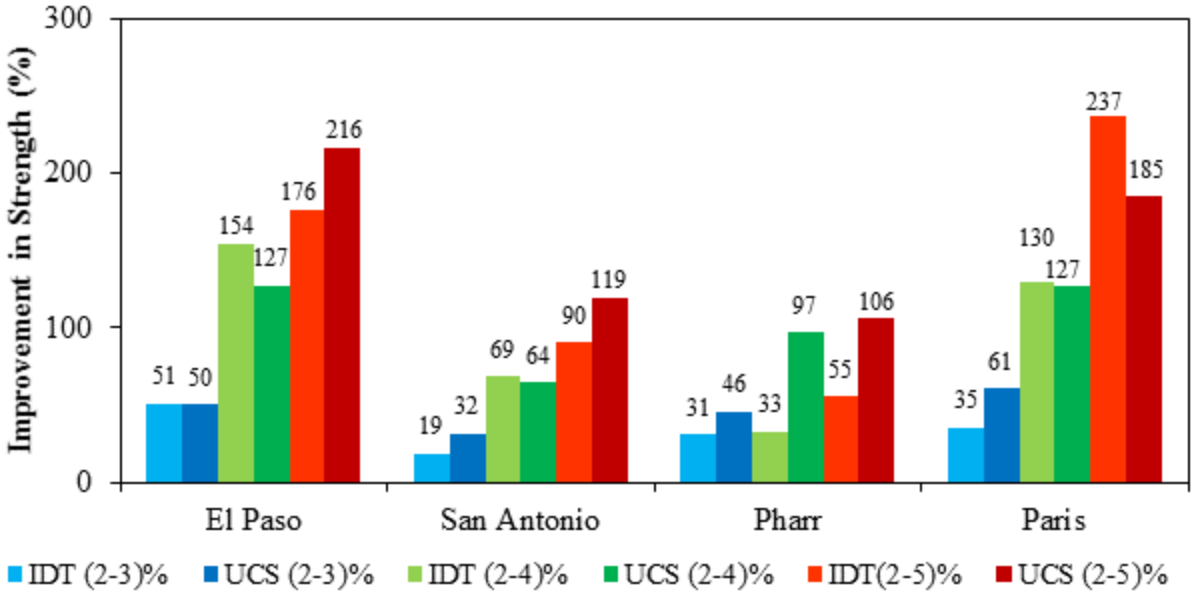

Figure 4.25: Improvements in Tensile and Compressive Strength Dynamic Indirect Diametrical Test (IDT).

SUBMAXIMAL MODULUS TEST

The stress-controlled Submaximal Modules test was performed on the 6 x 12 inch (152 x 305 mm) cylindrical stabilized specimens. The stress magnitudes applied to the specimens were selected based on the compressive strength values obtained from the UCS test. Strength portions of the UC strength values specifically 20, 40 and 60 percent, were applied for 5,000 repetitions for each variant. Figure 4.26 shows El Paso specimens fragmented after the Submaximal Modulus test. The loading intervals were 0.1 sec and the rest period was 0.9 sec per cycle with a total of 1 sec per cycle. It is important to mention that certain specimens failed before reaching 5,000 load applications at 60 percent of strength. Figure 4.27 illustrates the normalized permanent deformation after 5,000 load applications for the 7-day moist cured specimens at 20 percent UC strength. Since the percentage of strength applied is not the same for all variants, it is necessary to normalize the measured strain deformations by the stress amplitudes for proper comparison between different cement content and materials. For instance, 20 percent of UC

strength of a Pharr material with 2 percent cement content is significantly lower compared to Paris material with 5 percent cement content.

Figure 4.26: El Paso Specimens after Failure in the Submaximal Modulus Test.

Since higher stresses induce more deformation, the strains are normalized by the stress applied. Therefore, the results show the strain deformation per unit of stress applied. The results show a notable reduction in the final permanent deformation for all materials tested as cement content increases. Figure 4.27 clearly shows the deficit of the Pharr materials in terms of permanent deformation potential after 5,000 cycles for the 7-day moist cured specimens. As illustrated in figure 4.27, the magnitude of the permanent deformation, after 5000 load applications, observed for El Paso, San Antonio and Paris materials were close to each other.

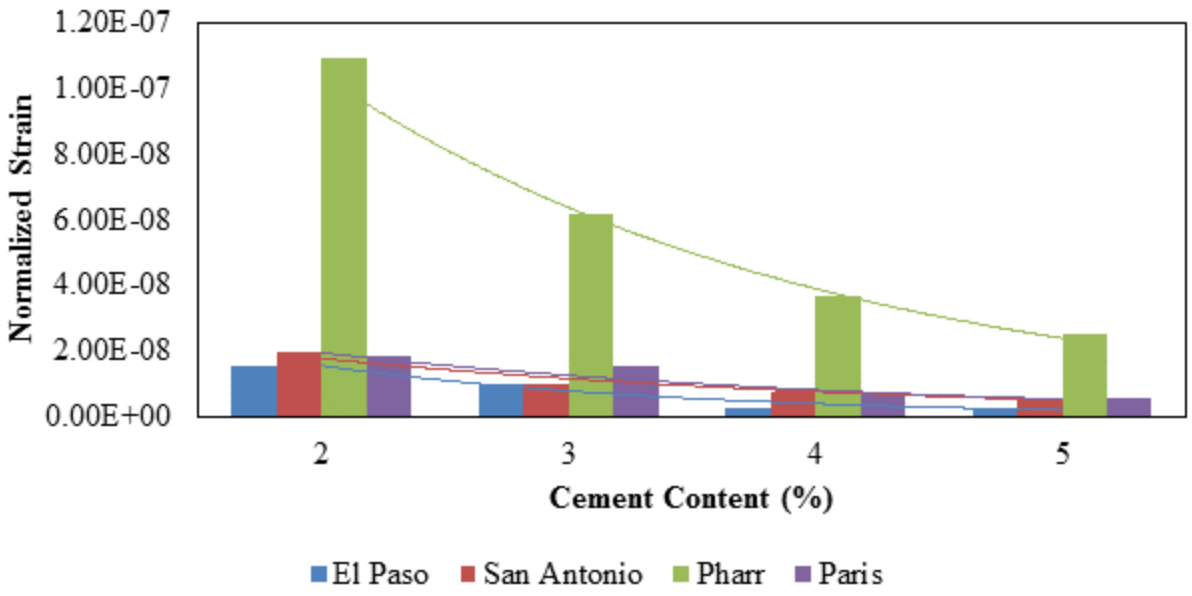

Figure 4.27: Plastic Deformations for 7-day Moist Cured Specimens.

Figure 4.28 represents the normalized plastic strains for the TST specimens. One interesting observation when comparing figures 4.27 and 4.28 results was the significant reduction of deformations of Pharr materials in the TST specimens. This could be attributed to the time-dependent nature of the pozzolanic reactions and their sensitivity to the rate and velocity of silica solubility in the mixes. The trends show that Pharr and San Antonio materials deform more than Paris and El Paso materials.

Figure 4.29 illustrates the reduction in the cumulative plastic deformation as cement content increases in the specimens for the 7-day moist cured condition. Comparable to the procedure presented for analysis of the previous tests, the deformations of the 2 percent cement content specimens were selected as the initial value to compare with the improvements at 3, 4 and 5 percent. The results demonstrated a notable reduction in the permanent deformation by increasing the cement content in all permutations of the experiment design. This positive influence of soil stabilization is more pronounced for El Paso specimens compared to Pharr

specimens. This confirms that soil stabilization reduces the permanent deformation under cyclic loading.

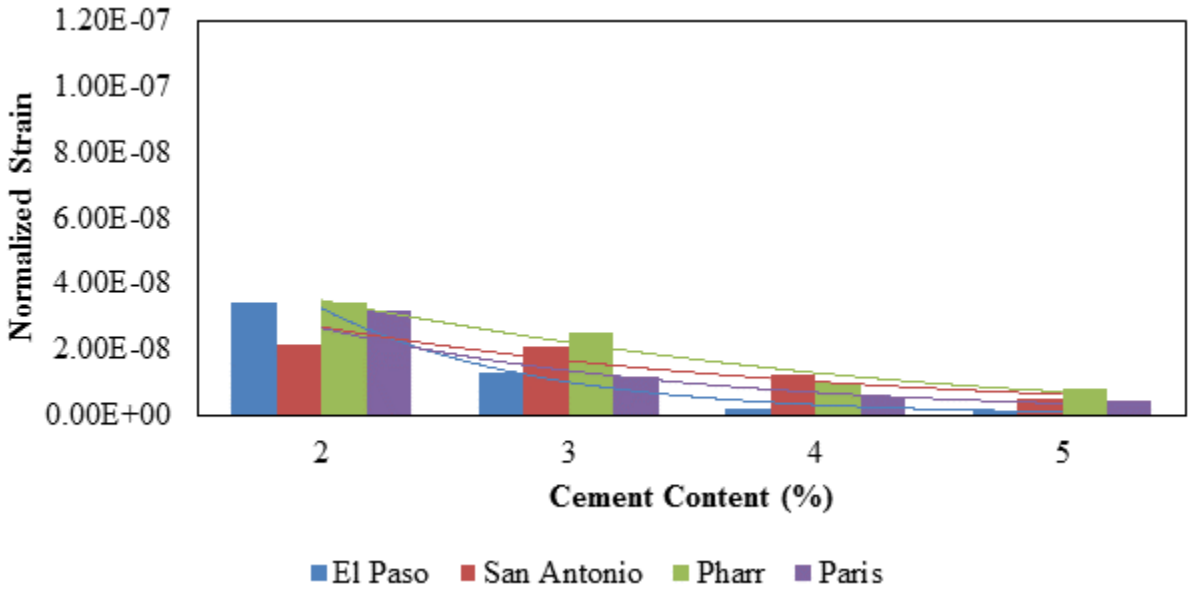

Figure 4.28: Plastic Deformations for 10-Day Capillary Soak Specimens.

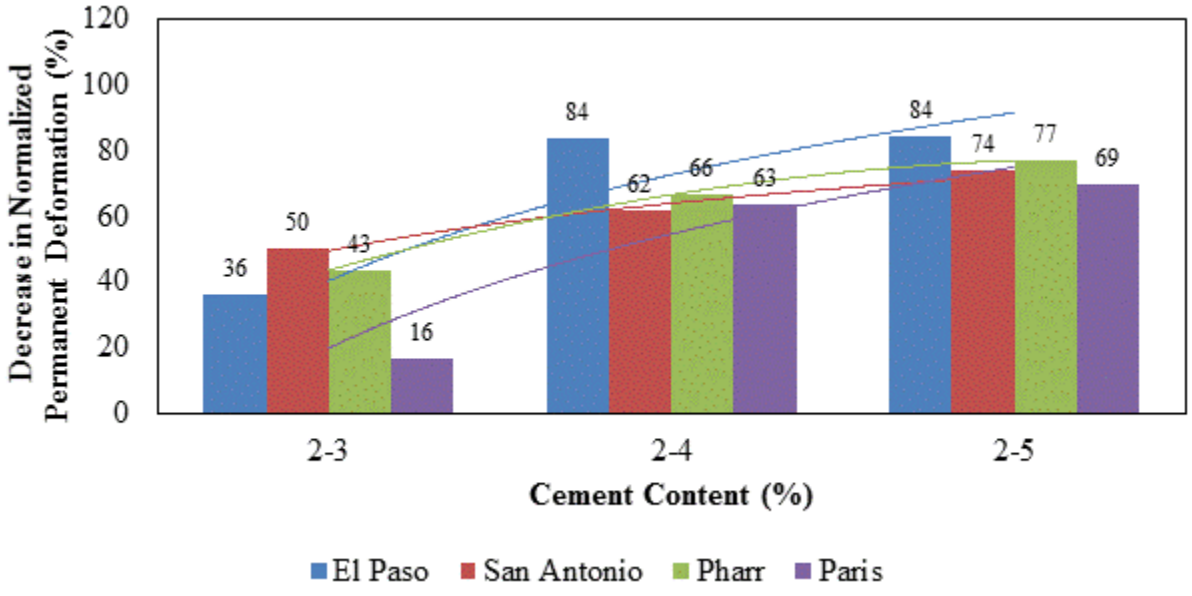

Figure 4.29: Reduction of Plastic Deformations after 5,000 cycles for 7-day Moist Cured Specimens.

A similar argument is valid for the TST specimens as illustrated in Figure 4.30. The trend of the data shows the reduction of plastic deformations by incremental increase of cement content in the mixes. One notable observation was the significant reduction of the normalized plastic deformation in the 10-day capillary soak specimens. Again, this could be attributed to the moisture intrusion when pozzolanic reaction occurs within the stabilized specimens. In conclusion, the trend analysis demonstrated that the Submaximal Modulus test properly captures the compressive dynamic performance of stabilized materials. However, the dynamic performance of the tensile component can be very different from the compressive component.

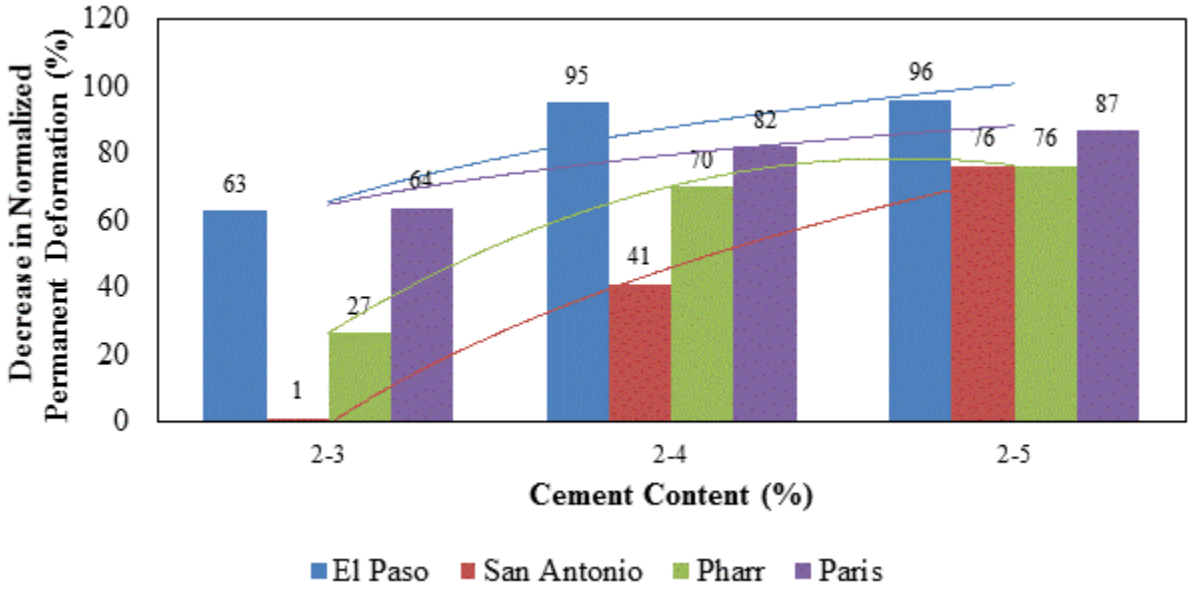

Figure 4.30: Reduction of Plastic Deformations after 5,000 cycles for 10-Day Capillary Soak Specimens.

DYNAMIC INDIRECT DIAMETRICAL TENSION (D-IDT) TEST

IDT specimens of 6 x 4.5 inch (152 x 114 mm) where subjected to dynamic stress-controlled protocol. The test setup and the sample geometry were similar to the static IDT test. Similarly, to Submaximal Modulus test, the dynamic load pulse amplitude was selected as fractions of the static IDT strength. Three incremental strength levels of 20, 40 and 60 percent of

IDT strength were cycled for 50,000 load repetitions to identify the permanent deformation of stabilized materials subjected to a high number of load cycles. The load applications were applied at frequency of three Hz. Additionally, the permanent deformations were normalized utilizing the same procedure presented in Submaximal Modulus test. In some cases, the specimens could not be tested for 50,000 load applications since the specimens reached failure before the completion of the test. Figure 4.31 shows the specimen setup and sample failure in the dynamic IDT test.

Figure 4.31: Dynamic Indirect Diametrical Test (IDT) (a) Specimen Setup (b) Fractured Specimen.

Figure 4.32 illustrates the normalized cumulative plastic deformations of the 7-day moist cured specimens after 50,000 cycles applied at 20 percent static IDT strength. The trend of the data clearly shows a favorable influence of the increasing stabilizer content to control the permanent deformation of stabilized specimens. This indicated that the IDT test applied to dynamic loading protocols properly captures the maximum tensile deformation of stabilized specimens. This is an important fact since many current design approaches utilize the tensile strain at the bottom fibers of the layer to predict the fatigue life of stabilized bases. Similarly, Figure 4.33 shows the normalized cumulative plastic deformations for TST samples.

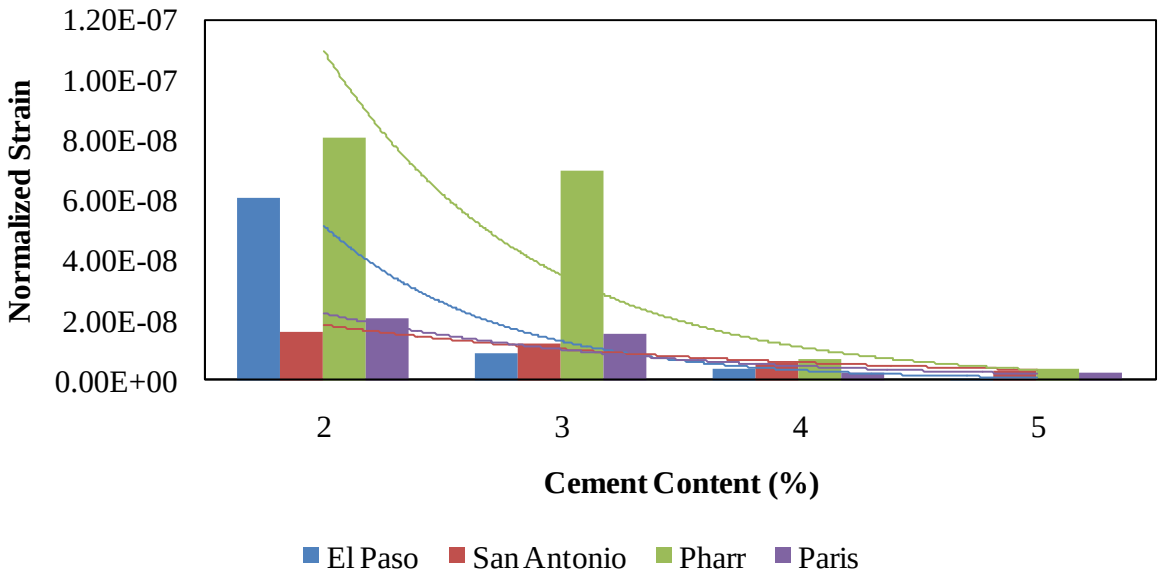

Figure 4.32: Cumulative Plastic Deformation after 50,000 Load Cycles for 20% Dynamic IDT for 7-Day Moist Cured Specimens.

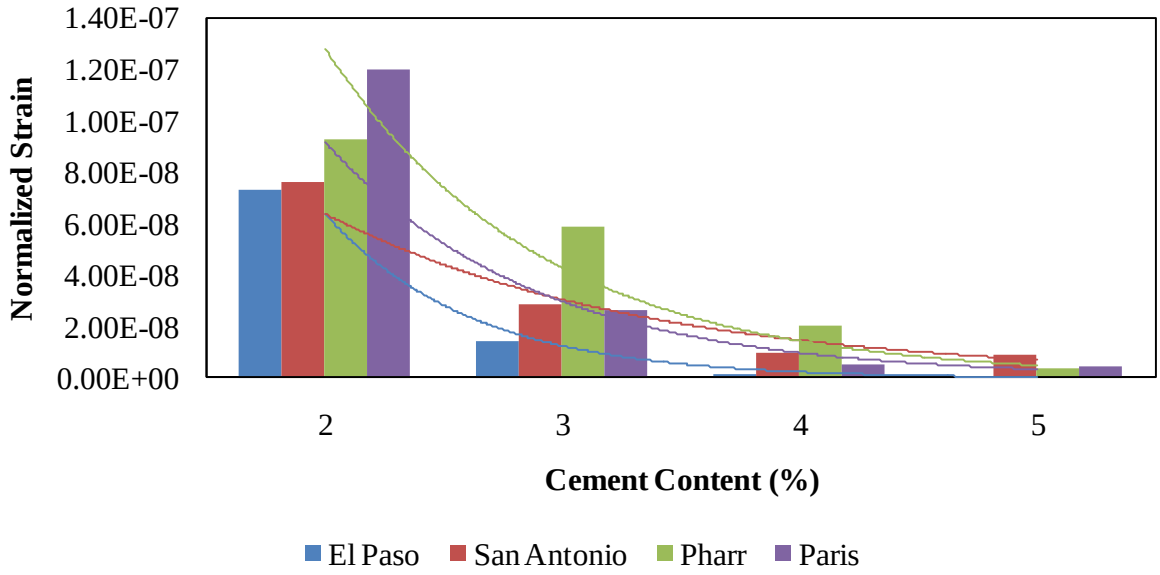

Figure 4.33: Cumulative Plastic Deformation after 50,000 Load Cycles for 20% Dynamic IDT for 10-Day Capillary Soak Specimens.

Figure 4.34 and 4.35 shows the percent reductions in the plastic deformation as cement content increases for 7-day moist cured and TST specimens respectively. An interesting observation illustrated in these figures is the fact that increasing the cement content from four to

five percent did not have a significant influence on reducing the plastic deformations after 50,000 load cycles. A reasonable explanation could be the fact that the permanent deformation curves have already reached an asymptotic behavior. Therefore, increasing the cement content has negligible influence on the permanent deformation of the specimens.

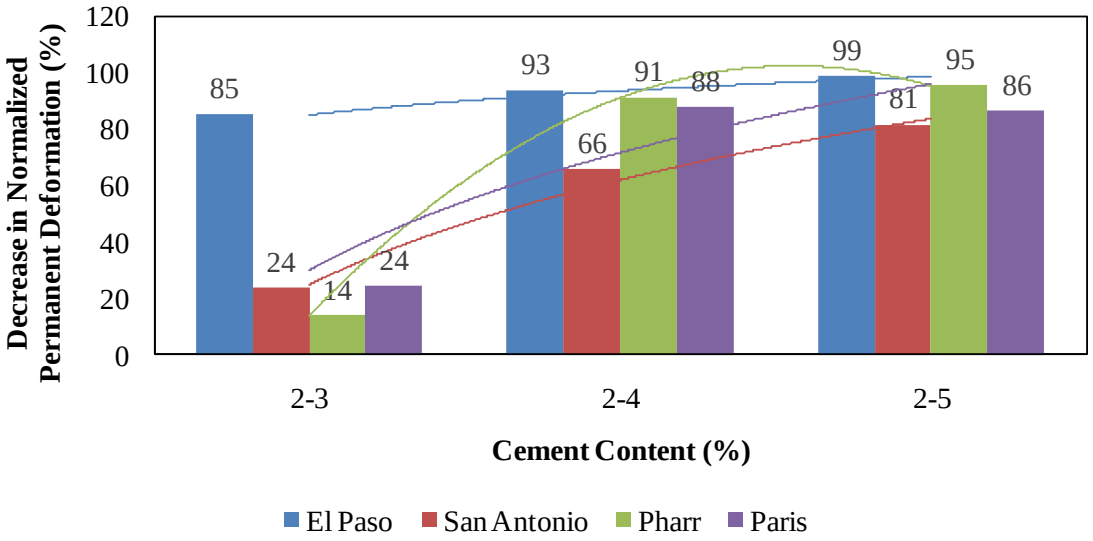

Figure 4.34: Percent Decrease in Plastic Deformation after 50,000 Load Cycles in Dynamic IDT Test for 7-Day Moist Cured Specimens.

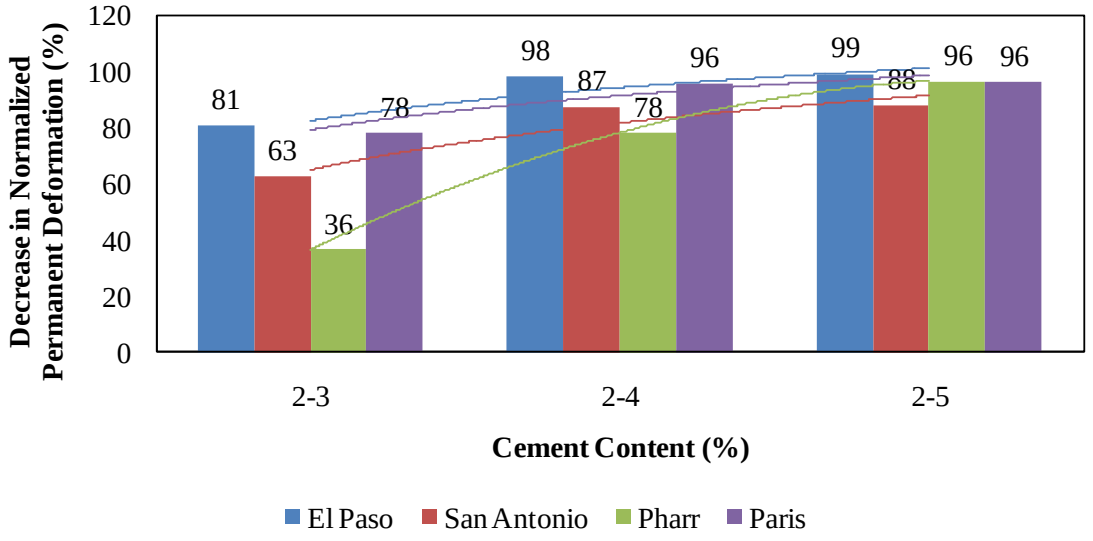

Figure 4.35: Percent Decrease in Plastic Deformation after 50,000 Load Cycles in Dynamic IDT Test for 10-Day Capillary Soak Specimens.

DIELECTRIC TEST

The moisture susceptibility potential of the stabilized specimens was determined by analysis of dielectric values using a Rainbow dielectric constant meter. The variations in the dielectric constant values are an indication of the change in the available moisture content within the pore structure of the specimens. The dielectric values of the TST specimen were measured every day for 10 consecutive days at five points at the top of the specimen as Figure 4.36 indicates. The locations were numbered in order to perform the measurements at the same locations.

Figure 4.36: Dielectric Test Set Up

The average values of the five measurements were then calculated and reported as the representative dielectric value for each variant of the experiment design. The results presented in all figures are for 6 x 12 inch (152 x 305 mm) specimens for all the permutations of the experiment design. Figure 4.37 shows the variations of the dielectric values of Paris specimens subjected to 10-day capillary soak at ambient temperature. The small variability of the dielectric

values during 10 days of testing for all stabilizer contents indicates that the unbound moisture was not able to travel and reach the top portion of the specimens. This is an indication of insignificant sensitivity of the selected aggregates to hold and transport moisture in the pore structure.

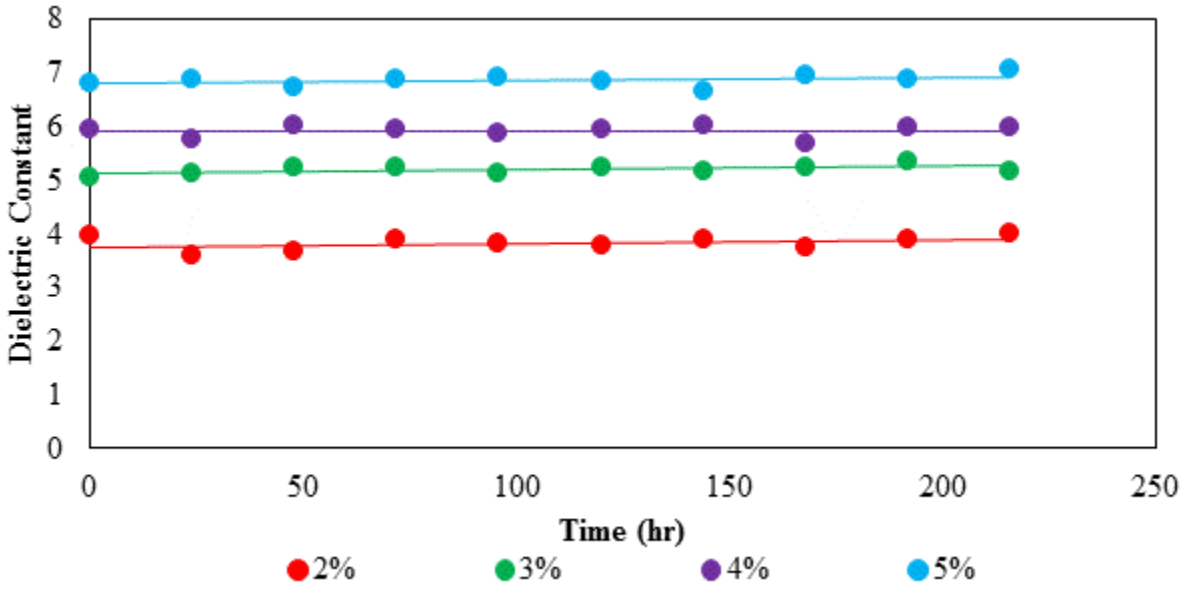

Figure 4.37: Variations of Dielectric Values for Paris Sandstone for 10 Day Capillary Soak Specimens

Figure 4.38 presents the cumulative results of the dielectric value measurements for 10-day capillary soak (TST) specimens. In order to initially develop this plot, the averages of the five point-measurements for each specimen were computed. Subsequently, the averages of the dielectric values for 10 consecutive days were calculated. In other words, every single bar in Figure 4.38 is the average of 50 data points [5 (measurements at the top of specimen) x 10 (days) =50]. Therefore, Figure 4.38 summarizes 800 dielectric value measurements into one plot. This provides valuable information for comparative analysis of the moisture susceptibility of the stabilized materials. One interesting observation that can be clearly observed from this figure is the lower dielectric constants for the Paris specimens when compared to other materials in the

experiment design. This could be attributed to either low moisture retention capacity of aggregates sources from the Paris district, or the consumption of the available moisture in strength gain reactions to improve the mechanical properties of the Paris specimens.

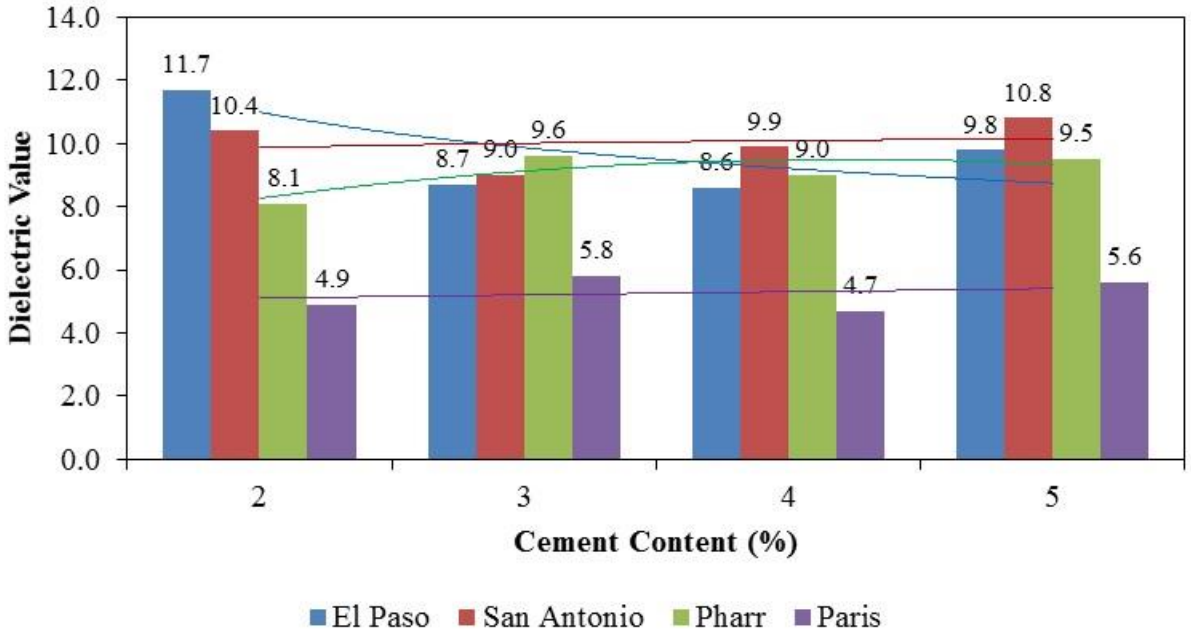

Figure 4.38: Dielectric Values for TST Curing Procedure Specimens

SEISMIC MODULUS TEST

The Free-Free Resonant Column (FFRC) test was utilized to estimate the small strain seismic moduli of the stabilized specimens. Additionally, it was used to measure the daily improvement on the stiffness properties for all variants in this study. The FFRC test was performed based on Tex-148-E (draft) procedure. This test was useful to recognize the improvement rate in stiffness properties as pozzolanic reactions occured in the specimens. Figure 4.39 through Figure 4.42 present the variations of seismic modulus test results for El Paso, San Antonio, Pharr, and Paris materials for 10 consecutive days. The data provided in these figures correspond to 6 x12 inch specimens for the TST curing procedure. As evidenced in Figure 4.39

through Figure 4.42, increasing the stabilizer contents resulted in higher small strain modulus values. The ascending pattern of the trends is an indication of the favorable influence of the provided moisture in contributing to the strength gain reactions. This information, combined with the observations presented in Figure 4.38, explains that the moisture is taken up into the curing process to make the specimens stiffer instead of having the moisture at the top of the specimen.

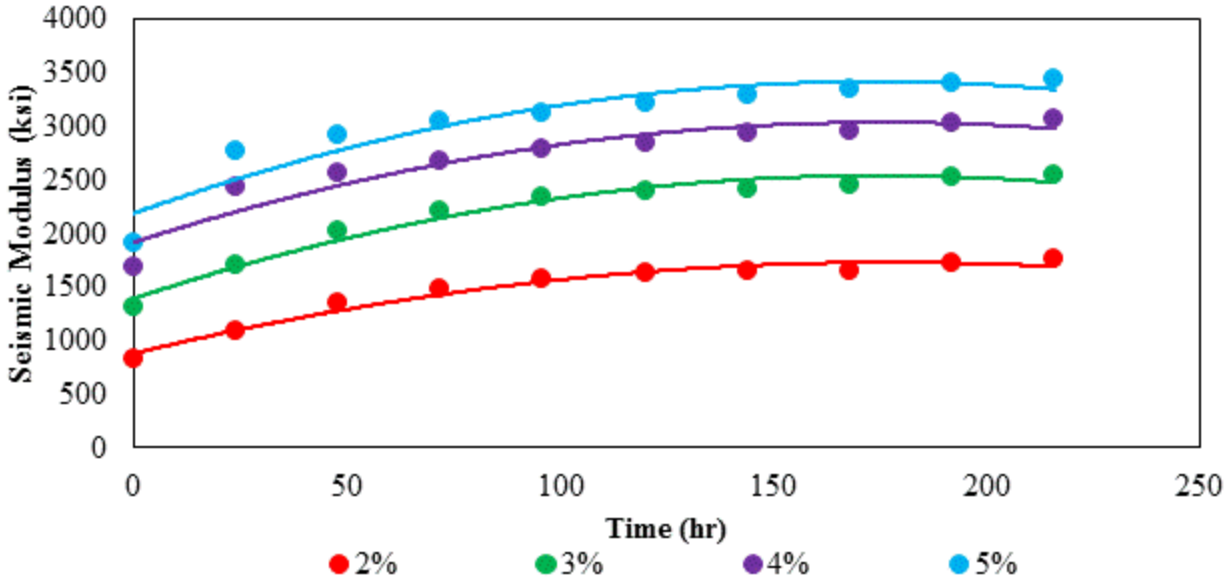

Figure 4.39: Variations of Seismic Modulus for Paris Sandstone for 10-Day Capillary Soak Specimens.

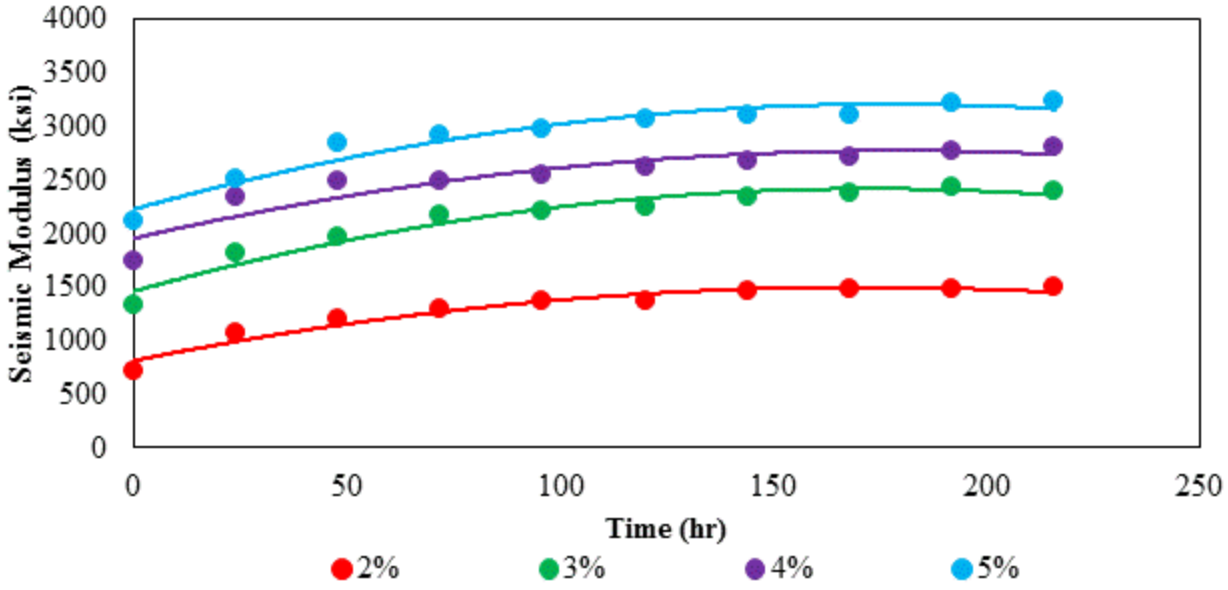

Figure 4.40: Variations of Seismic Modulus for El Paso Limestone for 10-Day Capillary Soak Specimens.

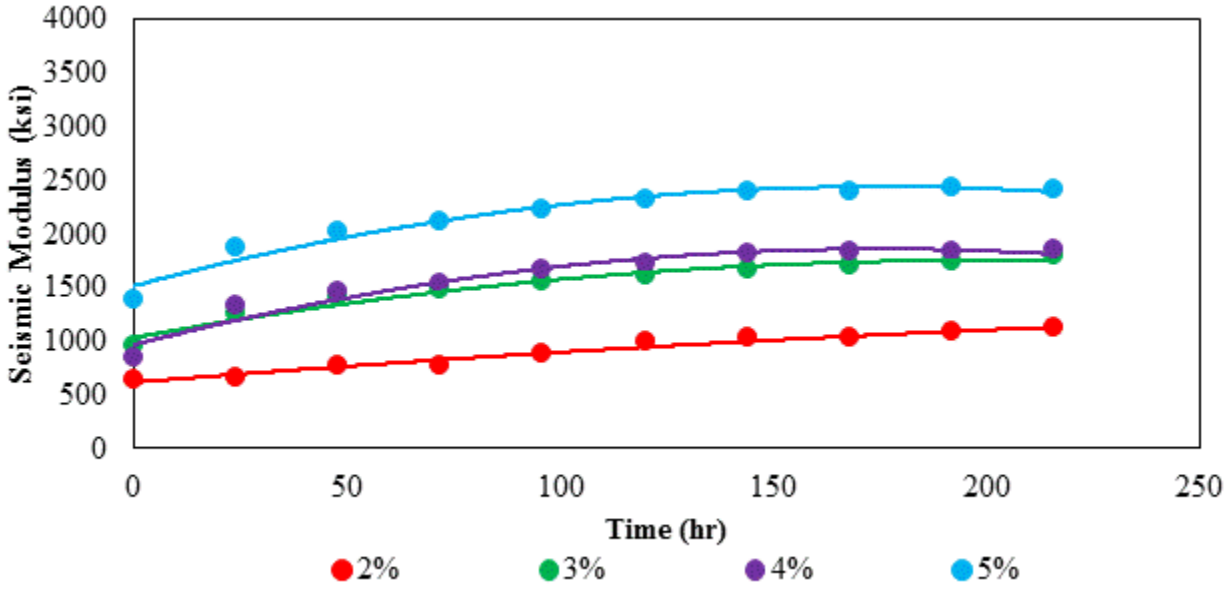

Figure 4.41: Variations of Seismic Modulus for San Antonio Limestone for 10-Day Capillary Soak Specimens.

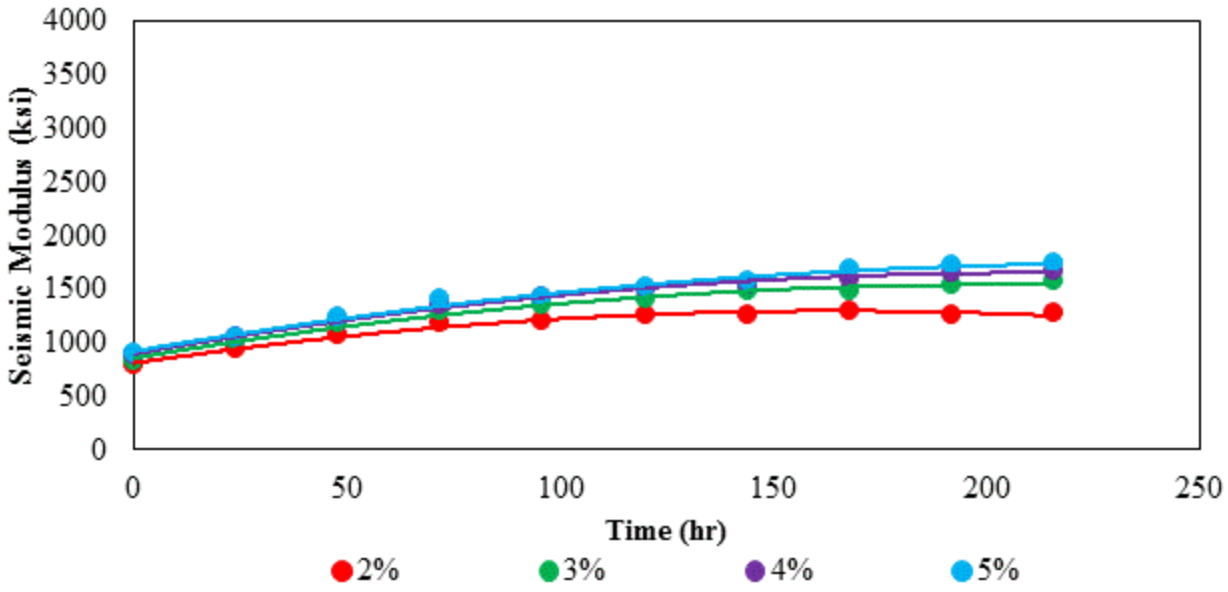

Figure 4.42: Variations of Seismic Modulus for Pharr Gravel for 10-Day Capillary Soak Specimens.

Figure 4.43 provides a comparative summary of the seismic modulus values for all the permutations of the experiment design. Similar to the method used to present the dielectric constant results, the calculated seismic modulus values were averaged over the 10 consecutive days to generate Figure 4.43. Therefore, each bar represents the average of 10 measurements, and the plot is generated based on 192 data points for each material or 768 total data points.

Figure 4.44 shows the improvements in the seismic modulus values with increasing stabilizer contents in the specimens. The seismic modulus improvements were calculated considering the lowest stabilizer content, two percent cement, as the reference level for each material. The rate of improvements, characterized by the slope of the trend lines is additional information provided in this plot. From Figure 4.44 is it observed that El Paso and Paris materials benefited considerably from the increase in the cement contents in the specimen mix compared to San Antonio and Pharr specimens subjected to TST curing conditioning.

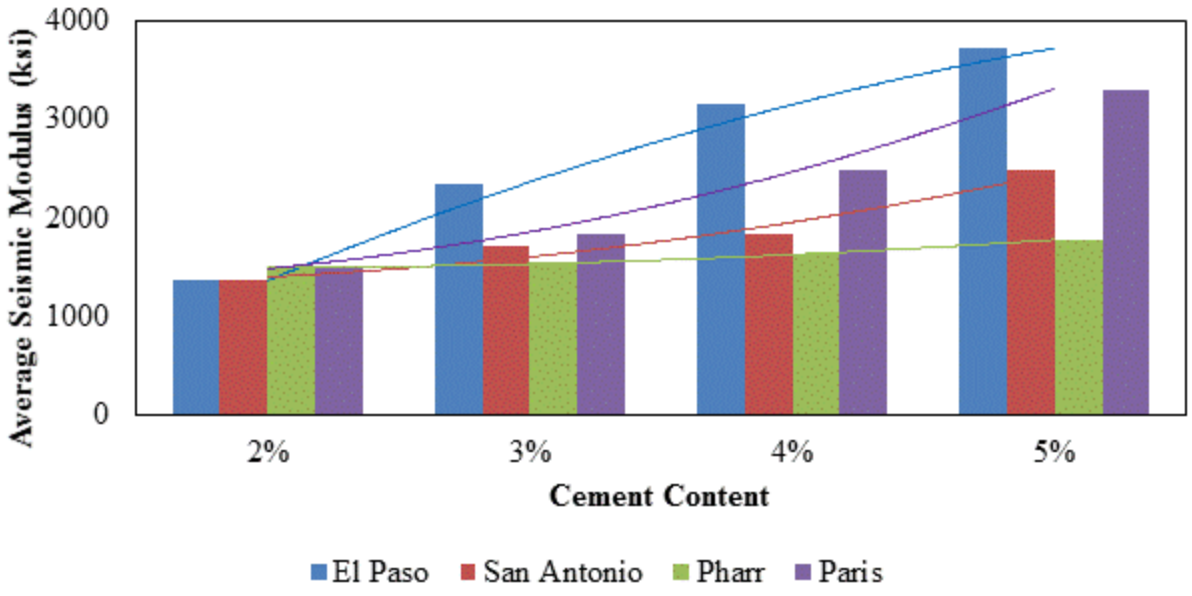

Figure 4.43: Average Seismic Modulus Values for 10-Day Capillary Soak Specimens.

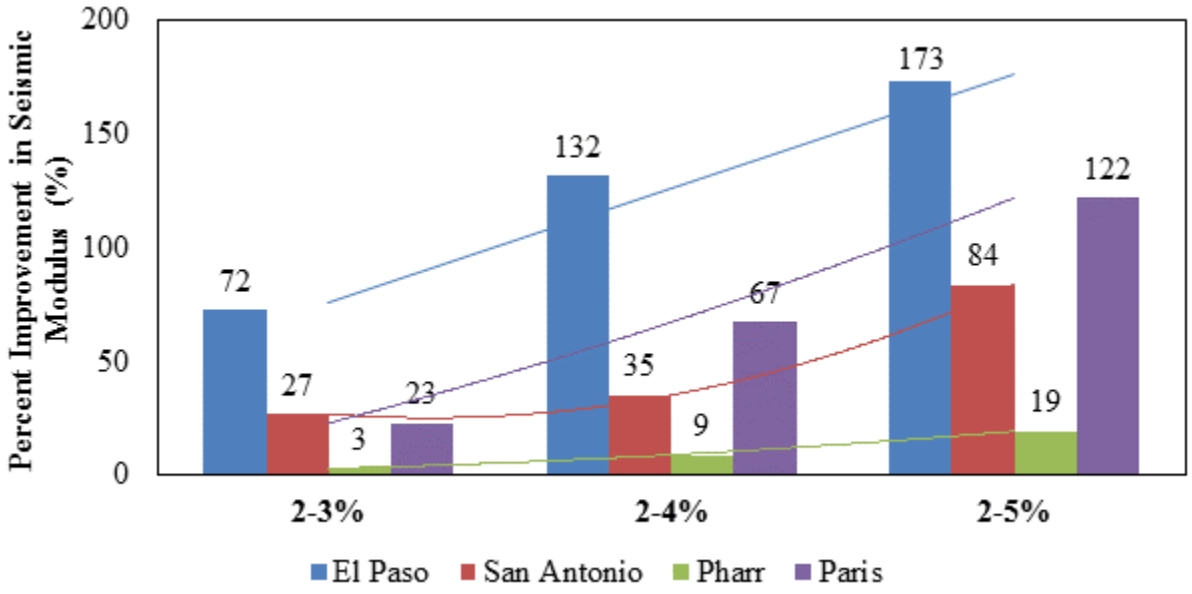

Figure 4.44: Improvements in Seismic Modulus for 10-Day Capillary Soak Specimens.

Chapter 5: Conclusion

INTRODUCTION

The fatigue performance models currently incorporated within the mechanistic design guides are regulated principally by the strength ratio and the modulus of rupture of stabilized specimens. However, an extensive review of the traditional four-point beam test revealed several theoretical and practical concerns presented in Chapter 1. Therefore, this study was conducted with the intention of providing an alternative testing protocol to characterize properly the tensile properties of stabilized granular materials.

According to the scope of this study, such a testing protocol should be practical to perform in the laboratory and it should be capable of proving precise and accurate results. Additionally, this new approach should be implemented on several materials with different mineralogies with a determined range of cement contents. In addition, this new procedure should be applied to specimens with different curing conditions, especially to specimens subjected to moisture susceptibility tests in the laboratory.

Based on the literature review presented in Chapter 2, the Indirect Diametrical Tension (IDT) test is an excellent candidate to replace ordinary methods in the laboratory. An experiment matrix was developed to achieve this objective where four different materials at four cement contents and two curing conditions were subjected to compressive and tensile testing procedures. Table 5.1 summarizes the material selection, gradation, curing conditions, cement contents and test procedures selected for this study.

Table 5.1: Experiment Design

<table>
<tr><th>Material Selection</th><th>Gradation</th><th>Curing Condition</th><th>Cement Content</th><th>Test Procedures</th></tr>
<tr><td rowspan="2">El Paso Limestone</td><td rowspan="5">Grade 4</td><td rowspan="3">7 day Moist Cured</td><td rowspan="5">2%, 3%, 4%, 5%</td><td>Unconfined Compressive Strength (UCS)</td></tr>
<tr><td rowspan="2">San Antonio Limestone</td><td>Submaximal Modulus</td></tr>
<tr><td>Static Indirect Diametrical Tension (S-IDT)</td></tr>
<tr><td>Pharr Siliceous Gravel</td><td rowspan="3">Ten Day Capillary Soak Suction (TST)</td><td>Dynamic Indirect Diametrical Tension (D-IDT)</td></tr>
<tr><td rowspan="2">Paris Sandstone</td><td>Dielectric Value</td></tr>
<tr><td>Free-Free Resonant Column (FFRC)</td></tr>
</table>

The main purpose of this study was to develop several testing protocols from the IDT test to replace the traditional four-point bending beam test. Additionally, the unconfined compressive strength test, and submaximal test were performed on all permutations of the experiment design to compute the strength and deformation potential of the stabilized materials subjected to compressive axial loads. The tensile mechanical behavior of the specimens was determined using the static IDT and the dynamic IDT tests developed in this study. The tensile laboratory test results were compared with the comprehensive tests results to confirm the theoretical results in terms of strength gaining and deformation reduction as cement content increased in the specimens. In other words, the laboratory data was validated based on the trend analysis of the results. Table 5.2 provides the total number of specimens used by each testing method in this project. The number of specimens prepared includes the re-tested variants considered for the replicates. Therefore, Table 5.2 provides the total number of specimen tested in each permutation in the experiment design.

Table 5.2: Specimen Tested for each Material.

Material	UCS	Static IDT	Dynamic IDT			Submaximal Modulus			Total
			20%	40%	60%	20%	40%	60%	
El Paso	26	24	30	32	25	14	16	16	183
San Antonio	17	16	20	20	24	18	19	19	153
Pharr	24	28	19	14	11	20	13	10	139
Paris	20	19	9	8	9	9	10	11	95
TOTAL	87	87	78	74	69	61	58	56	**570**

In addition to the mechanical strength and deformation tests, two curing conditions were incorporated in the experiment design to study the influence of moisture intrusion on the mechanical performance of the stabilized specimens. The constant nature of the dielectric value trends, when combined with increasing trends of seismic modulus, revealed the favorable role that moisture provides in developing pozzolanic reactions within the specimens.

DEVELOPMENT OF AN ALTERNATIVE LABORATORY TESTING PROTOCOL

In order to achieve the primary objective of the study, the following components were considered for the development and refinement of traditional testing procedures to be implemented in the tensile characterization of stabilized granular materials.

Practical Aspects

The proposed testing protocol derives from traditional testing methods (i.e., similarity to traditional split tension test). Consequently, laboratory personnel can easily perform this test. Additionally, the specimen sizes are similar to those of traditional dimensions in order to eliminate the requirement of obtaining new molds, sample extruder, etc. Figure 5.1 illustrates the dimension of the IDT specimens. The time consumed and the personnel required for the execution of the static IDT test is another important factor to take into consideration. The time

needed to accomplish the S-IDT test from the placement the specimen and set up of the test until completion is about 3-5 minutes, depending in the tensile strength magnitude of the stabilized specimen. Additionally, only one person is essential for the execution of this test, including handling and transportation of the specimen to the loading frame. The material required in this IDT test is less than 11 lb., a significantly lower quantity when compared to the 60 to 80 lb. of material required in the four-point bending beam test.

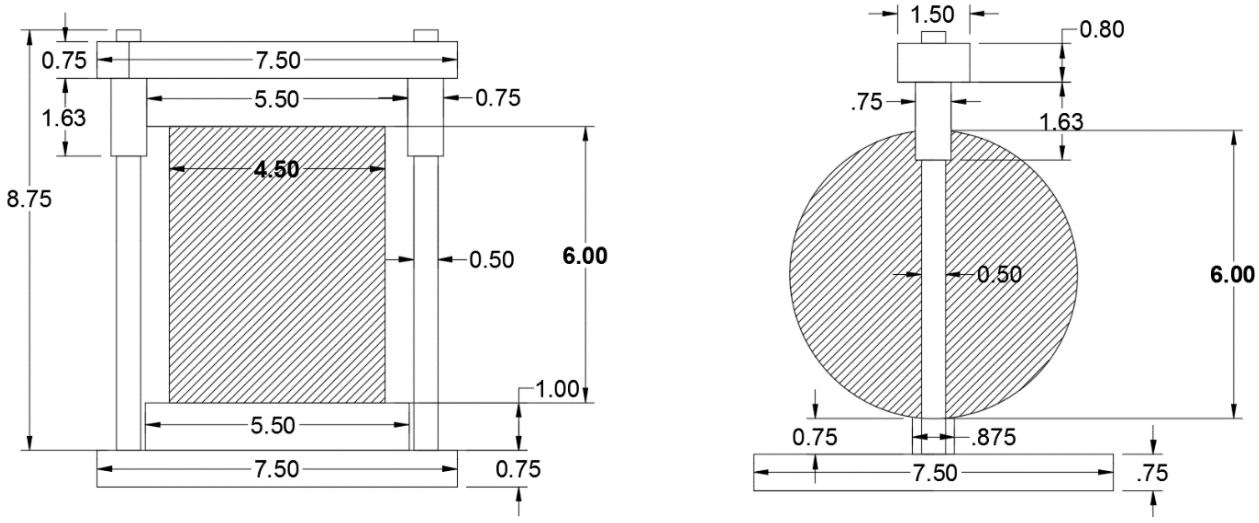

Figure 5.1: Dimensions of the Static IDT Test

Theoretical Aspects

In order to validate the data results of a new testing protocol; such test must follow theoretical principal with the least amount of uncertainty in the assumptions. For example, according to Mehta (2006) in the split tension test, a more uniform tensile stress distribution is observed along the failure plane of the specimens as Figure 5.2 indicates. The stress distribution clearly illustrates that around 85 percent of the cross section is acting uniformly in tension.

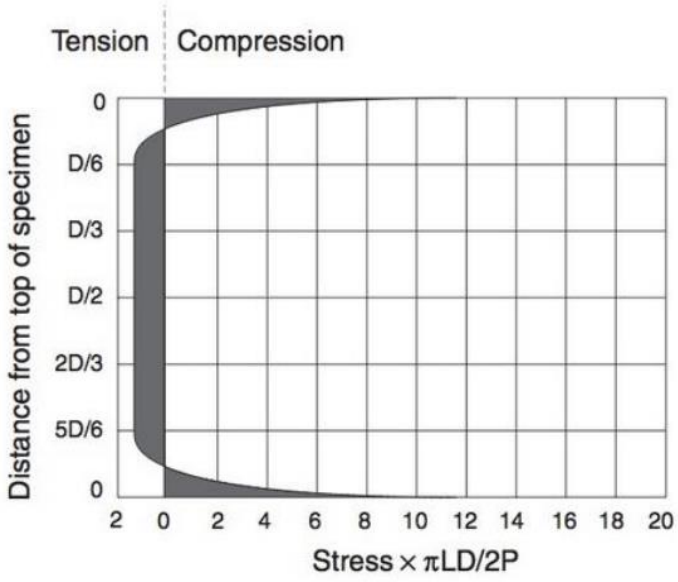

Figure 5.2: Diagrammatic Arrangements of the Split Tension Test Stress Distributions (Mehta 2006)

In order to prove the observations made by several previous researchers, a series of finite element analyses demonstrated the actual stress distribution of the IDT test. Figure 5.3 provides the stress distribution of 6 x 4.5 inch (152 x 114 mm) cylindrical specimen subjected to a strain controlled split tension test. The warmer colors in this plot (positive values of stresses) indicate tension and cooler colors (negative values) represent compression in the specimen. The compressive load applied on the rotated cylindrical specimen results in the failure of the sample in tension. These plots clearly show the capacity of this split tension test to induce relatively uniform tension along the axis of loading within the specimen. The top and bottom portions of the specimen experience compressional deformations however, the majority of the specimen experiences tension due the application of the axial compressive load.

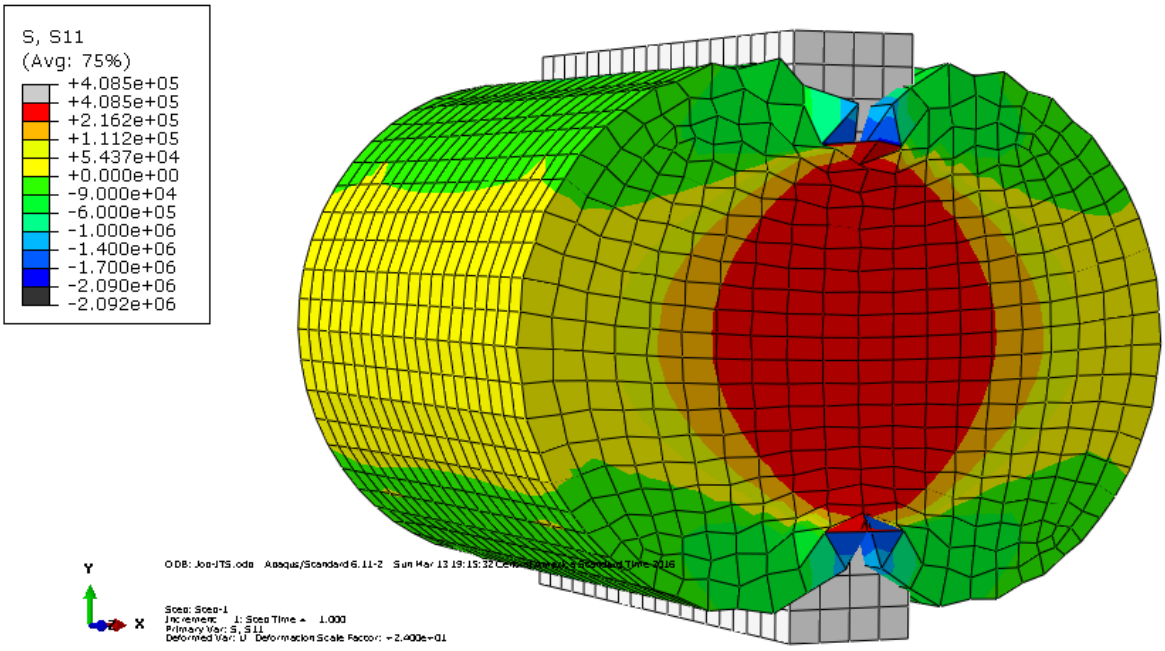

Figure 5.3: Distribution of the Stresses in the Indirect Diametrical Tensile Test.

The finite element analyses of the four-point beam test was compared with the traditional split tension test to develop a better understanding of the behavior of stabilized specimen in such tests. Figure 5.4 shows the side-by-side comparisons of stress distributions in cross section of the tensile tests. The nonlinear nature of the stresses in the four-point beam test imposes a systematic error for the calculations of the modulus of rupture of the stabilized materials.

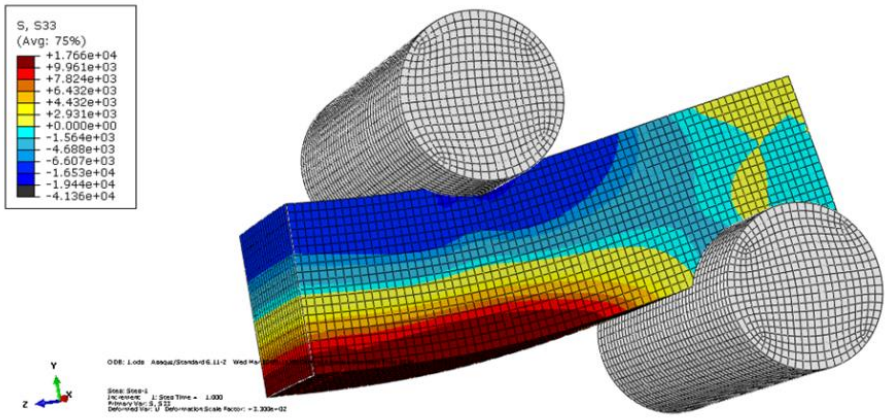

(a)

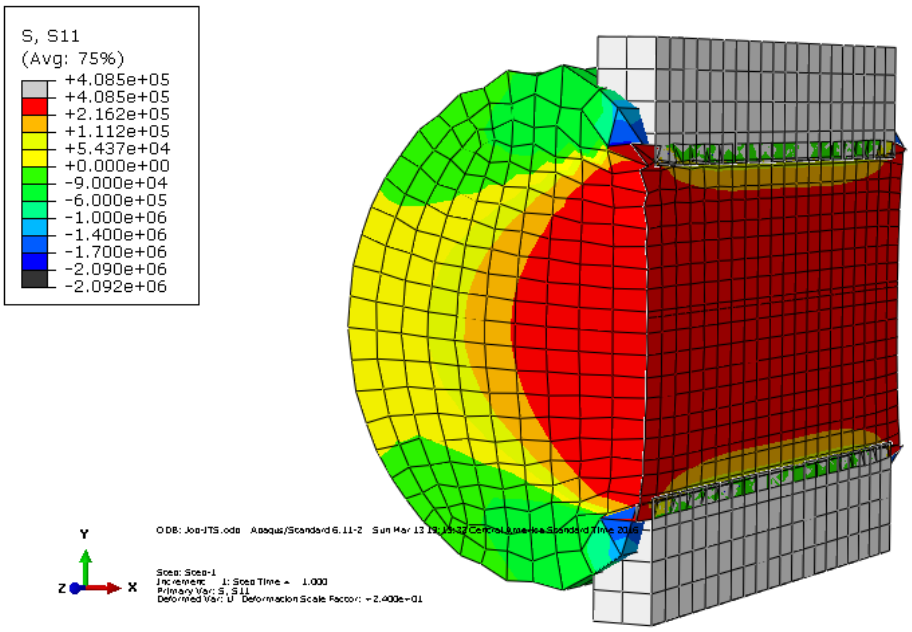

(b)

Figure 5.4: Nature of Stress Distributions in (a) Four-Point Beam Test (B) Indirect Diametrical Tension Test.

Hudson and Kennedy (1968) identified several modes of failure in the indirect diametrical test. They recognized that the idealized mode of failure is a straight crack along the frame supports where the tensile stress distributions exhibit higher magnitudes. Figure 5.5 (a) illustrates the idealized mode of failure according to Hudson and Figure 5.5 (b) represents the actual mode of failure for stabilized specimens in the split tension test for this study. The similitude in these two cases is extremely high; the crack in the stabilized specimen follows a relative linear shape along the failure plane. This is another indication of the validity of the IDT test as applied to stabilized materials.

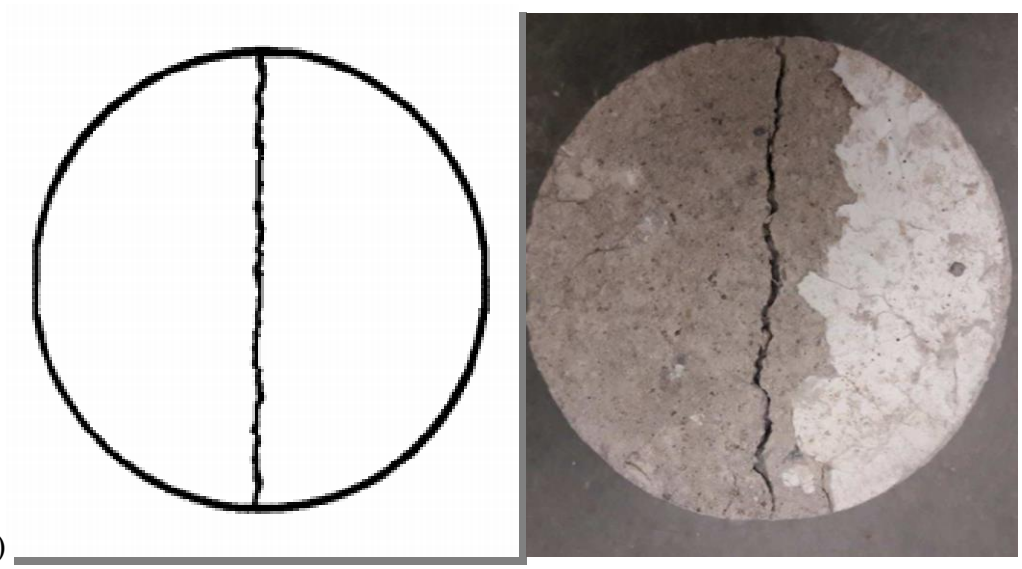

Figure 5.5: Mode of Failure of the IDT Test (a) Idealized Case (b) Actual Case

In conclusion, the finite element analysis of the slip tension test and the corroboration of the trend analysis of the static and dynamic IDT results validates the implementation of such test in stabilized specimens. This test is suitable for analyzing the influence of stabilizer content and aggregate mineralogy on the tensile behavior of cement treated granular materials. Additionally, this testing protocol is significantly easier to perform in the laboratory compared to the ordinary four-point bending beam test, especially for stabilized materials at low cement content. This study has demonstrated the different behavior of the compressive and tensile properties of stabilized materials such as; the degree of non-linearity, stress-strain relationships and level of improvement in strength ratio as cement content increases. Consequently, characterizing the tensile properties of stabilized specimens based on compressive testing procedures such as UCS test is not appropriate since the stress-strain relationships behave very differently in tension and compression. Additionally, the increments of cement content in the specimens do not have the same level of enhancement of tensile and compressive strengths.

RECOMMENDATIONS AND FUTURE WORK

This study has proposed a new testing procedure for the characterization of the tensile properties of stabilized systems. Such tensile properties involve fatigue performance under cyclic loading conditions that the base layer experiences thought its service life. For this reason, the Dynamic IDT test can be implemented for the fatigue characterization of stabilized systems based on the results presented in this study. The expansion and continuation of the D-IDT test is a suitable alternative to develop a fatigue model and characterizing the fatigue performance of stabilized systems in the laboratory. Additionally, this study suggests the inclusion of more materials into the experiment design such as Recycled Asphalt Pavement (RAP) and Recycled Concrete Aggregate (RCA). In conclusion, the database developed in this study provides valuable information to develop a full laboratory characterization of stabilized systems in terms of fatigue performance to predict the life cycle of stabilized base layers in the field.

SUMMARY OF THE MAJOR POINTS

This section provides a quick resume of the major findings of this study along the chapters:

I. Cement base stabilization is an exercise commonly implemented along U.S. since it reduces the thickness of the pavement layers.

II. Reflective cracks propagate from cement treated bases to the surface layers causing a deleterious effect in the performance of pavement layers therefore proper characterization of the tensile properties of stabilized base layers is extremely important.

III. New mechanical-empirical design approaches utilize the modulus of rupture as a decisive component that controls the fatigue life of stabilized base layers.

IV. The traditional testing method, the four-point bending beam test has demonstrated practicality issues associated with specimen de-molding, handling, transportation,

uniformity of compaction of large beams in the laboratory for lightly stabilized materials.

V. Finite element analyses of the four-point bending beam test revealed the systematic error associated with the assumption of linear stress distribution for the determination of the modulus of rupture in the test

VI. An extensive literature search illustrated that the several procedures derived from ordinary tests, such as the UCS and split tension tests, correspond to the current state of practice for the tensile characterization of stabilized materials.

VII. After the development of an experiment matrix, the results showed that the behavior of stabilized specimens is very different in compression and tension conditions therefore; the author does not recommend characterizing the tensile properties from compressive procedures.

VIII. The trend analysis of the post processed data from both dynamic and static IDT tests indicated the validation of the determination of the tensile strength of cement treated materials with different mineralogies, stabilized at different cement content, and different curing conditions.

IX. Based on the theoretical principals of the split tension test, the mode of failure of stabilized specimens corresponds to the idealized mode of failure where the assumptions in the equations validate the results.

X. This study suggests the extension and continuation of the D-IDT test for the use of fatigue performance characterization of stabilized base layers under cyclic loading conditions.

References

Adaska, W. S., Luhr, D. R., 2004. Control of Reflective Cracking in Stabilized Bases. 5th international RILEM Conference, Limoges, France.

Ashtiani R., D. N. Little and E. Masad. 2007. Evaluation of Impact of Fines on the Performance of Lightly Cement Stabilized Aggregate Systems Transportation Research Record (TRR): Journal of Transportation Research Board, No. 2026, Transportation Research Board of National Academics, Washington D.C. ,2007, pp.81-88.

Arnold, G., and Morkel, C. 2012. Development of tensile fatigue criteria for bound materials. NZ Transport Agency research report 463.

Burns, S. and Tillman, A. K. 2006. Evaluation of the Strength of Cement-Treated Aggregate for Pavement Bases. Virginia Transportation Research Council VTRC 06-CR7

Flintsch, G. W., Diefenderfer, B. K., and Nunez, O. 2008. Composite pavement systems: Synthesis of design and construction practices. Virginia Transportation Research Council, Report No. FHWA/VTRC 09-CR2, Charlottesville, Virginia.

Gaspard, J. K. (2000) "Evaluation of Cement Treated Base Courses." Louisiana Transportation Research Center, Technical Assistance Report Number 00-1TA.

Gnanendran, C. T., and Piratheepan, J. 2008. Indirect diametrical tensile testing with internal displacement measurement and stiffness determination. Geotechnical Testing Journal, 32(1), 1-10.

Gnanendran, C. T., and Piratheepan, J. 2008. Dynamic Modulus and Fatigue Testing of Lightly Cementitiously Stabilized Granular Pavement Materials. ASCE Airfield and Highway Pavements.

Gnanendran, C. T., and Piratheepan, J. 2010. Determination of fatigue life of a granular base material lightly stabilized with slag lime from indirect diametric tensile testing. Journal of Transportation Engineering (ASCE), 136(8), 736-745.

Gupta, S., Ranaivoson, A., Edil, T., Benson, C., Sawangsuriya, A. 2007. Pavement design using unsaturated soil technology. Final Research Report submitted to Minnesota Department of Transportation, Report No. MN/RC-2007-11, University of Minnesota, Minneapolis.

Grieb, W. E., Werner, G. 1962. Comparison of the Splitting Tensile Strength of Concrete with Flexural and Compressive Strengths. Public Roads, Vol 32, No 5, pp 97-106.

Hudson, W.R, Kennedy, T.W. 1968. An Indirect Tensile Test for Stabilized Materials. Center of Highway Research, The University of Texas at Austin. Research Report Number 98-1.

Khalid, A. H. 2000. A comparison between bending and diametric fatigue test for bituminous material. Materials and Structures Vol. 33 457-465.

Khoury, N. N., and Zaman, M. M. 2007. Environmental effects on durability of aggregates stabilized with cementitious materials. Journal of Materials in Civil Engineering (ASCE), 19(1), 41-48.

Li, Y., Metcalf, I. J. B., Romanoschi, S. A., and Rasoulian, M. 1999. Performance and failure modes of Louisiana asphalt pavements with soil-cement bases under full-scale accelerated loading. Transportation Research Record 1673, 600, 9-15. 100

Mahasantipiya, S. 2000. Performance analysis of bases for flexible pavement. Dissertation submitted for award of Doctor of Philosophy, College of Engineering and Technology, Ohio University.

Majumder, B. K., Das, A., and Pandey, B. B. 1999. Cement treated marginal aggregates for roads. Journal of Materials in Civil Engineering (ASCE), 11(3), 257-265.

Mbaraga, N. A., Jenkins, J. K., and Van de Ven, M., 2013. Influence of beam geometry and aggregate size on the flexural strength and elastic moduli of cement stabilized materials. TRB 2014 Annual Meeting. University of Stellenbosh Institute of Integrated Engineering and Technology, Stellenbosh, Western Cape, South Africa.

Midgley, L., and Yeo, R. 2008. The development and evaluation of protocols for the laboratory characterisation of cemented materials. Austroads Technical Report APT-T101-08.

Molenaar, A.A.A., and Pu, B. (2002) Prediction of Fatigue Cracking in Cement Treated Base Courses. Delft University of Technology, the Netherlands.

Nazarian S., Yuan D., and Williams R. R. 2003. A simple method for determining modulus of base and subgrade materials. ASTM STP 1437, ASTM, West Conshohocken, PA, 152-164.

Papacostas, A. 2013. Prediction of Flexural Strength and Breaking Strain of Cemented Materials: Laboratory Study. AUSTROADS TECHNICAL REPORT AP-T251-13

Paul, D. K., and Gnanendran, C. T. 2013. Stress–strain behavior and stiffness of lightly stabilized granular materials from UCS testing and their predictability. International Journal of Pavement Engineering, 14:3, 291-308

Paul, D. K., and Gnanendran, C. T. 2012. Characterization of Lightly Stabilized Granular Base Materials by Flexural Beam Testing and Effects of Loading Rate. Geotechnical Testing Journal, Vol. 35, No. 5.

Puppala, A. J., Hoyos, L. R., and Potturi, A. K. 2011. Resilient moduli response of moderately cement-treated reclaimed asphalt pavement aggregates. Journal of Materials in Civil Engineering (ASCE), 23(7), 990-998.

Scullion, T., Uzan, J., Hilbrich, S., and Chen, P. 2008. Thickness Design Systems for Pavements Containing Soil-Cement Bases. SN2863, Portland Cement Association, Skokie, Illinois.

Scullion, T., Sebesta, S., Estakhri, C., Harris, P., Shon, C., Harvey O., and Rose-Harvey, K. 2012. Full-Depth Reclamation: New Test Procedures and Recommended Updates to Specifications. Texas Transportation Institute FHWA/TX-11/0-6271-2 101

Sobhan, K., Das, B.M. 2007. Durability of soil–cements against fatigue fracture. Journal of Materials in Civil Engineering (ASCE), 19(1), 26-32.

Texas Department of Transportation Designation: Tex-101-E Part II. 2010. Preparing Soil and Flexible Base Materials. Texas Department of Transportation.

Texas Department of Transportation Designation: Tex-113-E. 2011. Laboratory Compaction Characteristics and Moisture-Density Relationships of Base Materials. Texas Department of Transportation.

Texas Department of Transportation Designation: Tex-120-E. 2012. Soil-Cement Testing. Texas Department of Transportation.

Texas Department of Transportation Designation: Tex-144-E (Draft) 2006. Tube Suction Test. Texas Department of Transportation.

Texas Department of Transportation Standard Specifications Book 2014. Standard Specifications for Construction and Maintenance of Highways, Streets, and Bridges. Texas Departement of Transportation.

Thaulow, S. 1957. Tensile Splitting Test and High Strength Concrete Test Cylinders. Journal of the American Concrete Institute, Vol 28, No 7, Paper 53-38, pp 699-705.

White, D.J., Handy, R.L., 2015. Cement Stabilization of Embankment Materials. Center for Earthworks Engineering Research, Iowa State University.

Yan, W., Weihong, X., and Xiaotong, F. 2011. Studies on fatigue behaviors of cement stabilized macadam mixture. Emerging Technologies for Material, Design, Rehabilitation, and Inspection of Roadway Pavements, Geotechnical Special Publication No. 218 ASCE.

Zhou, F., Fernado E., and Sculion T. 2010. Development, Calibration, and Validation of Performance Prediction Models for the Texas M-E Flexible Pavement Design System. Texas Transportation Institute FHWA/TX-10/0-5798-2

Appendix A

SURVEY FOR TXDOT RESEARCH PROJECT 0-6812

District: _____Contact Person: _____

Telephone number and e-mail: _____

1. Do you use Portland cement to stabilize the base layers in your district?

☐ Often ☐ Sometimes ☐ Never

2. If often or sometimes, in your judgment how many such projects have been completed in the last 5 years or are scheduled to be constructed in the near future in your district?

_____Project(s).

3. Please indicate the percentage of cement content that you typically use for the stabilization of the aggregate base layers (check all that applies).

☐ 2% ☐ 3% ☐ 4%

☐ 5% ☐ 6% ☐ Other (please specify in %) _____

4. The cement content is usually estimated based on

☐ Local experience ☐ Laboratory testing ☐ District/Area office preference

☐ Other (please specify) _____.

5. Are there any strength requirements for cement-stabilized base in your district? If so, what are the typical requirements?

☐ Yes ☐ No

6. Are there any other requirements for cement-stabilized base in your district? If so, what are they?

☐ Yes ☐ No

7. Please indicate the most common aggregate type(s) and the quarries you used to obtain aggregates for cement stabilized base layers.

☐ Limestone from _Hanson Perch Hill_____ ☐ Granite from _____

☐ Gravel from _____ ☐ Other (please specify) _____

8. As per Item 275, please indicate the Grade that you most frequently use for cement stabilized base layers.

☐ Grade 1 ☐ Grade 2 ☐ Grade 3 ☐ Grade 4

9. Could you please comment on any area that this research should address to help you?

_____

10. Do you mind if we contact you for more information?

☐ Yes ☐ No

Appendix B

UNCONFINED COMPRESSIVE STRENGTH DATA

Table B.1: Unconfined Compressive Strength Data

Test	Material	Curing Condition	Cement Content (%)	Max Load (lb)	
				Set 1	Set 2
Unconfined Compressive Strength	El Paso	7 Day Moist Cured	2	8674	7579
			3	11697	12729
			4	17914	19043
			5	23755	27617
		10-Day TST	2	5082	8021
			3	11710	12577
			4	19077	18635
			5	25509	20130
	San Antonio	7 Day Moist Cured	2	6300	9973
			3	10962	10459
			4	13394	13345
			5	16800	18860
		10-Day TST	2	6642	8209
			3	10713	10426
			4	12283	11634
			5	14806	12007
	Pharr	7 Day Moist Cured	2	3205	3818
			3	5212	5033
			4	6705	7103
			5	6914	7553
		10-Day TST	2	3995	4090
			3	5212	5108
			4	7893	6567
			5	9250	8372
	Paris	7 Day Moist Cured	2	7800	10041
			3	13857	14780
			4	20725	19850
			5	27413	23420
		10-Day TST	2	7913	9874
			3	17207	15324
			4	22884	18555
			5	27280	29411

Appendix C

STATIC INDIRECT DIAMETRICAL TEST DATA

Table C.1: Static Indirect Diametrical Test Data

Test	Material	Curing Condition	Cement Content (%)	Max Load (lb)	
				Set 1	Set 2
Static Indirect Diametrical Test	El Paso	7 Day Moist Cured	2	1796	1478
			3	2191	2634
			4	3698	4047
			5	4568	4008
		10-Day TST	2	1791	806
			3	2338	1851
			4	3622	3679
			5	5144	4024
	San Antonio	7 Day Moist Cured	2	1731	2168
			3	2829	1807
			4	3084	3407
			5	3508	3894
		10-Day TST	2	1064	1111
			3	1421	2335
			4	2905	2604
			5	3618	3370
	Pharr	7 Day Moist Cured	2	1822	2083
			3	2445	2579
			4	2496	2670
			5	2963	3197
		10-Day TST	2	1657	1697
			3	1814	2069
			4	2042	2240
			5	2665	2406
	Paris	7 Day Moist Cured	2	1292	1254
			3	1952	1614
			4	3551	2590
			5	4542	4663
		10-Day TST	2	699	971
			3	2094	1428
			4	2985	2322
			5	4058	4246

Appendix D

SUBMAXIMAL MODULUS TEST DATA

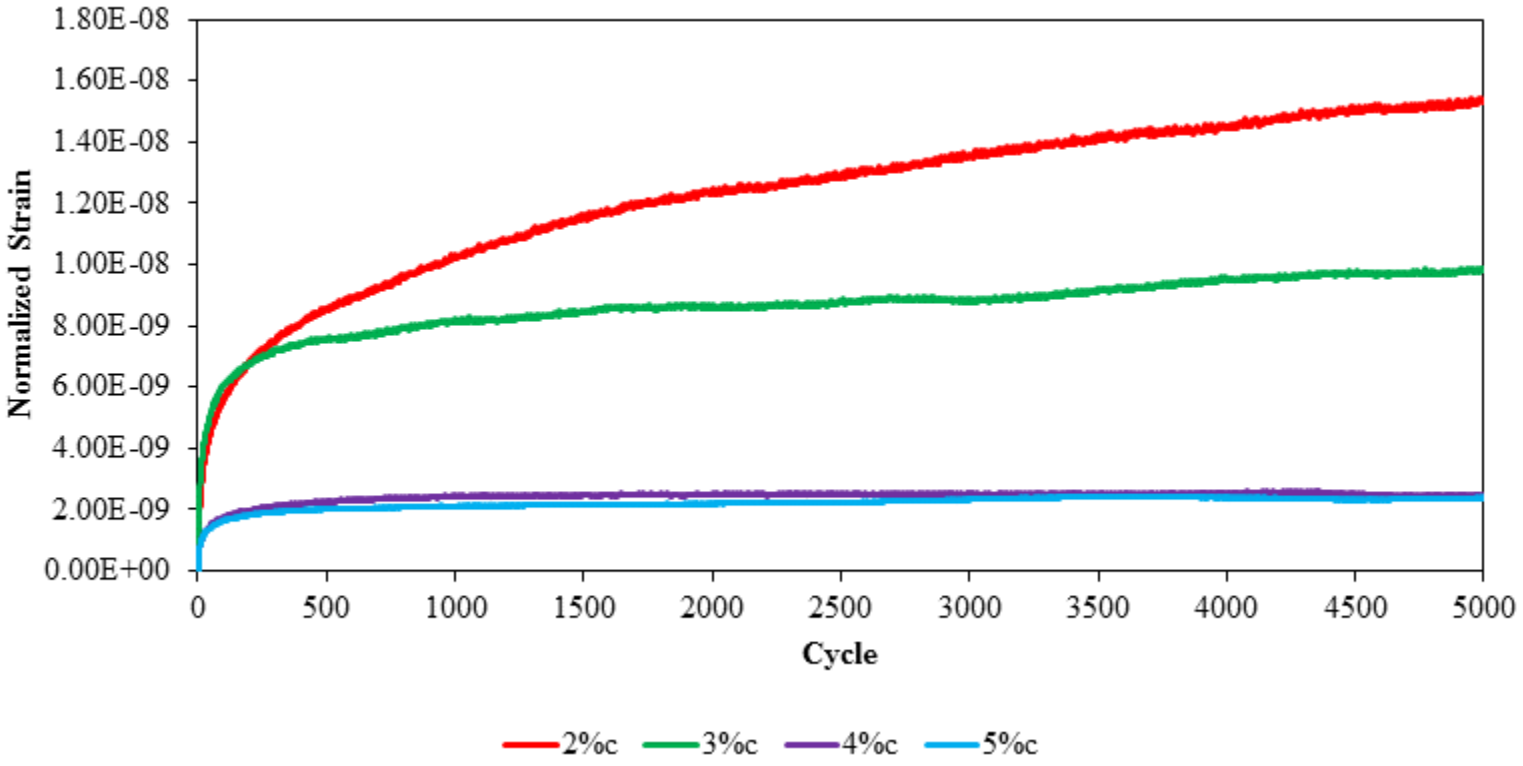

Figure D.1: Permanent Deformation for El Paso Material @20% UCS Strength for 7 day Moist Cured Samples.

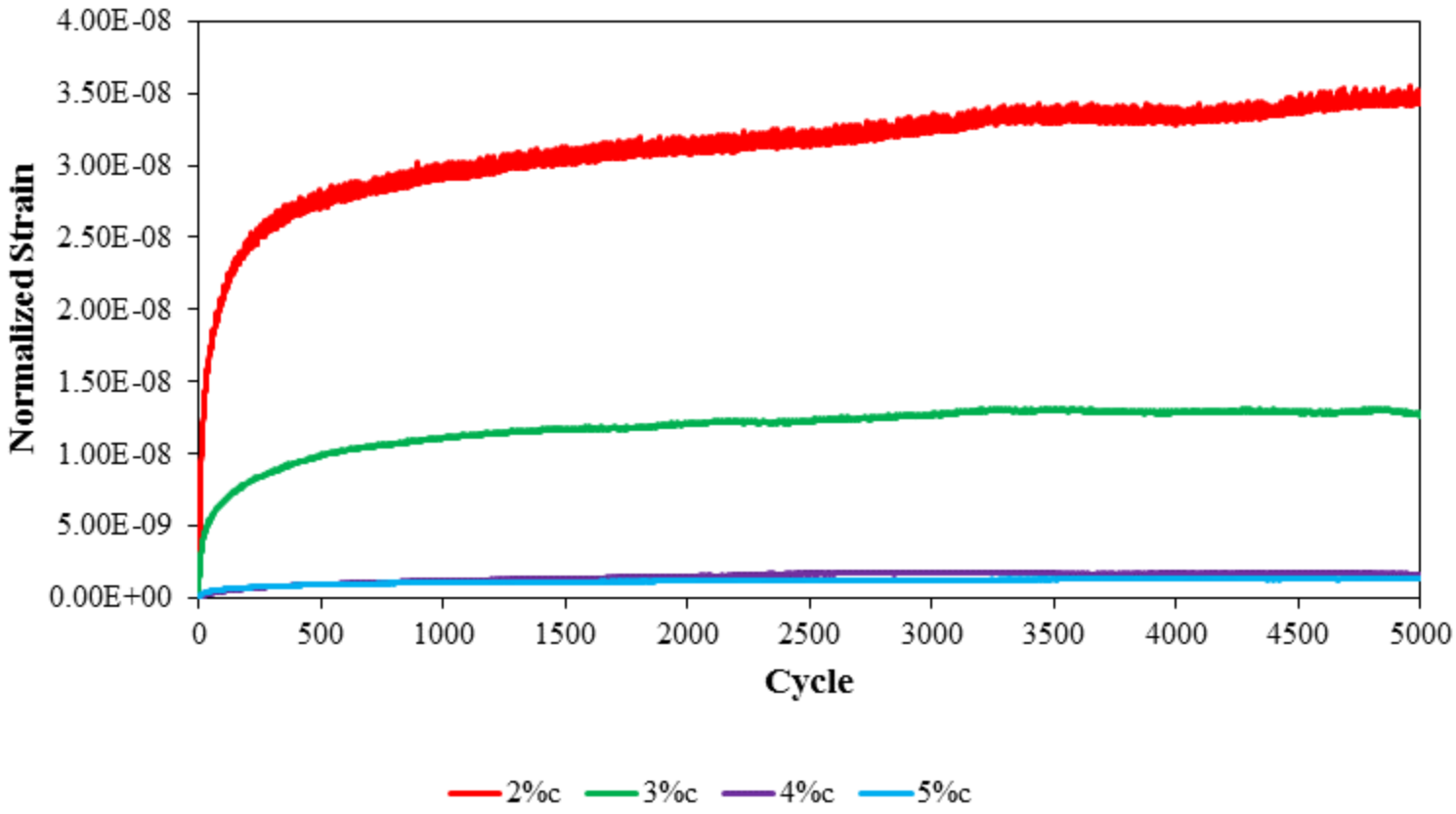

Figure D.2: Permanent Deformation for El Paso Material @20% UCS Strength for 10 Day Capillary Soak Samples.

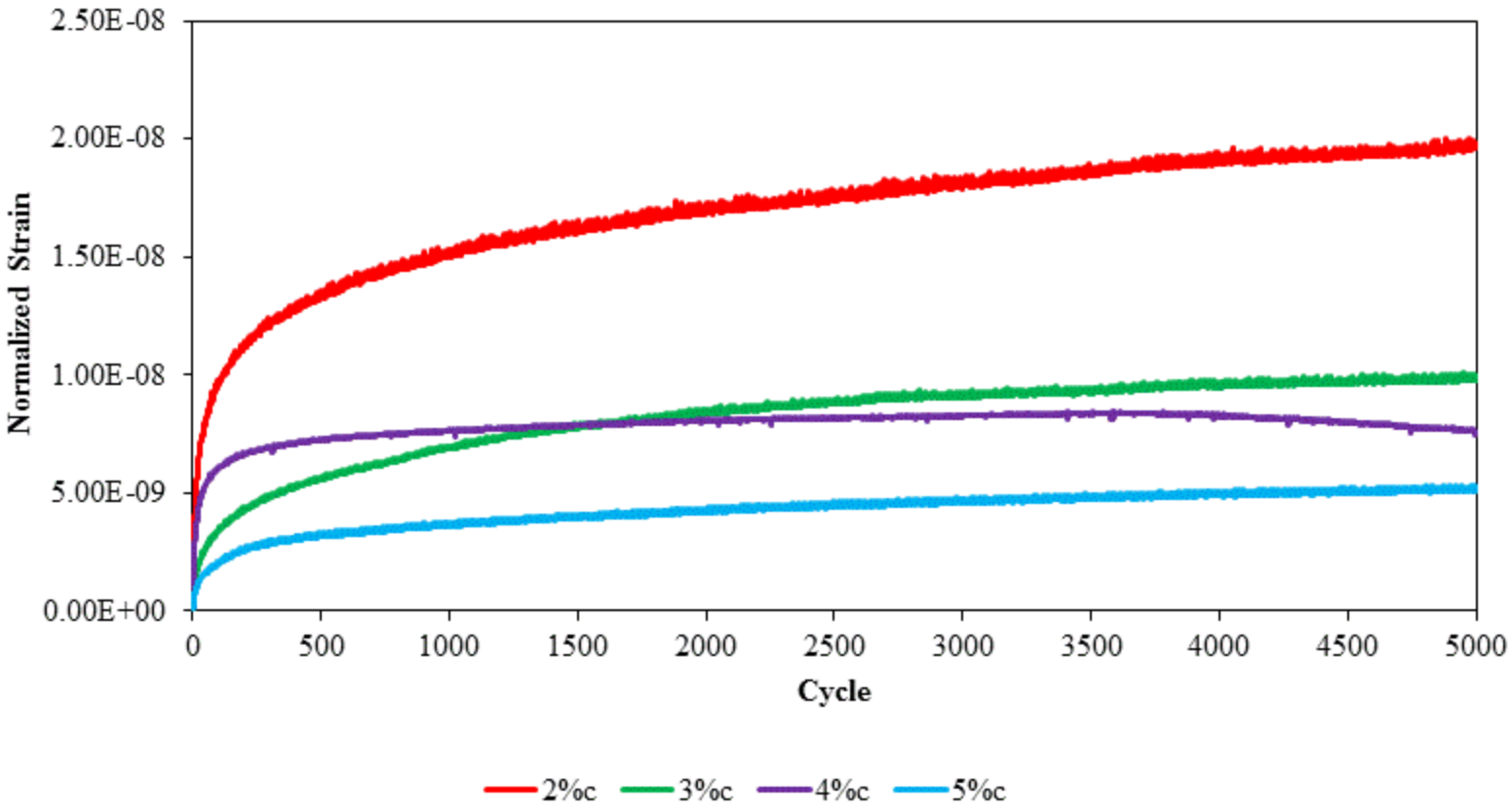

Figure D.3: Permanent Deformation for San Antonio Material @20% UCS Strength for 7 day Moist Cured Samples.

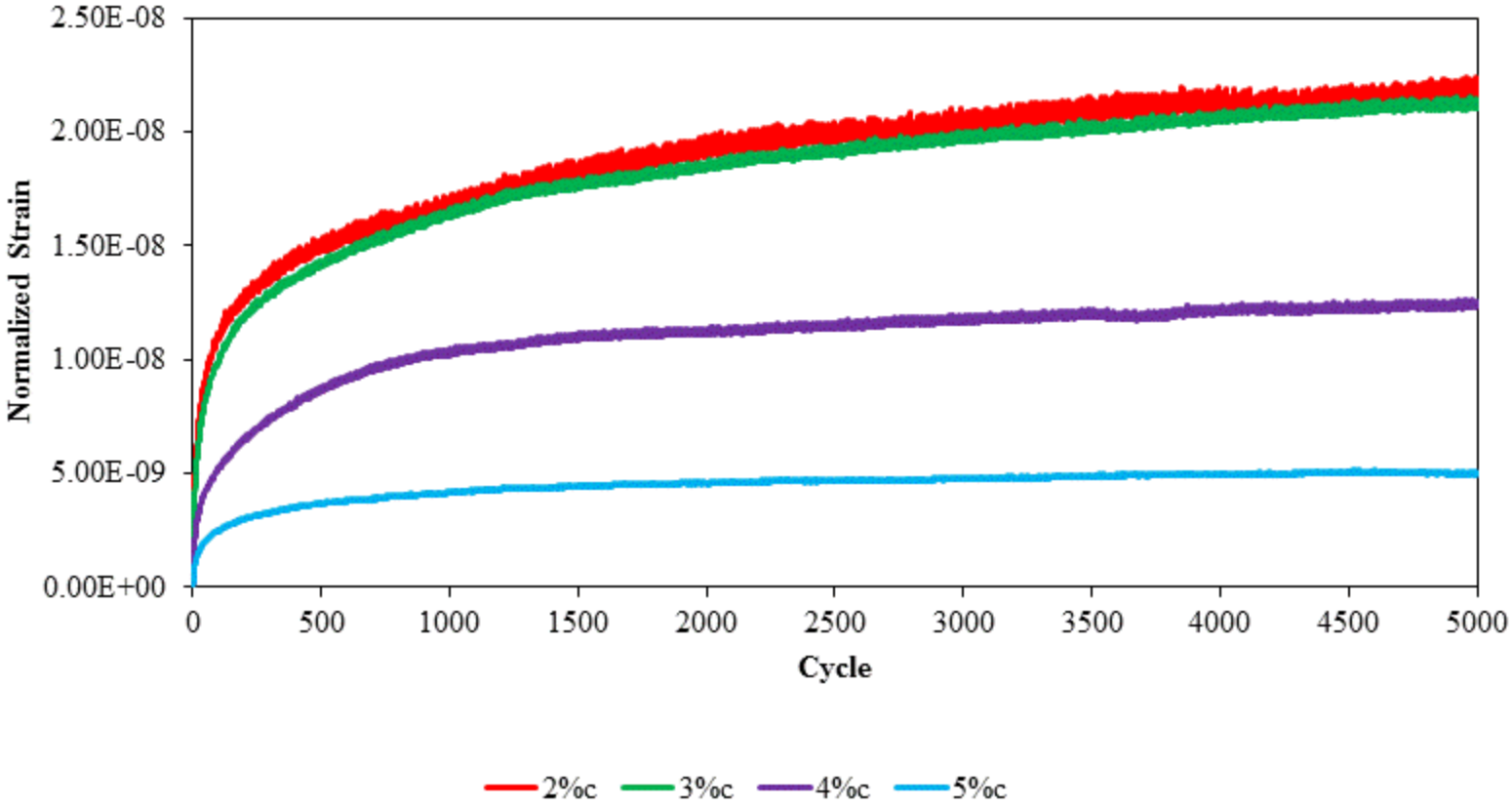

Figure D.4: Permanent Deformation for San Antonio Material @20% UCS Strength for 10 Day Capillary Soak Samples.

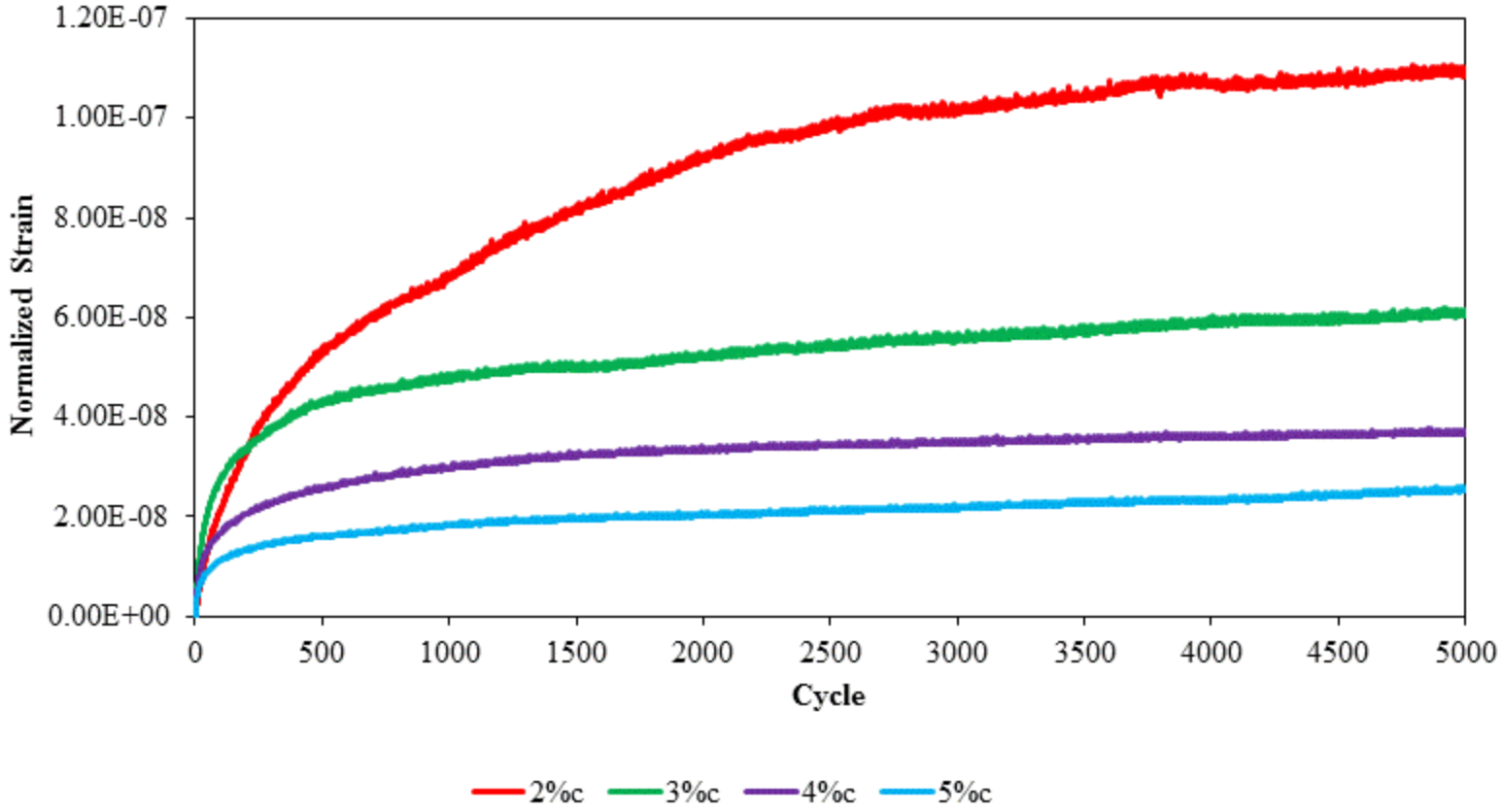

Figure D.5: Permanent Deformation for Pharr Material @20% UCS Strength for 7 day Moist Cured Samples.

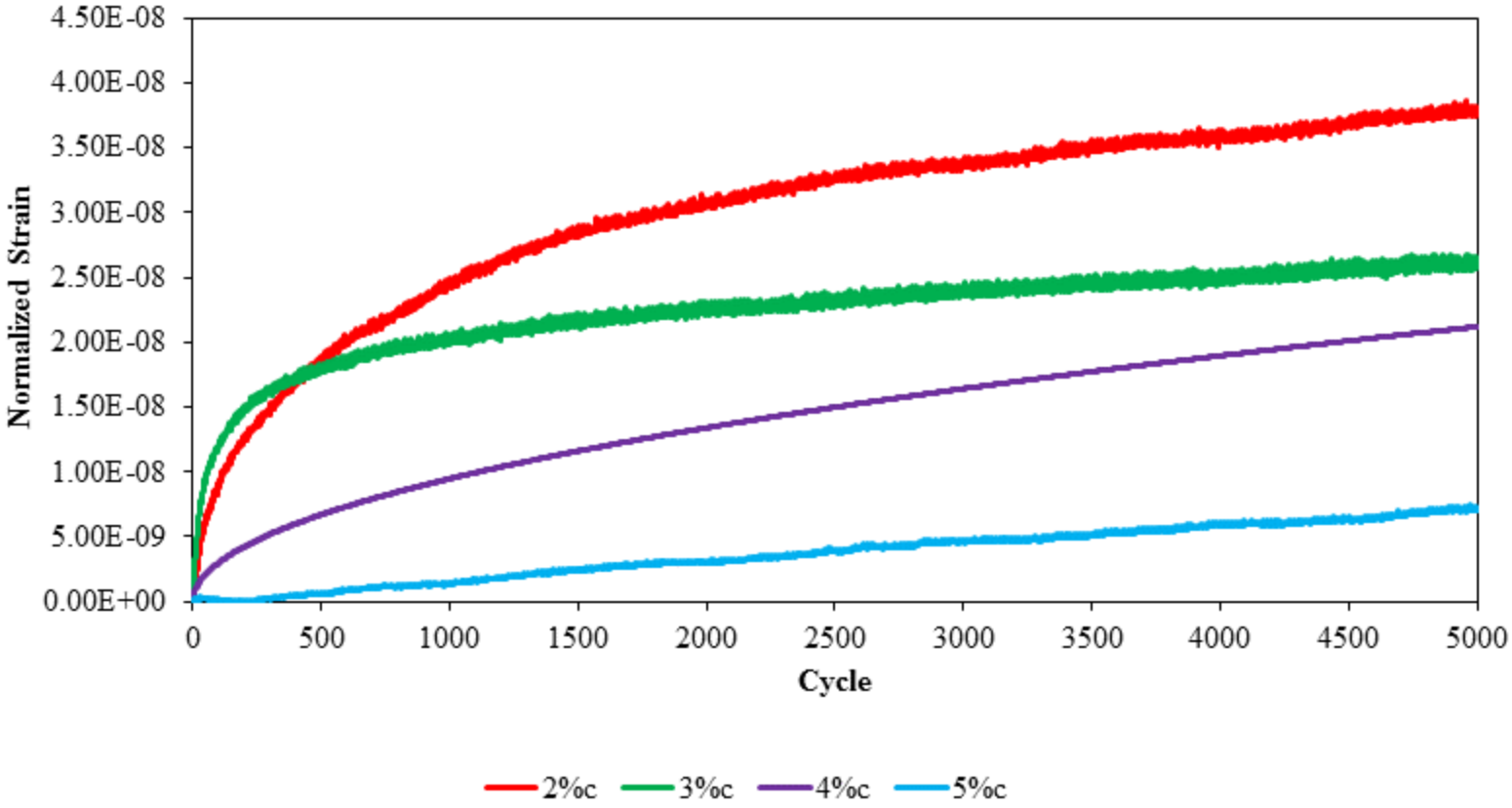

Figure D.6: Permanent Deformation for Pharr Material @20% UCS Strength for 10 Day Capillary Soak Samples.

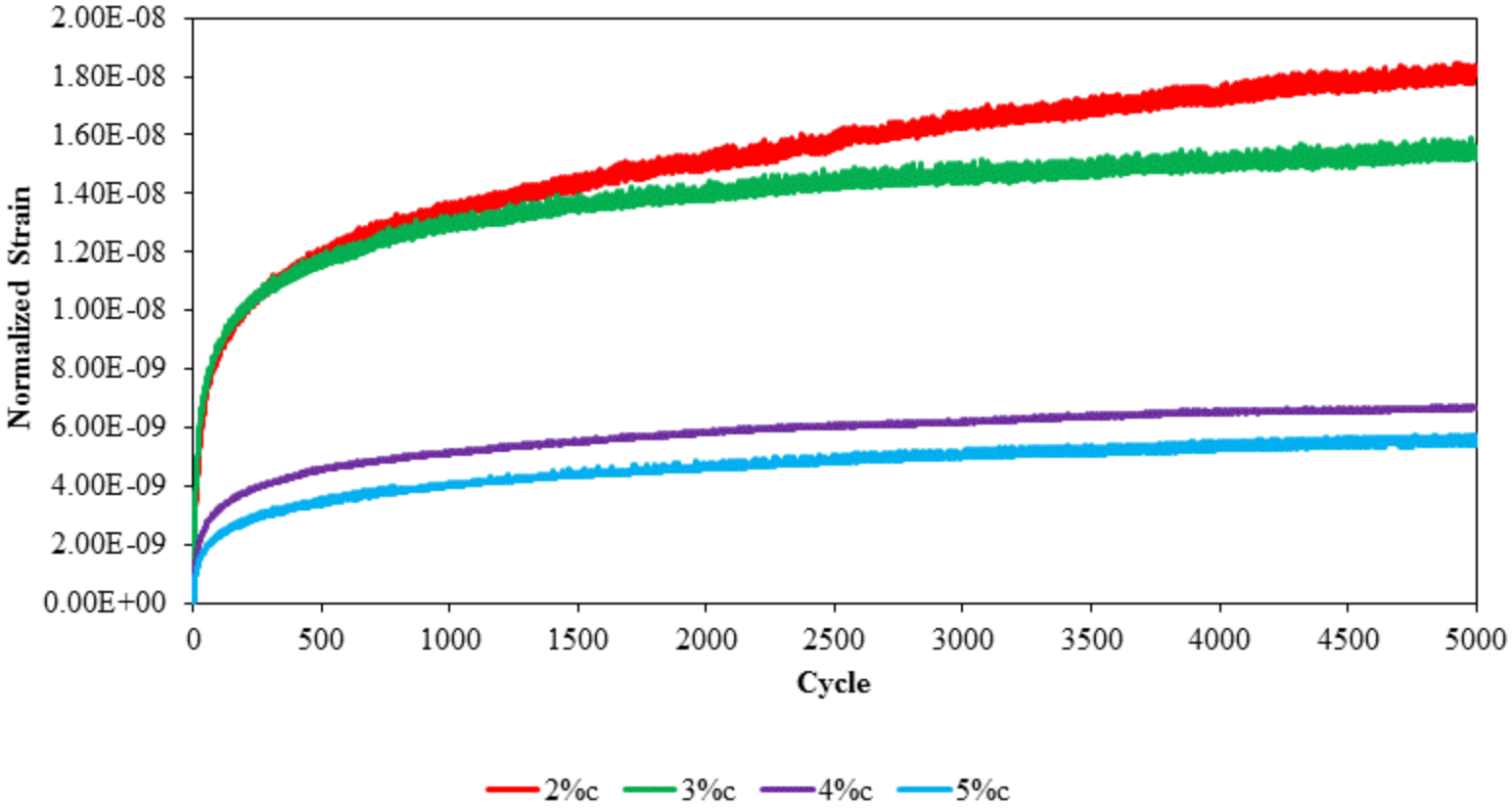

Figure D.7: Permanent Deformation for Paris Material @20% UCS Strength for 7 day Moist Cured Samples.

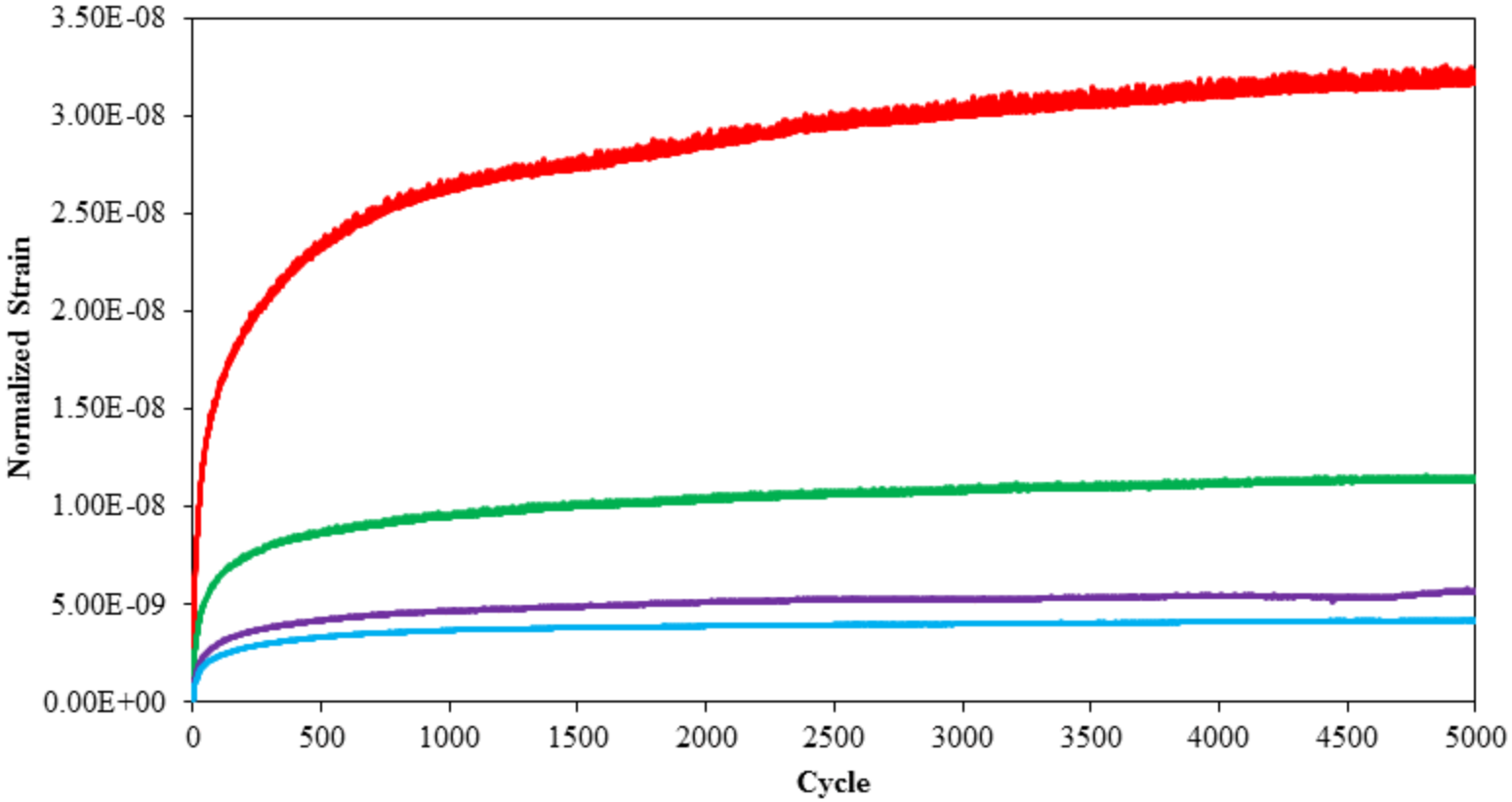

Figure D.8: Permanent Deformation for Paris Material @20% UCS Strength for 10 Day Capillary Soak Samples.

Appendix E

DYNAMIC IDT TEST DATA

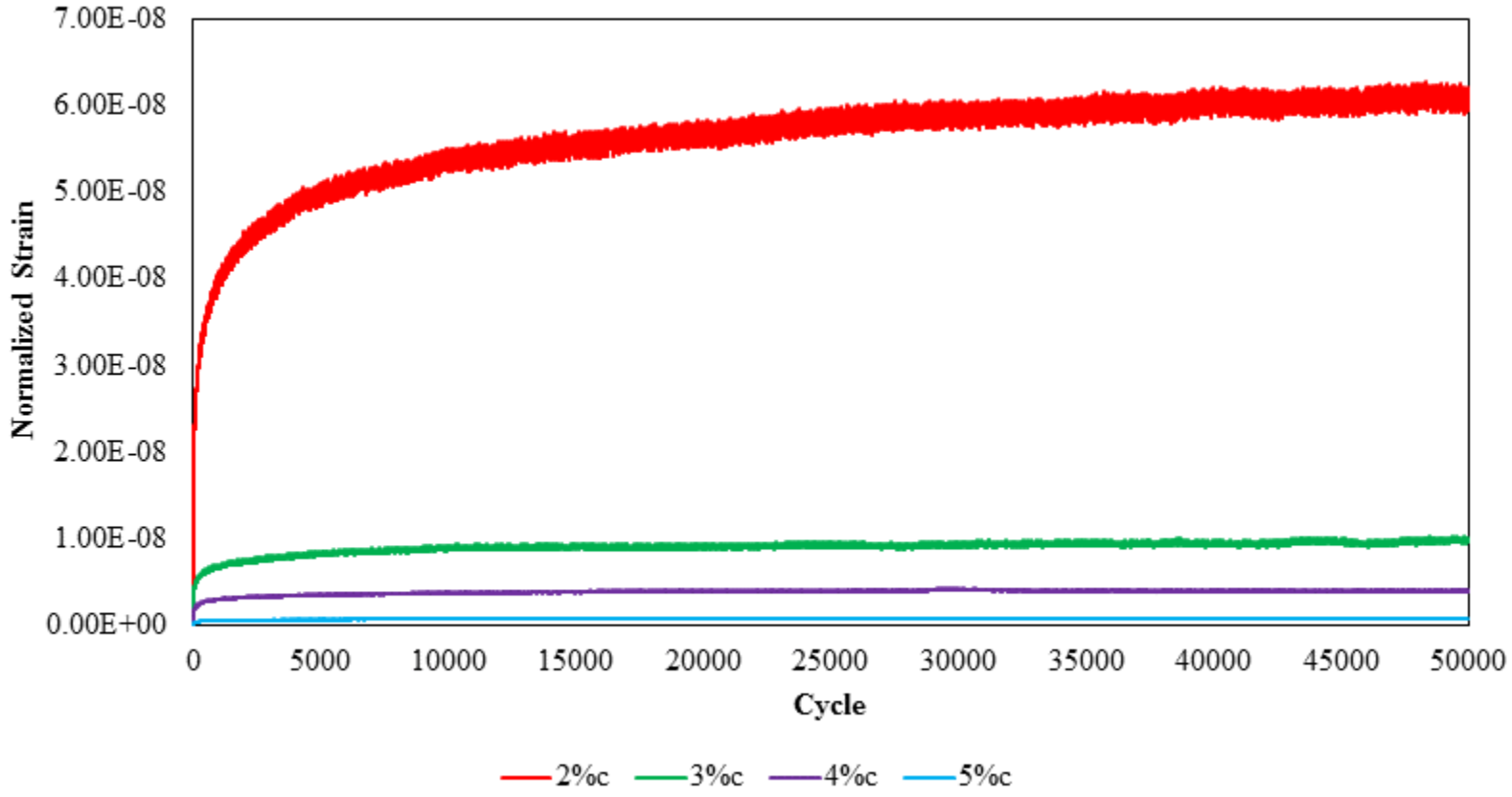

Figure E.1: Permanent Deformation for El Paso Material @20% IDT Strength for 7 day Moist Cured Samples.

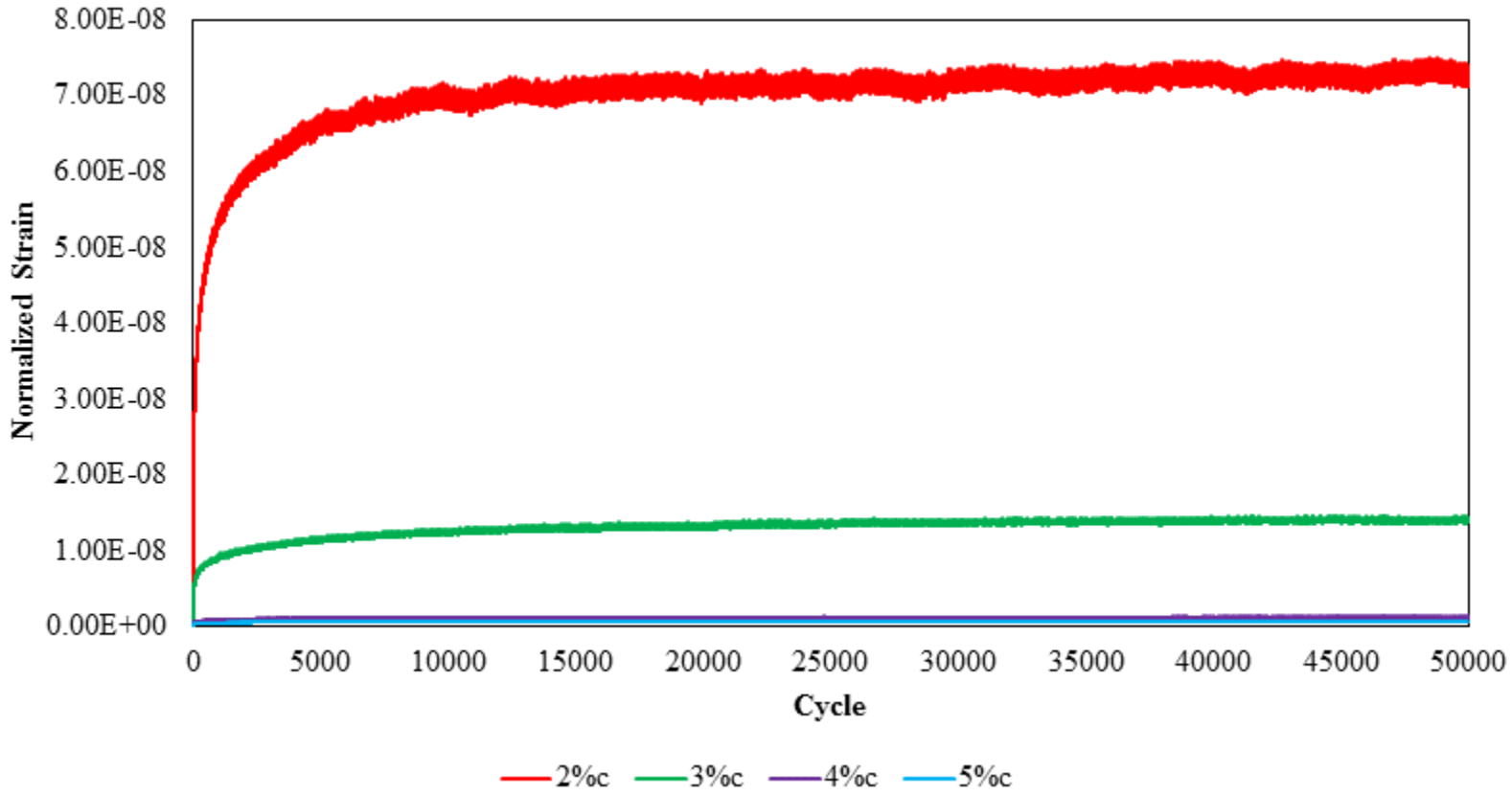

Figure E.2: Permanent Deformation for El Paso Material @20% IDT Strength for 10 Day Capillary Soak Samples.

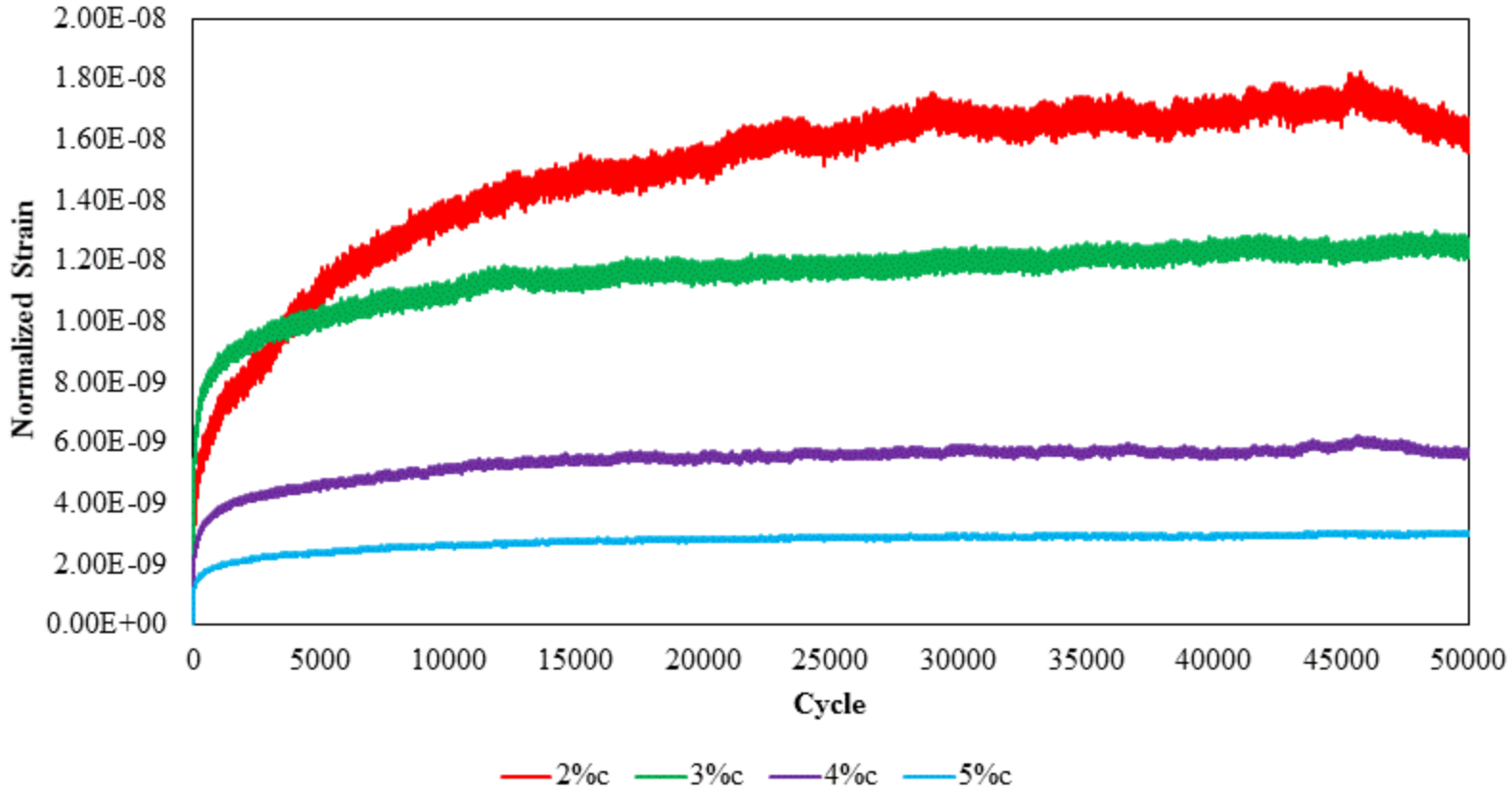

FigureE.3: Permanent Deformation for San Antonio Material @20% IDT Strength for 7 day Moist Cured Samples.

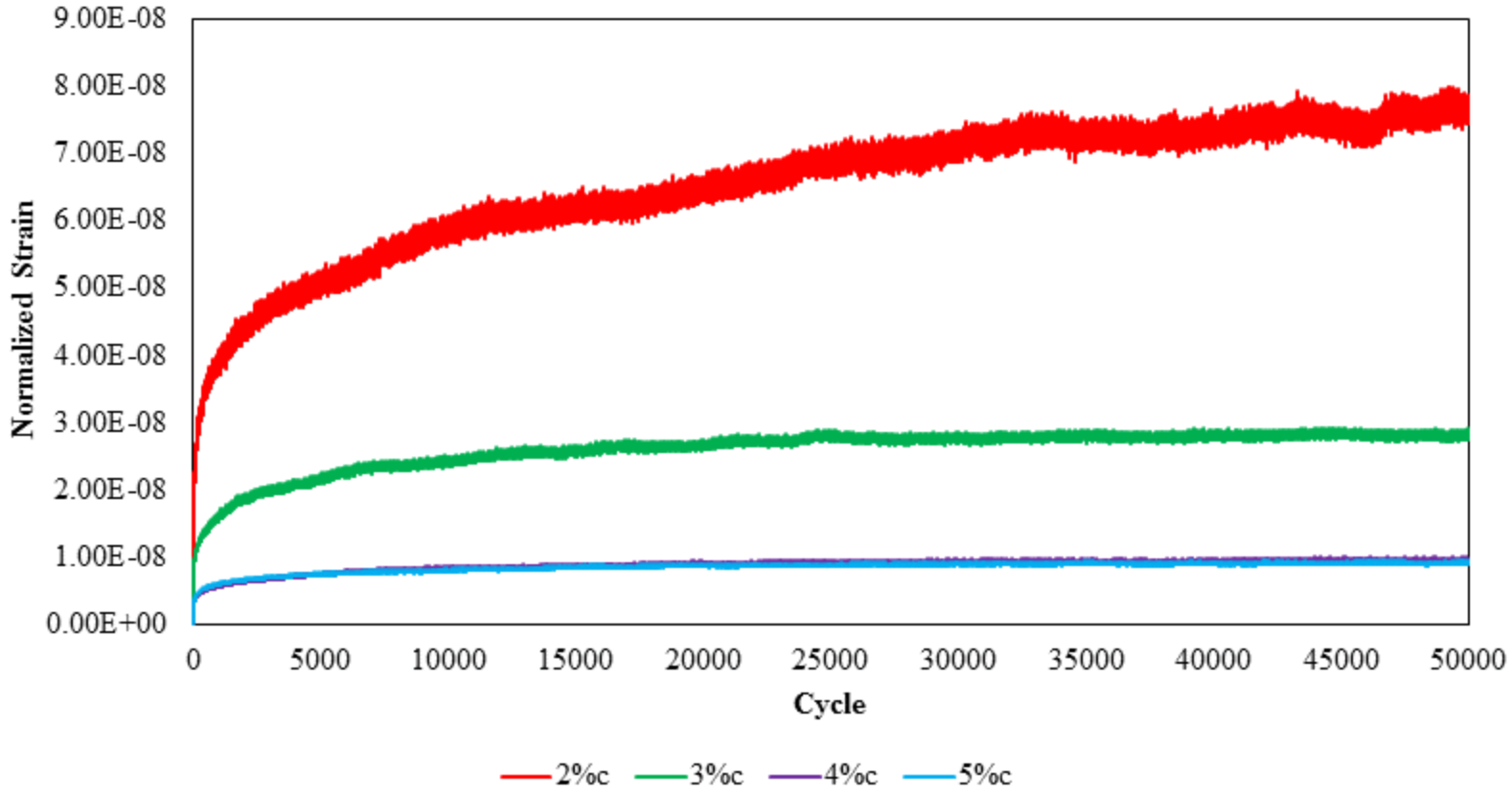

Figure E.4: Permanent Deformation for San Antonio Material @20% IDT Strength for 10 Day Capillary Soak Samples.

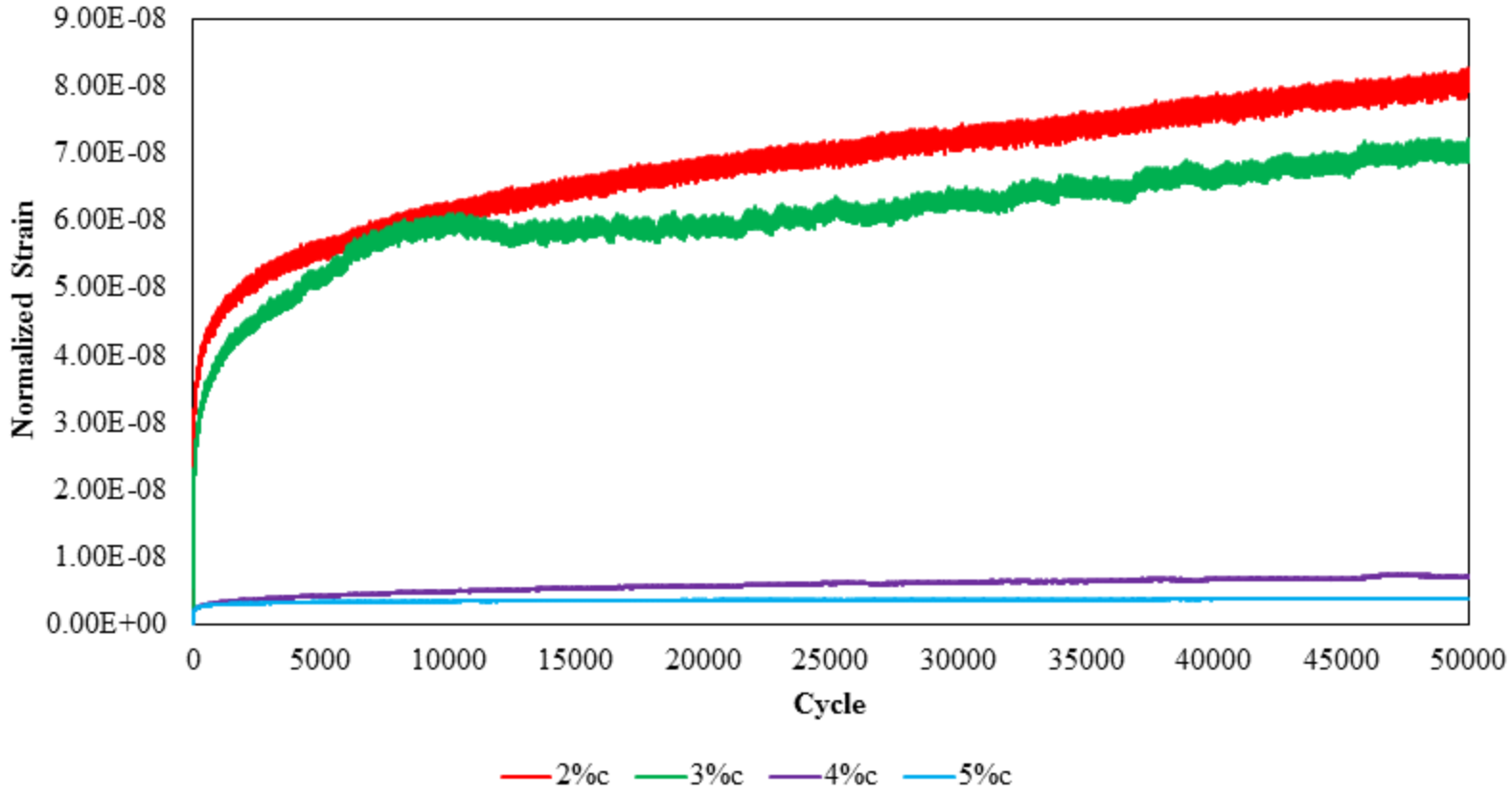

Figure E.5: Permanent Deformation for Pharr Material @20% IDT Strength for 7 day Moist Cured Samples.

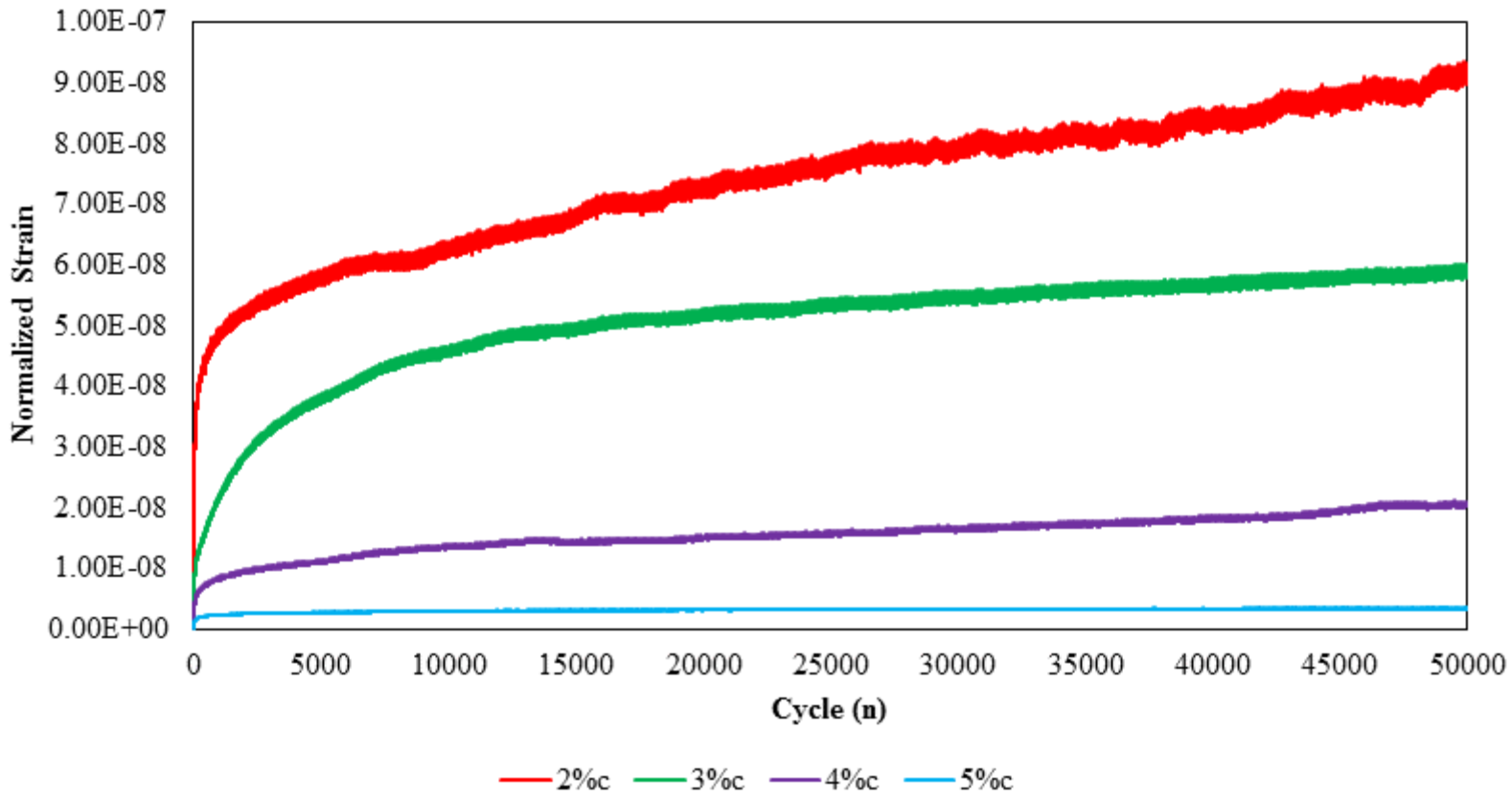

Figure E.6: Permanent Deformation for Pharr Material @20% IDT Strength for 10 Day Capillary Soak Samples.

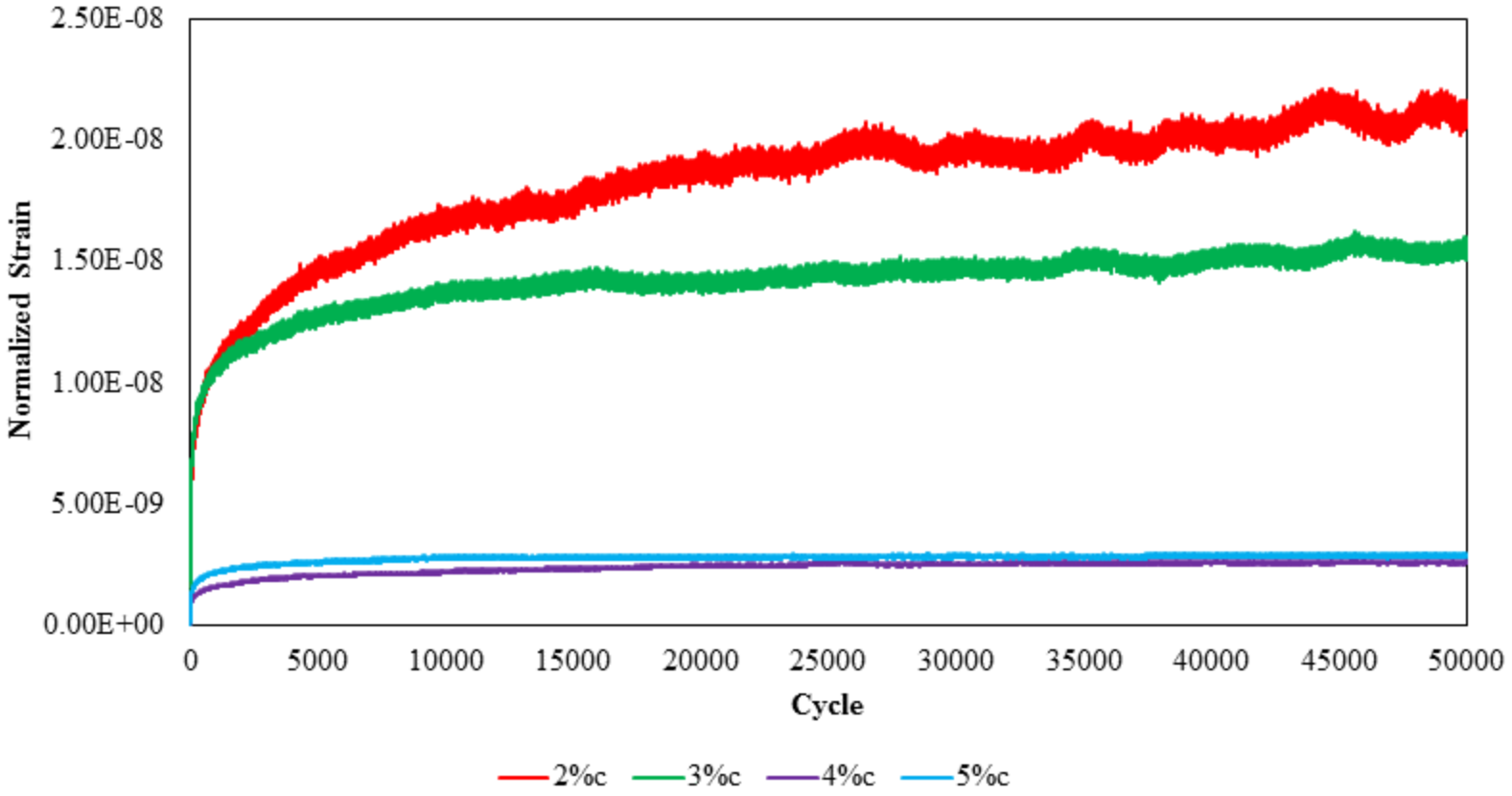

Figure E.7: Permanent Deformation for Paris Material @20% IDT Strength for 7 day Moist Cured Samples.

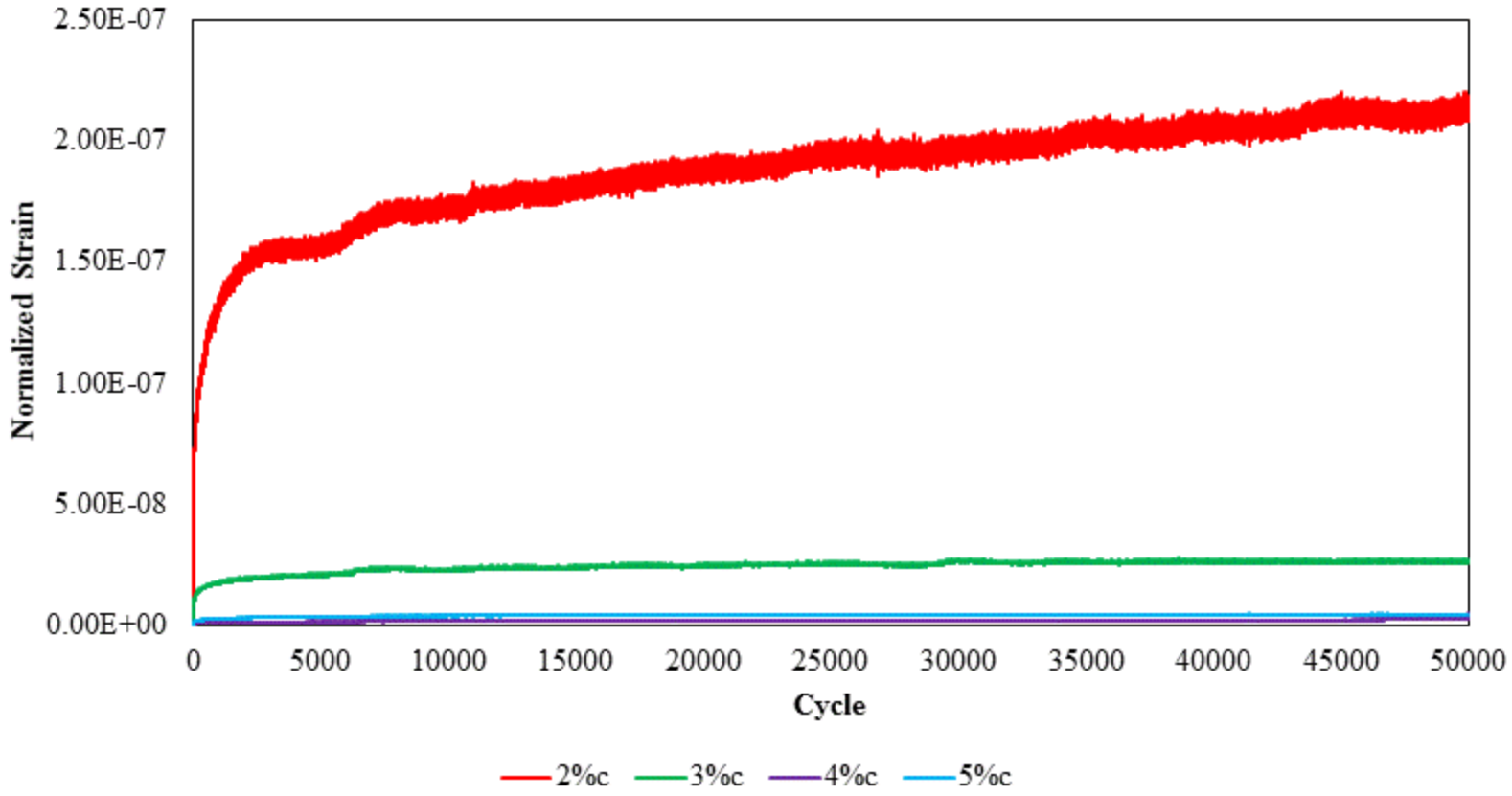

Figure E.8: Permanent Deformation for Paris Material @20% IDT Strength for 10 Day Capillary Soak Samples.

Curriculum Vita

Jose Tarin was born in Mexico where he lived and studied until his high school graduation in 2009. Then, he decided to start his bachelor degree in Civil Engineering at the University of Texas at El Paso. During his last semester at the university, he was invited directly from Dr. Reza Ashtiani to work and participate in a Texas Department of Transportation project related to soil stabilization. Then, he worked as a research assistant at the Center of Transportation of Infrastructure Systems where he performed several test such as Unconfined compressive strength test, indirect diametrical tensile test, free-free resonant column test, dielectric value test, capillary soak suction test. He finished his masters degree in May of 2017.

Contact Information: jatarin2@miners.utep.edu

This thesis was typed by Jose Antonio Tarin